

# Synthesis of $[\text{Os}(\text{bpy})_2(\text{py})(\text{OH}_2)](\text{PF}_6)_x$ Substituted Pyridine Complexes; Characterization of a Singly Bridged $\text{H}_3\text{O}_2^-$ Ligand

## Supplementary Information

Jiangtian Sun,<sup>a</sup> Jingwen Sun,<sup>a</sup> Brandon J. Jolly,<sup>a</sup> Martin-Louis Y. Riu,<sup>a</sup> Tyler A. Kerr,<sup>a</sup> Yi-An Lai,<sup>a</sup> Michael J. Pung,<sup>a</sup> Chong Liu<sup>\*a,b</sup> and Matthew Nava<sup>\*a</sup>

<sup>a</sup>Department of Chemistry and Biochemistry, University of California, Los Angeles, Los Angeles, CA, 90095, USA

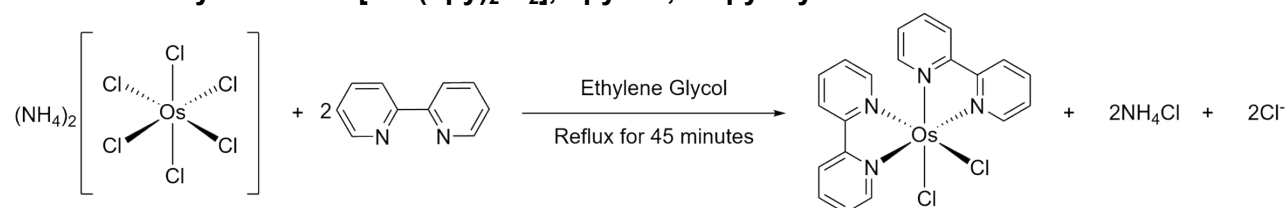
<sup>b</sup>California NanoSystems Institute, University of California, Los Angeles, Los Angeles, CA, 90095, USA

## Table of Contents

Section S1. Synthesis of $[\text{Os}^{\text{II}}(\text{bpy})_2\text{Cl}_2]$ , bpy = 2,2 bipyridyl .....	2
Section S2. Synthesis of $[\text{Os}^{\text{II}}(\text{bpy})_2\text{CO}_3]$ , bpy = 2,2 bipyridyl .....	5
S2.1 Synthesis and characterization of $[\text{Os}^{\text{II}}(\text{bpy})_2\text{CO}_3]$ .....	5
S2.2 Dimerization and Oligomerization of $[\text{Os}^{\text{II}}(\text{bpy})_2(\text{OH}_2)_2]^{2+}$ .....	9
Section S3. Synthesis of $[\text{Os}(\text{bpy})_2(\text{OH}_2)(\text{py})](\text{PF}_6)_x$ (py=pyridine, 4-methoxypyridine, 4-methylpyridine, 4-cyanopyridine, 4-cholopyridine, 4-pyridylmethylphosphonic acid, 4-N-(pyridin-4-ylmethyl)-N,N,N-trimethylammonium) .....	11
S3.1 Determination of the impurity peaks in Figure 2A and pyridinium salt .....	11
S3.2 Choice of solvent systems .....	14
S3.3 Choice of precipitation agents .....	15
S3.4 Synthesis of $[\text{Os}(\text{bpy})_2(\text{OH}_2)(\text{py})](\text{PF}_6)_2$ (py=pyridine, 4-methoxypyridine, 4-methylpyridine) .....	16
S3.4.1 Oxidation of $[\text{Os}(\text{bpy})_2(\text{OH}_2)(\text{py})](\text{PF}_6)_2$ .....	17
S3.4.2 Diffusion coefficient measurement of $[\text{Os}(\text{bpy})_2(\text{OH}_2)(\text{py})](\text{PF}_6)_2$ (py=pyridine) ....	23
S3.4.3 ICP-MS analysis of the Chloride content in $[\text{Os}(\text{bpy})_2(\text{OH}_2)(\text{py})](\text{PF}_6)_2$ (py=4-methylpyridine) .....	34
S3.5 Synthesis of $[\text{Os}(\text{bpy})_2(\text{OH}_2)(\text{py})](\text{PF}_6)_2$ (py=4-cyanopyridine, 4-cholopyridine) .....	35
S3.6 Synthesis of $[\text{Os}(\text{bpy})_2(\text{OH}_2)(\text{py})](\text{PF}_6)_x$ (py=4-pyridylmethylphosphonic acid, 4-N-(pyridin-4-ylmethyl)-N,N,N-trimethylammonium) .....	44
S3.6.1 Diffusion coefficient measurement of $[\text{Os}(\text{bpy})_2(\text{OH}_2)(\text{py})](\text{PF}_6)_2$ (py = 4-N-(pyridin-4-ylmethyl)-N,N,N-trimethylammonium) .....	56
S3.7 Synthesis and diffusion coefficient measurement of $[\text{Os}(\text{bpy})_3](\text{PF}_6)_2$ (bpy=2,2'-bipyridine) .....	58
Section S4. Pyridine derivatives that could not be synthesized with the general procedure	61
Section S5. Single Crystal X-ray Crystallography .....	66
S5.1 Single crystal structure of complex $[\text{Os}(\text{bpy})_2(\text{py})(\text{OH}_2)][\text{Cl}]_{0.66}[\text{PF}_6]_{1.33}$ (py = 4-methylpyridine) .....	66
S5.2 Single crystal structure of complex $\{[\text{Os}^{\text{II}}(\text{bpy})_2(\text{py})]_2(\mu\text{-O}_2\text{H}_3)\}(\text{PF}_6)_5$ (py = 4-N-(pyridin-4-ylmethyl)-N,N,N-trimethylammonium) .....	84
S5.3 Single crystal structure of dinuclear complex 6 .....	105

Ammonium hexachloroosmate(IV) (99.99% metals basis), 2,2'-bipyridine (99+%), pyridine (99+%, for spectroscopy), sodium hexafluorophosphate (99+%), L-(+)-Ascorbic acid (99+%), 2-bromopyridine (99%), 4-bromopyridine hydrochloride (99%) and trimethylamine (1M soln. in THF) were purchased from Thermo Fisher Scientific and used as received. Ethylene glycol (99.8%), diethyl ether ( $\geq 99.0\%$ ), sodium hydrosulfite (sodium dithionite,  $\geq 82\%$  (RT)), sodium carbonate ( $\geq 99.5\%$ ), ethanol ( $\geq 95.0\%$ ), boric acid ( $\geq 99.5\%$ ), acetic acid (glacial,  $\geq 99.7\%$ ), phosphoric acid (crystalline,  $\geq 99.999\%$  trace metals basis), 2-propanol ( $\geq 99.5\%$ ), 4-chloropyridine hydrochloride (99%), 4-pyridylmethylphosphonic acid (4-pyridylmethylphosphonic acid), acetone ( $\geq 99.5\%$ ), 2-methoxypyridine (98%), quinoline (98%) and 1,8-naphthyridine were purchased from Sigma-Aldrich and used as received. 4-methoxypyridine (98%), 4-methylpyridine (98%) and 4-cyanopyridine (98%) were purchased from Oakwood Chemical and used as received. All the isotopes for NMR analysis were purchased from Cambridge Isotope Laboratories. The other common chemicals and solvents used, not mentioned above, were purchased from Sigma-Aldrich, Thermo Fisher Scientific, Oakwood Chemical and AA Blocks. UV-Vis spectra were collected using a Cary 5000 UV-Vis-NIR spectrophotometer. Cyclic voltammetry was performed with a BioLogic SP-50e potentiostat. A three-electrode setup was used, consisting of a glassy carbon working electrode (CH Instruments, diameter 3 mm), a platinum wire counter-electrode (CH Instruments) and an Ag/AgCl (1 M KCl) reference electrode (CH Instruments, with 1 M KCl as the electrolyte). All solutions, unless specified, were purged with  $N_2$  prior to the collection of electrochemical data. IR spectra were collected by an Agilent Cary 600 Series FTIR Spectrometer. Emission spectra were collected by a HORIBA TCSPC spectrofluorometer with a slit width set to 5 nm. The compounds bulk purities were checked by either elemental analysis (CE-440 Elemental Analyzer) or inductively coupled mass spectrometry (ICPMS, Agilent 8800 ICP-MS triple Quad). NMR spectra were obtained on a Bruker AV400 spectrometer. 2D-DOSY spectra were recorded on a NEO 600 spectrometer. The size of the FID was 32. The standard Bruker pulse program, ledbpgp2s, employing a stimulated echo sequence and 2 spoil gradient was utilized. The diffusion gradient level was 2% - 95% (GPZ6, maximum 95%); the gradient length (P30, the total gradient defocusing time) was 1000  $\mu s$ ; and the diffusion delay (D20) was 0.059999 s. Individual rows of the quasi-2-D diffusion databases were phased and baseline corrected.

### Section S1. Synthesis of $[Os^{II}(bpy)_2Cl_2]$ , bpy = 2,2 bipyridyl



[Os<sup>II</sup>(bpy)<sub>2</sub>Cl<sub>2</sub>] was synthesized according to a literature procedure.<sup>1</sup> In a 250 mL round-bottom flask, (NH<sub>4</sub>)<sub>2</sub>OsCl<sub>6</sub> (2.00 g, 4.55 mmol, 1.00 equiv) and bpy (1.44 g, 9.22 mmol, 2.03 equiv) in ethylene glycol (100 mL) were heated to reflux (200 °C) for 45 min under N<sub>2</sub>. After the reaction mixture cooled to room temperature, saturated aqueous sodium dithionite solution (100 mL) was added to reduce excess Os(III) to Os(II). After stirring for 30 minutes, the purple-black precipitate was isolated by filtration, washed with cold water (50 mL) to remove [Os(bpy)<sub>3</sub>]<sup>2+</sup> and other ionic products, and washed with diethyl ether (200 mL). The product was dried under dynamic vacuum overnight (2.1 g, 80% yield). <sup>1</sup>H NMR (400 MHz, DMSO-*d*<sub>6</sub>, 298 K) 9.67 – 9.61 (m, 2H), 8.58 – 8.51 (m, 2H), 8.33 (dd, *J* = 8.6, 1.5 Hz, 2H), 7.59 – 7.50 (m, 4H), 7.30 – 7.17 (m, 4H), 6.76 (ddd, *J* = 7.5, 6.0, 1.5 Hz, 2H); <sup>13</sup>C NMR (101 MHz, DMSO-*d*<sub>6</sub>, 298 K) δ 164.64, 162.06, 151.72, 151.38, 134.40, 132.12, 126.58, 126.18, 123.67, 122.72.

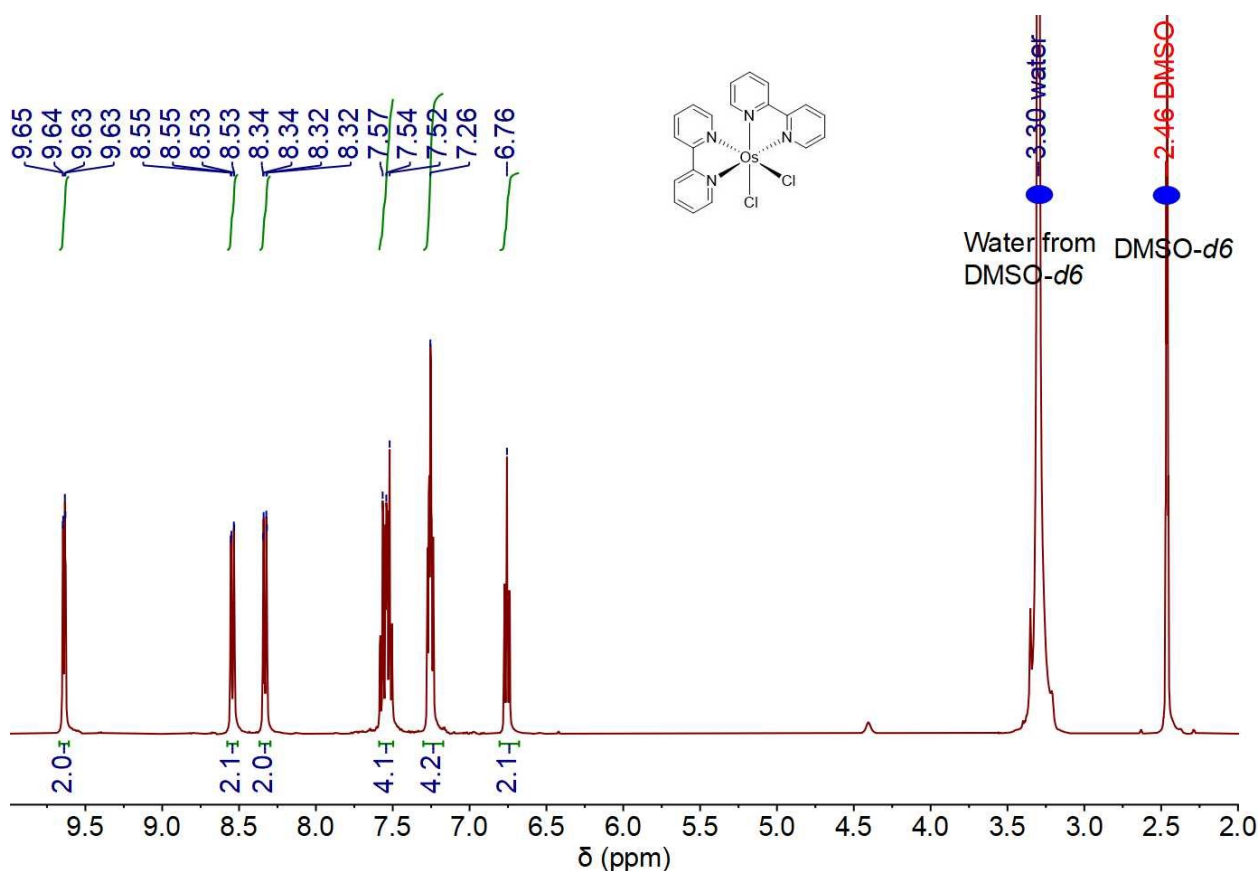


**Figure S1.** <sup>1</sup>H NMR spectrum of [Os<sup>II</sup>(bpy)<sub>2</sub>Cl<sub>2</sub>] (400 MHz, DMSO-*d*<sub>6</sub>, 298 K)

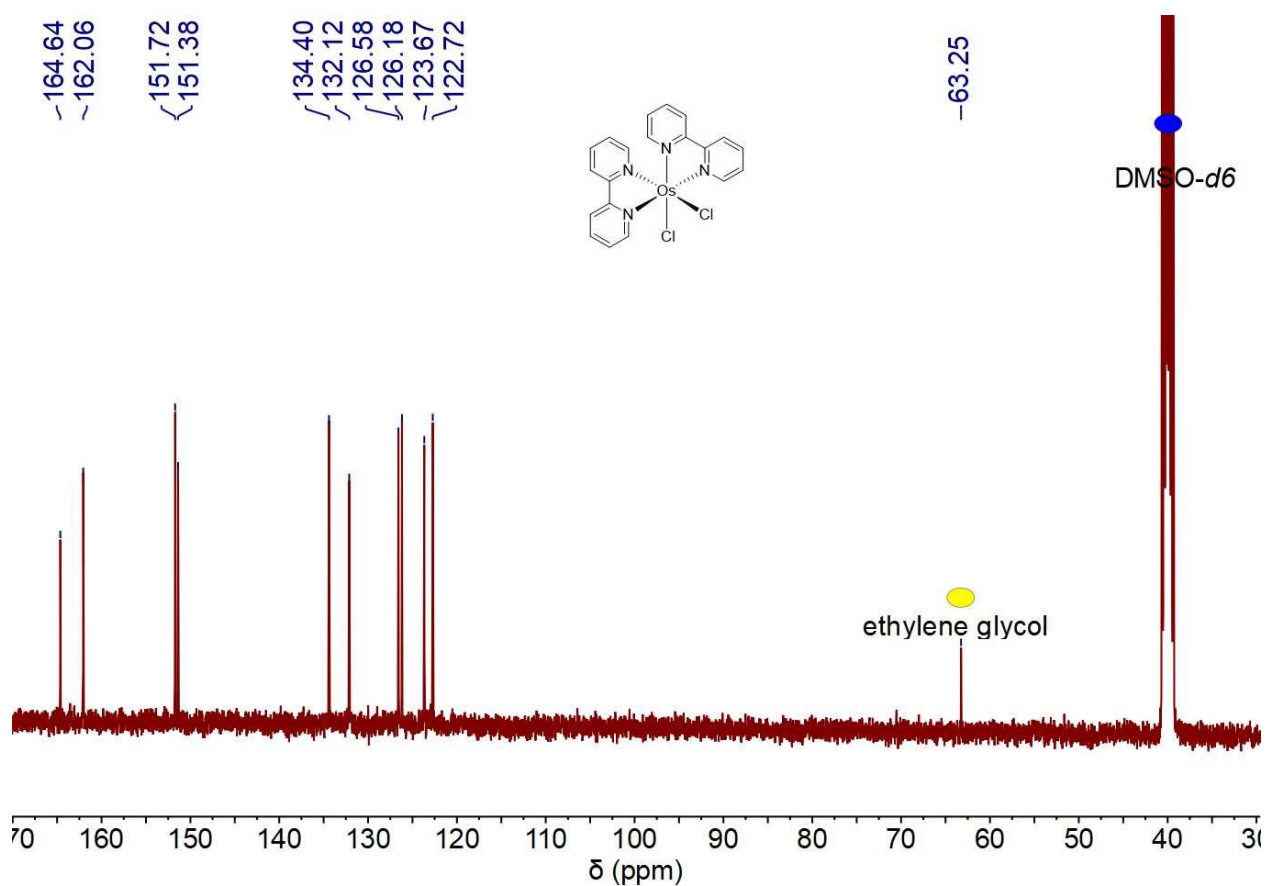


**Figure S2.**  $^{13}\text{C}$  NMR spectrum of  $[\text{Os}^{\text{II}}(\text{bpy})_2\text{Cl}_2]$  (101 MHz,  $\text{DMSO-}d_6$ , 298 K)

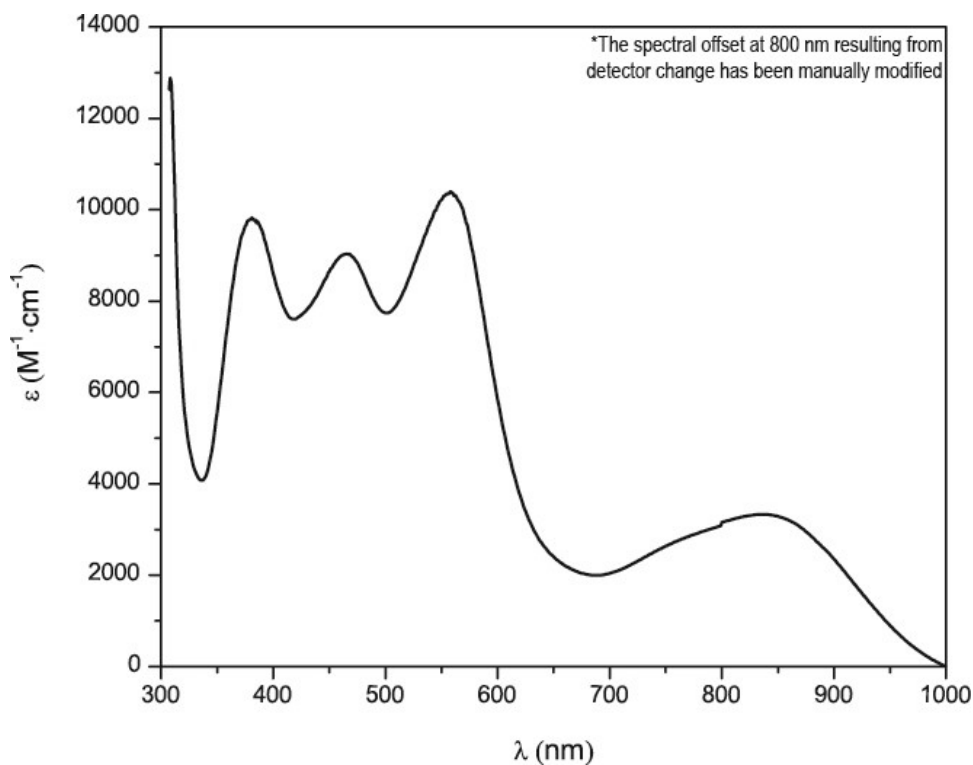


**Figure S3.** UV-Vis spectrum of  $[\text{Os}^{\text{II}}(\text{bpy})_2\text{Cl}_2]$  in  $\text{CH}_2\text{Cl}_2$ . Concentration of  $[\text{Os}(\text{bpy})_2\text{Cl}_2] = 0.39 \text{ mM}$ ;  $\lambda_{\text{max}}$ : 381 nm,  $9828 \text{ M}^{-1} \text{ cm}^{-1}$ ; 466 nm,  $9032 \text{ M}^{-1} \text{ cm}^{-1}$ ; 558 nm,  $10400 \text{ M}^{-1} \text{ cm}^{-1}$ ; 836 nm,  $3328 \text{ M}^{-1} \text{ cm}^{-1}$ .

Data recorded matches data from the literature.<sup>1</sup> \*The data points between 800 nm and 1000 nm were manually adjusted by lowering them to align with the data point at 799 nm.

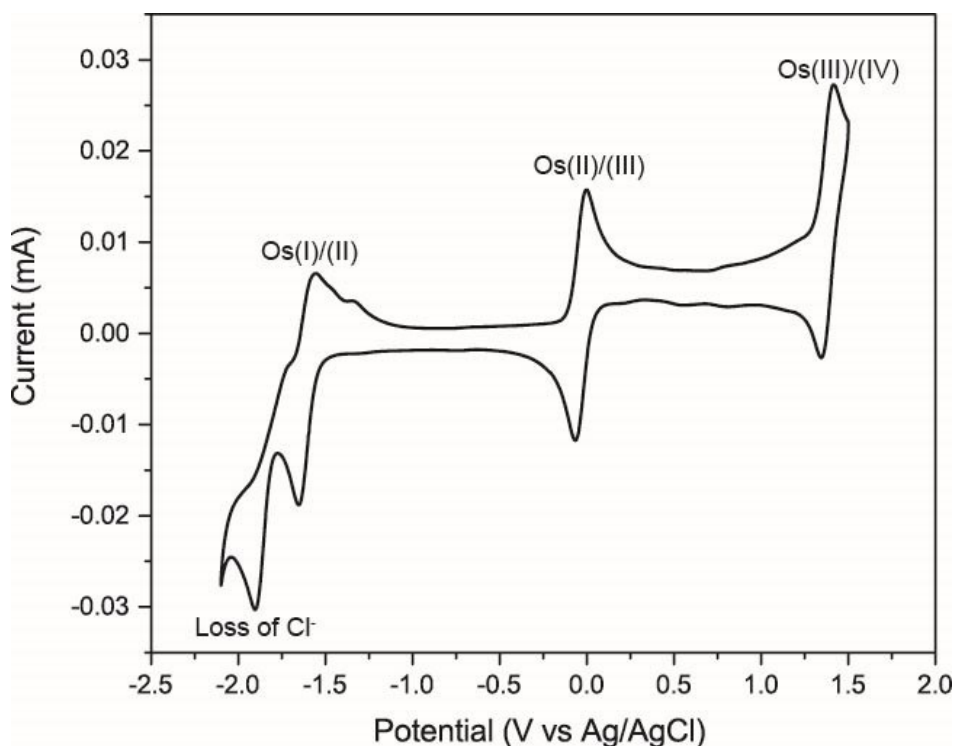
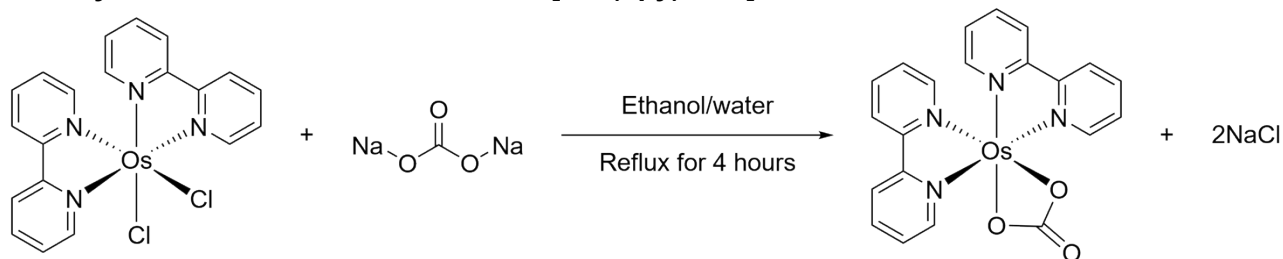


**Figure S4.** CV traces of  $[\text{Os}(\text{bpy})_2\text{Cl}_2]$  in MeCN with 0.1 M tetrabutylammonium perchlorate (TBAP) as the electrolyte. Concentration of  $[\text{Os}(\text{bpy})_2\text{Cl}_2] = 2 \text{ mM}$ ; scan rate = 200 mV/s. Reversible waves at  $-1.604 \text{ V vs Ag/AgCl}$  ( $\text{Os}^{\text{I/II}}$ ),  $-0.034 \text{ V vs Ag/AgCl}$  ( $\text{Os}^{\text{II/III}}$ ) and  $1.381 \text{ V vs Ag/AgCl}$  ( $\text{Os}^{\text{III/IV}}$ ) and irreversible wave at  $-1.903 \text{ V vs Ag/AgCl}$  (Loss of  $\text{Cl}^-$ ).<sup>1</sup> \* $\text{N}_2$  must be purged into the electrochemical cell to remove dissolved  $\text{O}_2$  in MeCN.

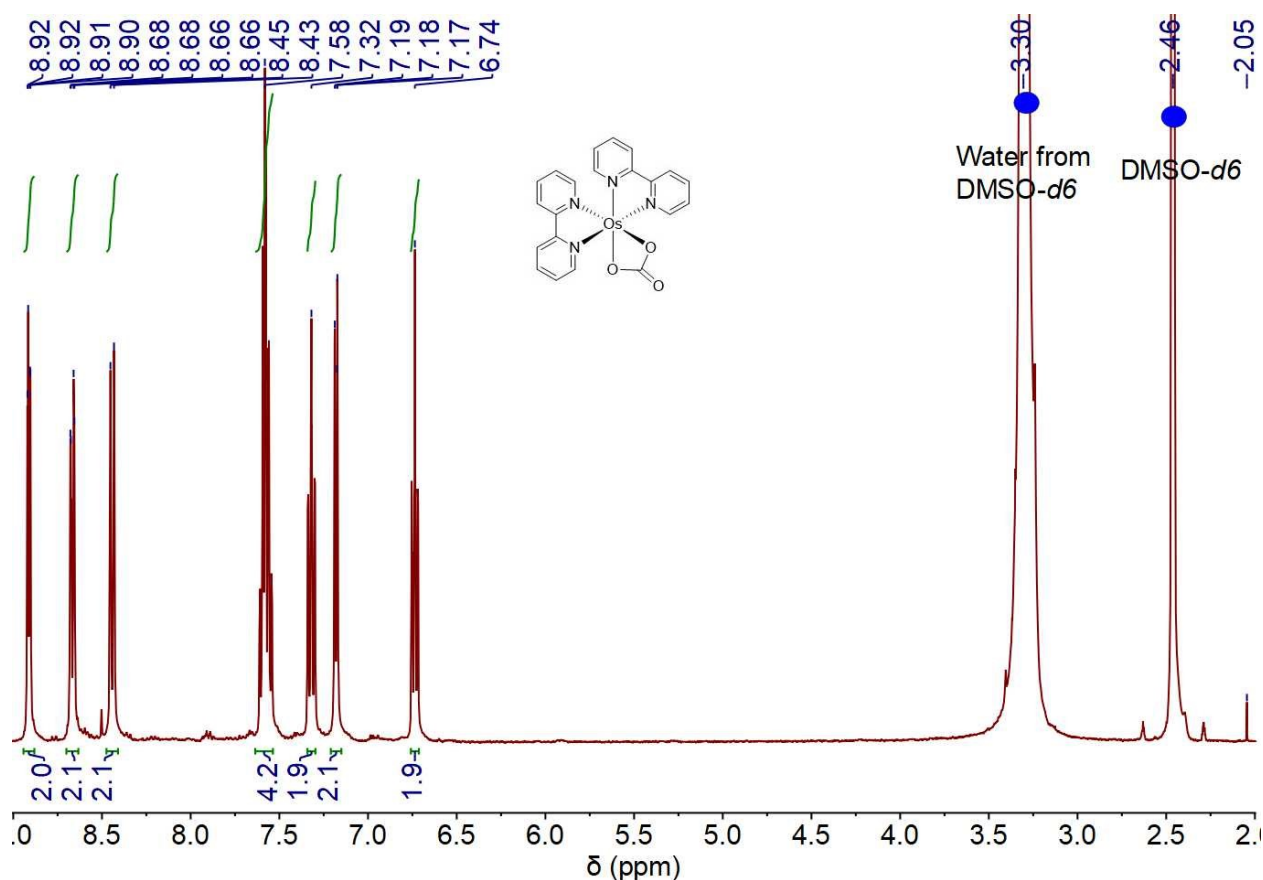
## Section S2. Synthesis of $[\text{Os}^{\text{II}}(\text{bpy})_2\text{CO}_3]$ , bpy = 2,2 bipyridyl

### S2.1 Synthesis and characterization of $[\text{Os}^{\text{II}}(\text{bpy})_2\text{CO}_3]$

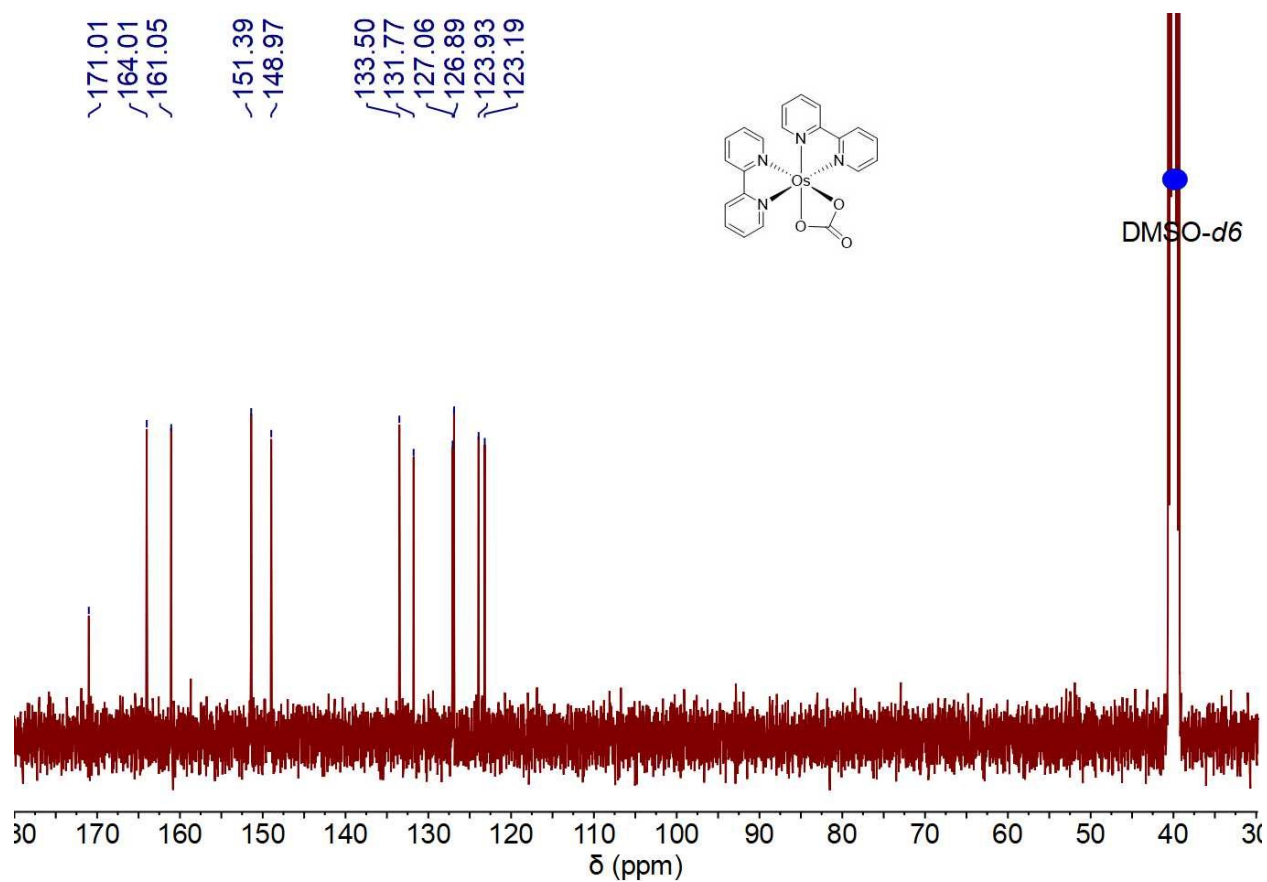


$[\text{Os}^{\text{II}}(\text{bpy})_2\text{CO}_3]$  was synthesized according to a modified literature procedure.<sup>2</sup> In a 250 mL round-bottom flask,  $[\text{Os}(\text{bpy})_2\text{Cl}_2]$  (2.50 g, 3.34 mmol, 1.00 equiv) was dissolved in ethanol (55 mL). Concentrated aqueous solution of sodium carbonate (0.25 M, 110 mL, 27.5 mmol, 8.23 equiv) was then added. The mixture was heated to reflux under  $\text{N}_2$  for 2 hours. After the reaction mixture cooled to room temperature, solid sodium carbonate (16.5 g, 155.7 mmol, 46.62 equiv) was added to the

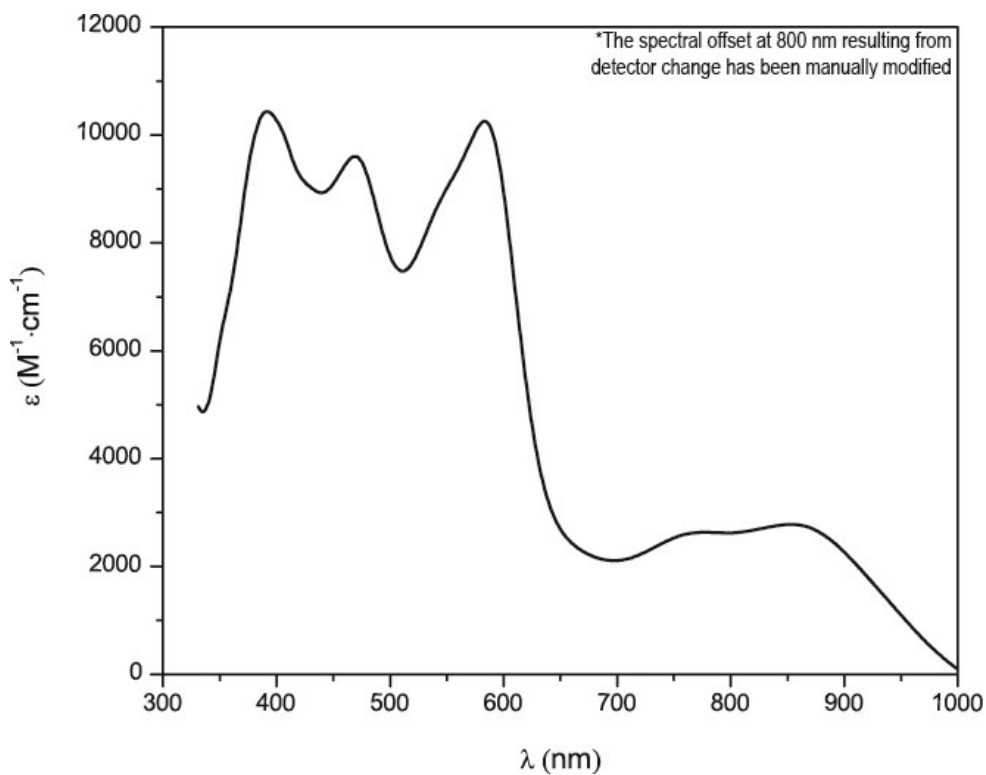
solution. The mixture was heated again to reflux for 2 hours under  $N_2$ . After the reaction mixture cooled to room temperature, the ethanol was removed under reduced pressure, affording a black precipitate which was collected by filtration and washed with sodium hydroxide solution (100 mL,  $pH > 9$ ) and then with diethyl ether (100 mL). The black solid was dried at room temperature under dynamic vacuum overnight (1.6 g, 85% yield).  $^1H$  NMR (400 MHz,  $DMSO-d_6$ , 298 K)  $\delta$  8.94 – 8.88 (m, 2H), 8.70 – 8.63 (m, 2H), 8.44 (dt,  $J = 8.2, 1.2$  Hz, 2H), 7.58 (pd,  $J = 7.4, 1.8$  Hz, 4H), 7.32 (ddd,  $J = 8.4, 7.3, 1.3$  Hz, 2H), 7.18 (dt,  $J = 6.0, 1.1$  Hz, 2H), 6.74 (ddd,  $J = 7.3, 6.0, 1.4$  Hz, 2H);  $^{13}C$  NMR (101 MHz,  $DMSO-d_6$ , 298 K)  $\delta$  171.01, 164.01, 161.05, 151.39, 148.97, 133.50, 131.77, 127.06, 126.89, 123.93, 123.19.



**Figure S5.**  $^1H$  NMR spectrum of  $[Os^{II}(bpy)_2CO_3]$  (400 MHz,  $DMSO-d_6$ , 298 K)

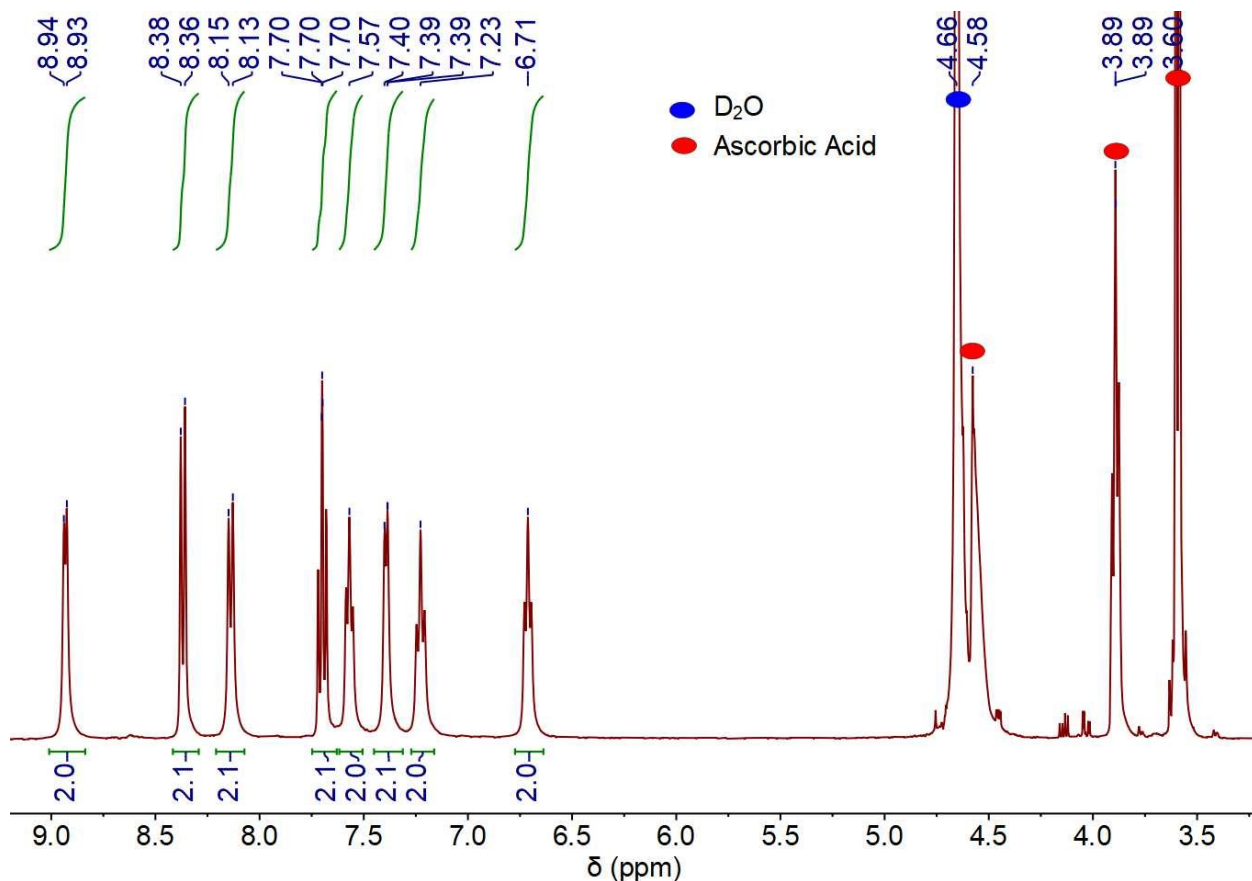


**Figure S6.**  $^{13}\text{C}$  NMR spectrum of  $[\text{Os}^{\text{II}}(\text{bpy})_2\text{CO}_3]$  (101 MHz, DMSO- $d_6$ , 298 K)

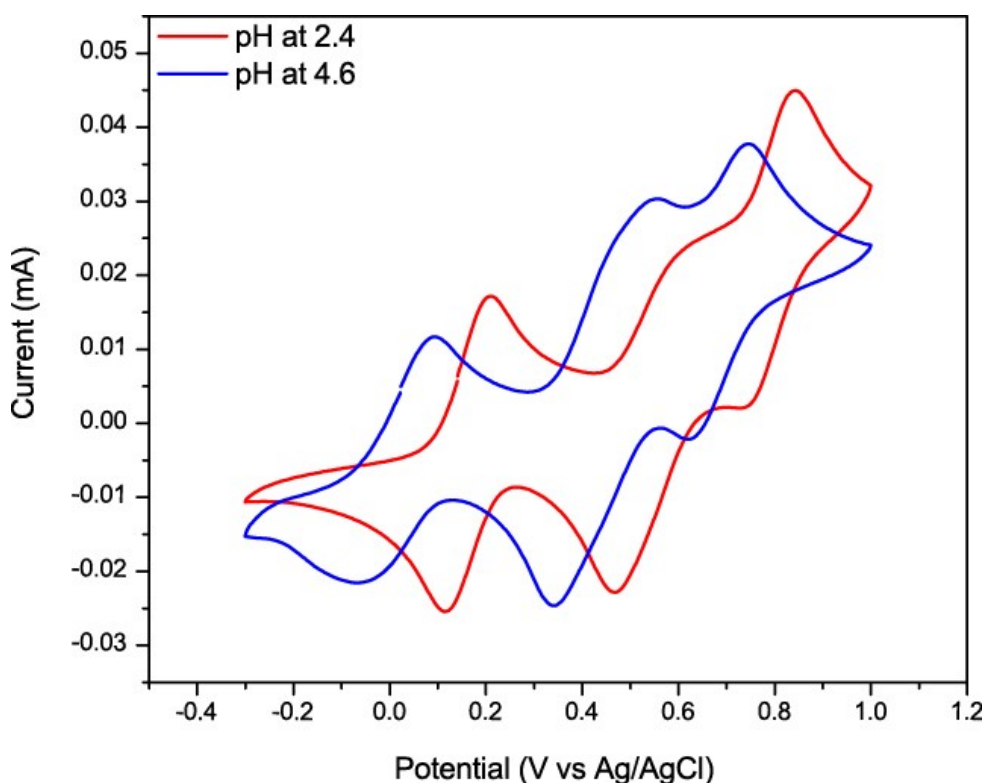


**Figure S7.** UV-Vis spectrum of  $[\text{Os}^{\text{II}}(\text{bpy})_2\text{CO}_3]$  in  $\text{CH}_2\text{Cl}_2$ . Concentration of  $[\text{Os}^{\text{II}}(\text{bpy})_2\text{CO}_3]$  = 0.284 mM;  $\lambda_{\text{max}}$ : 391 nm, 10436  $\text{M}^{-1} \text{cm}^{-1}$ ; 469 nm, 9604  $\text{M}^{-1} \text{cm}^{-1}$ ; 583 nm, 10255  $\text{M}^{-1} \text{cm}^{-1}$ ; 854 nm, 2780  $\text{M}^{-1}$

cm<sup>-1</sup>. Data recorded matches with data from literature.<sup>1</sup> \*The data points between 800 nm and 1000 nm were manually adjusted by lowering them to align with the data point at 799 nm.



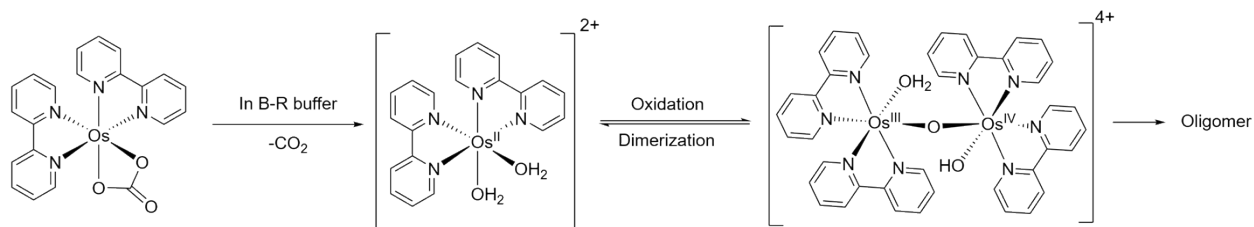
**Figure S8.** <sup>1</sup>H NMR spectrum of [Os<sup>II</sup>(bpy)<sub>2</sub>(OH<sub>2</sub>)<sub>2</sub>]<sup>2+</sup> resulting from [Os<sup>II</sup>(bpy)<sub>2</sub>CO<sub>3</sub>] in ascorbic acid solution (2 equiv). <sup>1</sup>H NMR (400 MHz, D<sub>2</sub>O, 298K) δ 8.93 (d, *J* = 5.7 Hz, 2H), 8.37 (d, *J* = 8.2 Hz, 2H), 8.14 (d, *J* = 8.2 Hz, 2H), 7.70 (ddd, *J* = 8.8, 7.8, 1.4 Hz, 2H), 7.57 (t, *J* = 6.5 Hz, 2H), 7.45 – 7.31 (m, 2H), 7.23 (t, *J* = 7.8 Hz, 2H), 6.71 (t, *J* = 6.8 Hz, 2H).



**Figure S9.** CV traces of  $[\text{Os}^{\text{II}}(\text{bpy})_2(\text{OH}_2)_2]^{2+}$  resulting from  $[\text{Os}^{\text{II}}(\text{bpy})_2\text{CO}_3]$  in 0.01 M aqueous  $\text{HBF}_4$ . Concentration of  $[\text{Os}^{\text{II}}(\text{bpy})_2\text{CO}_3] = 2 \text{ mM}$ ; scan rate = 100 mV/s. At pH 2.4: reversible waves at 0.162 V vs Ag/AgCl ( $\text{Os}^{\text{III}}$ ), 0.524 V vs Ag/AgCl ( $\text{Os}^{\text{III/IV}}$ ) and 0.792 V vs Ag/AgCl ( $\text{Os}^{\text{III/IV}}$ ).<sup>2</sup>

### S2.2 Dimerization and Oligomerization of $[\text{Os}^{\text{II}}(\text{bpy})_2(\text{OH}_2)_2]^{2+}$

$[\text{Os}^{\text{II}}(\text{bpy})_2(\text{OH}_2)_2]^{2+}$  is in equilibrium with its dimer in Britton–Robinson buffer (B-R buffer) which is an aqueous solution of a mixture of 0.04 M boric acid, 0.04 M phosphoric acid and 0.04 M acetic acid that has been titrated to the desired pH with 0.2 M sodium hydroxide.  $[\text{Os}^{\text{II}}(\text{bpy})_2(\text{OH}_2)_2]^{2+}$  is readily oxidized by air and dimerizes to form  $[(\text{bpy})_2(\text{OH}_2)\text{Os}^{\text{III}}\text{OOs}^{\text{IV}}(\text{OH})(\text{bpy})_2]^{4+}$  followed by oligomerization; therefore, avoiding oligomers formation is important to maximizing the yield of  $[\text{Os}(\text{bpy})_2(\text{OH}_2)(\text{py})](\text{PF}_6)_2$ .<sup>2,3</sup>



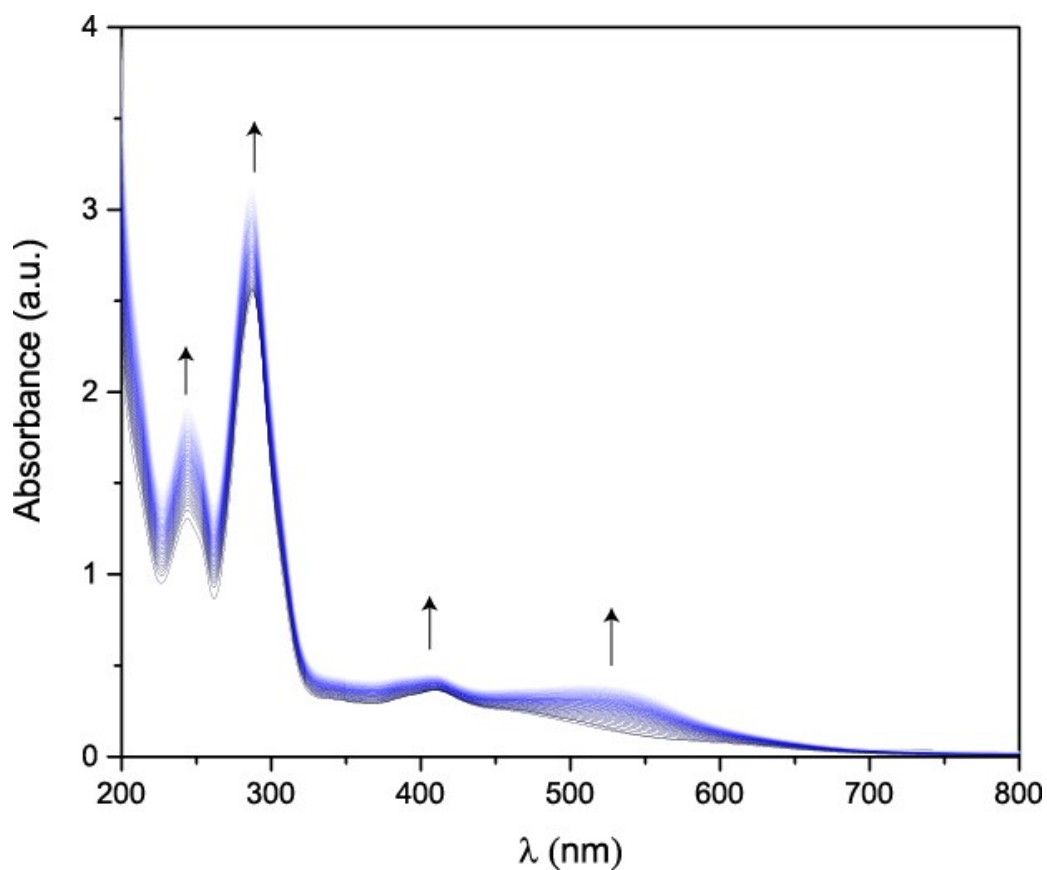


**Figure S10.** UV-Vis spectra of  $[\text{Os}(\text{bpy})_2(\text{OH}_2)_2]^{2+}$  in B-R buffer at pH=6.78 to illustrate the instability of the diwater adduct. Concentration of  $[\text{Os}(\text{bpy})_2(\text{OH}_2)_2]^{2+} = 0.74$  mM; Each UV-Vis measurement was taken at half-hour intervals, with a total monitoring time of 20 hours. The growth of the peak at 513 nm corresponds to the formation of the dinuclear  $[(\text{bpy})_2(\text{OH}_2)\text{Os}^{\text{III}}\text{O}(\text{OH})\text{Os}^{\text{IV}}(\text{OH})(\text{bpy})_2]^{4+}$ .<sup>3</sup>

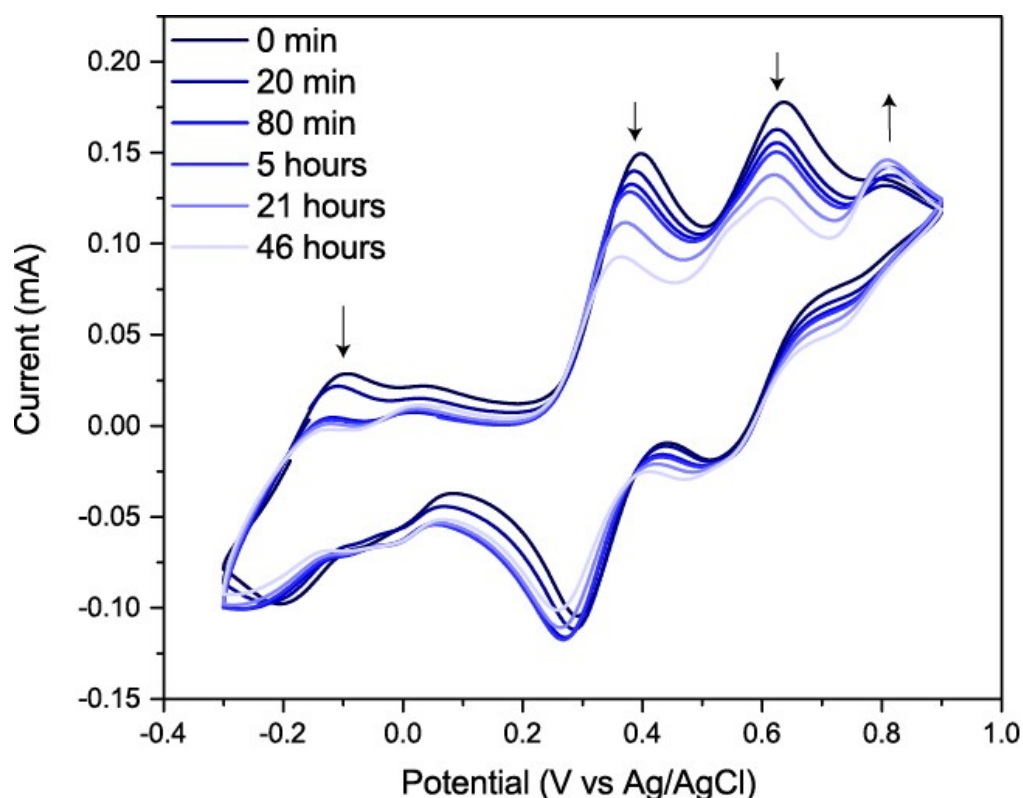
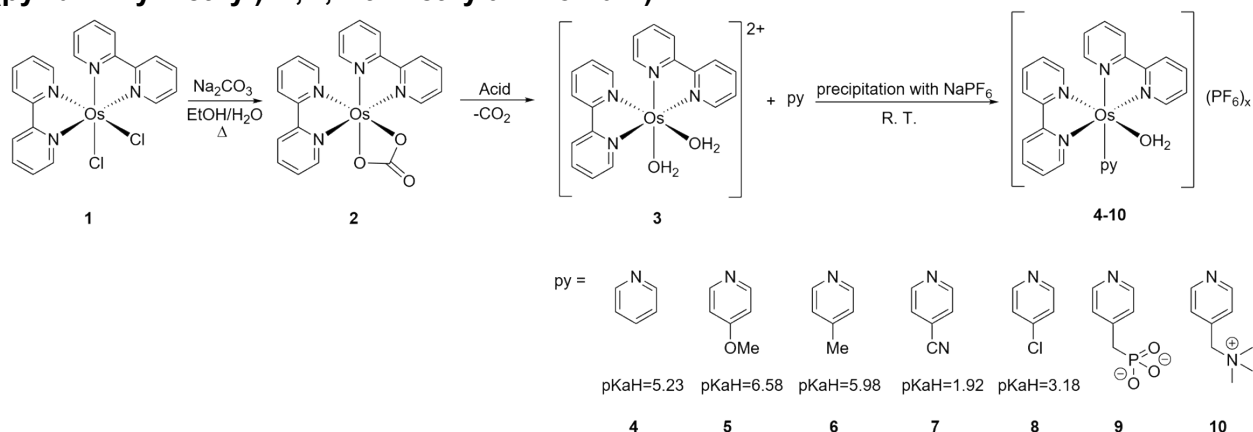


**Figure S11.** CV traces of  $[\text{Os}^{\text{II}}(\text{bpy})_2(\text{OH}_2)_2]^{2+}$  resulting from  $[\text{Os}^{\text{II}}(\text{bpy})_2\text{CO}_3]$  in B-R buffer at pH=6.80. Concentration of  $[\text{Os}^{\text{II}}(\text{bpy})_2(\text{OH}_2)_2]^{2+} = 17 \text{ mM}$ ; scan rate = 100 mV/s. Loss of peaks for  $[\text{Os}^{\text{II}}(\text{bpy})_2(\text{OH}_2)_2]^{2+}$  suggests the formation of oligomers.

**Section S3. Synthesis of  $[\text{Os}(\text{bpy})_2(\text{OH}_2)(\text{py}^{\text{L}})](\text{PF}_6)_x$  ( $\text{py}^{\text{L}} = \text{pyridine, 4-methoxypyridine, 4-methylpyridine, 4-cyanopyridine, 4-chloropyridine, 4-pyridylmethylphosphonic acid, 4-N-(pyridin-4-ylmethyl)-N,N,N-trimethylammonium}$ )**



**S3.1 Determination of the impurity peaks in Figure 2A and pyridinium salt**

We hypothesize that the impurity peaks 0.15 and 0.57 V in Figure 2A correspond to  $[\text{Os}^{\text{II}}(\text{bpy})_2(\text{py})(\text{Cl})]^+$  and  $[\text{Os}^{\text{II}}(\text{bpy})_2(\text{py})_2]^{2+}$ , respectively. To test our hypothesis, we added NaCl and

pyridine to a 2 mM B-R buffer solution of  $[\text{Os}(\text{bpy})_2(\text{OH}_2)(\text{py})](\text{PF}_6)_2$  (py=pyridine) and monitored the change CV traces.

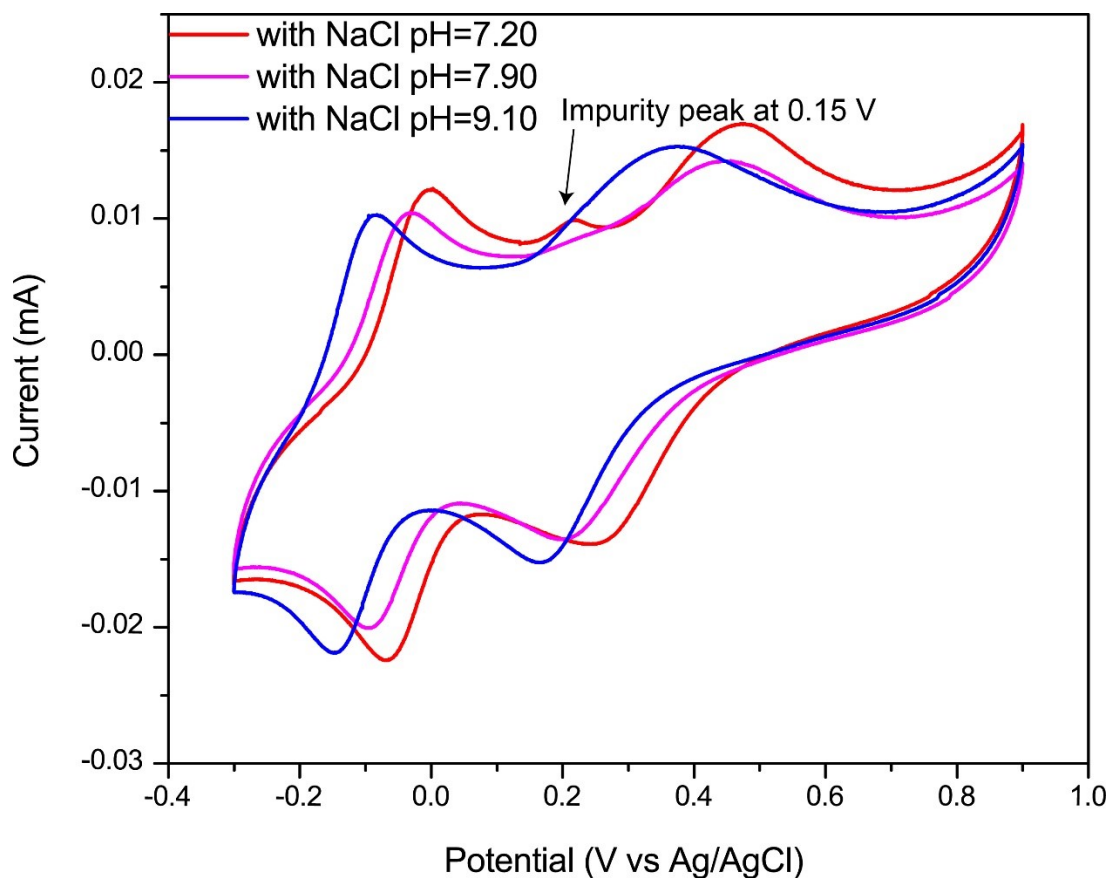


**Figure S12.** CV traces of  $[\text{Os}(\text{bpy})_2(\text{OH}_2)(\text{py})](\text{PF}_6)_2$  (py=pyridine) in B-R buffer with NaCl (500 equiv) at room temperature with stirring for 12 hours. Concentration of  $[\text{Os}(\text{bpy})_2(\text{OH}_2)(\text{py})](\text{PF}_6)_2 = 2 \text{ mM}$ ; scan rate = 100 mV/s.

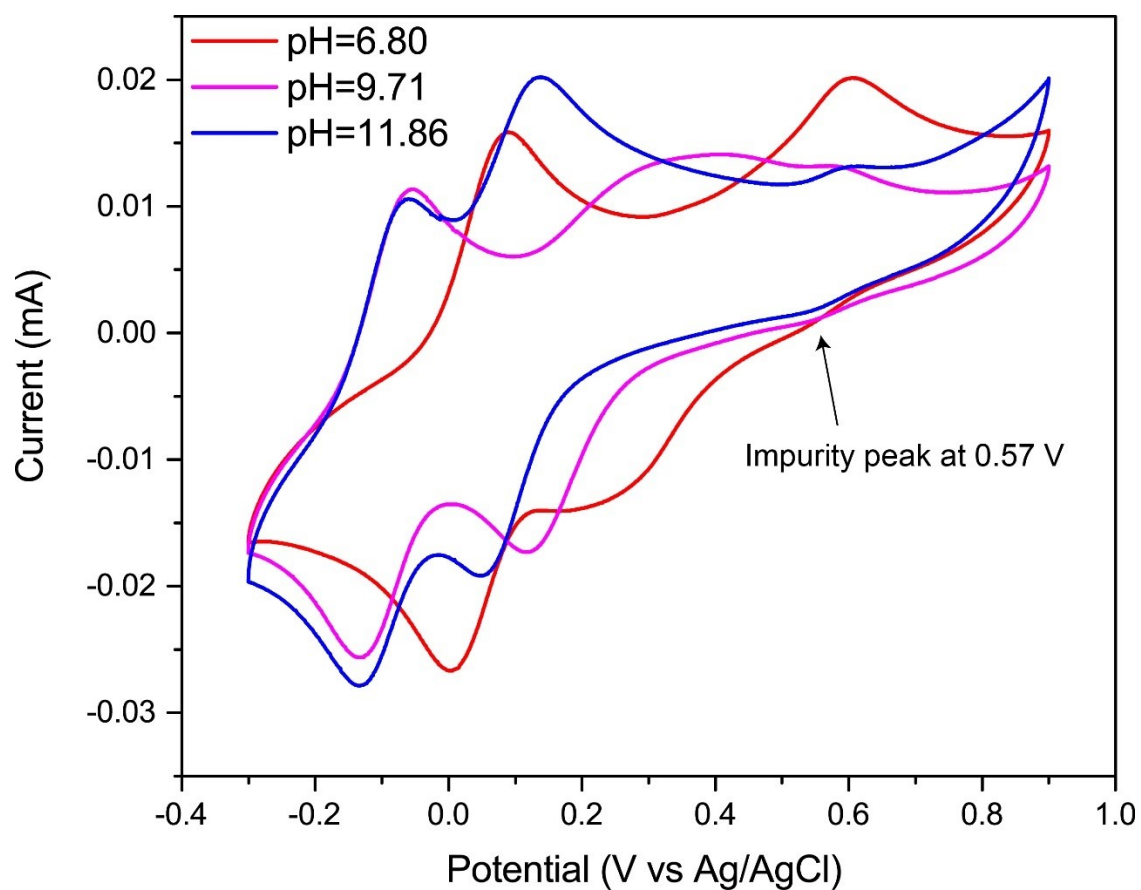


**Figure S13.** CV traces of  $[\text{Os}(\text{bpy})_2(\text{OH}_2)(\text{py})](\text{PF}_6)_2$  (py=pyridine) in B-R buffer with pyridine (200 equiv) at 50 °C heating with stirring for 12 hours. Concentration of  $[\text{Os}(\text{bpy})_2(\text{OH}_2)(\text{py})](\text{PF}_6)_2 = 2$  mM; scan rate = 100 mV/s.

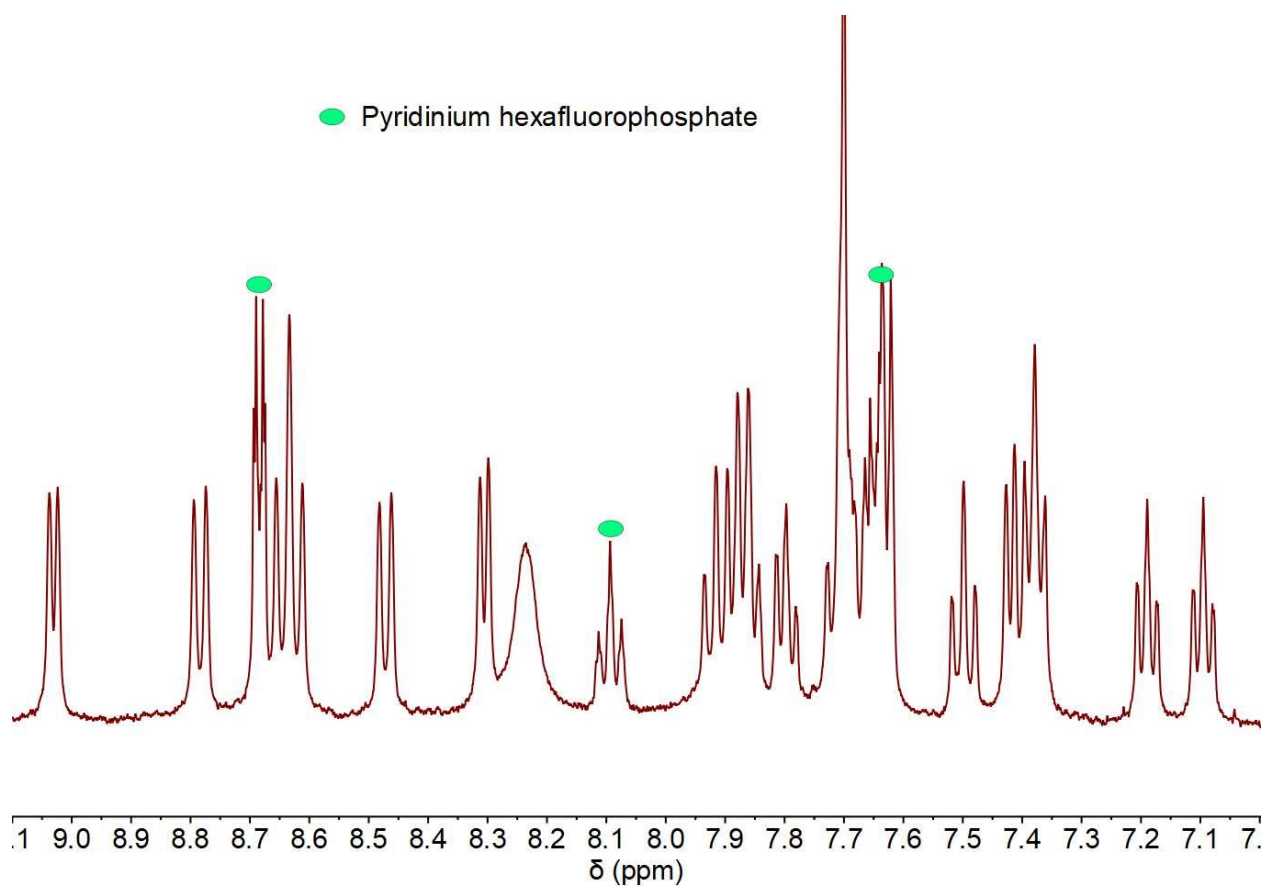


**Figure S14.** <sup>1</sup>H NMR spectrum of [Os(bpy)<sub>2</sub>(OH<sub>2</sub>)(py)](PF<sub>6</sub>)<sub>2</sub> (py=pyridine) mixed with pyridinium hexafluorophosphate (400 MHz, DMSO, 298 K).

### S3.2 Choice of solvent systems

B-R buffer (pH 6.8) was identified as an ideal reaction medium as opposed to 0.1 M H<sub>2</sub>SO<sub>4</sub> due to suppressed formation of disubstituted pyridine [Os<sup>II</sup>(bpy)<sub>2</sub>(py)<sub>2</sub>] and other impurities.

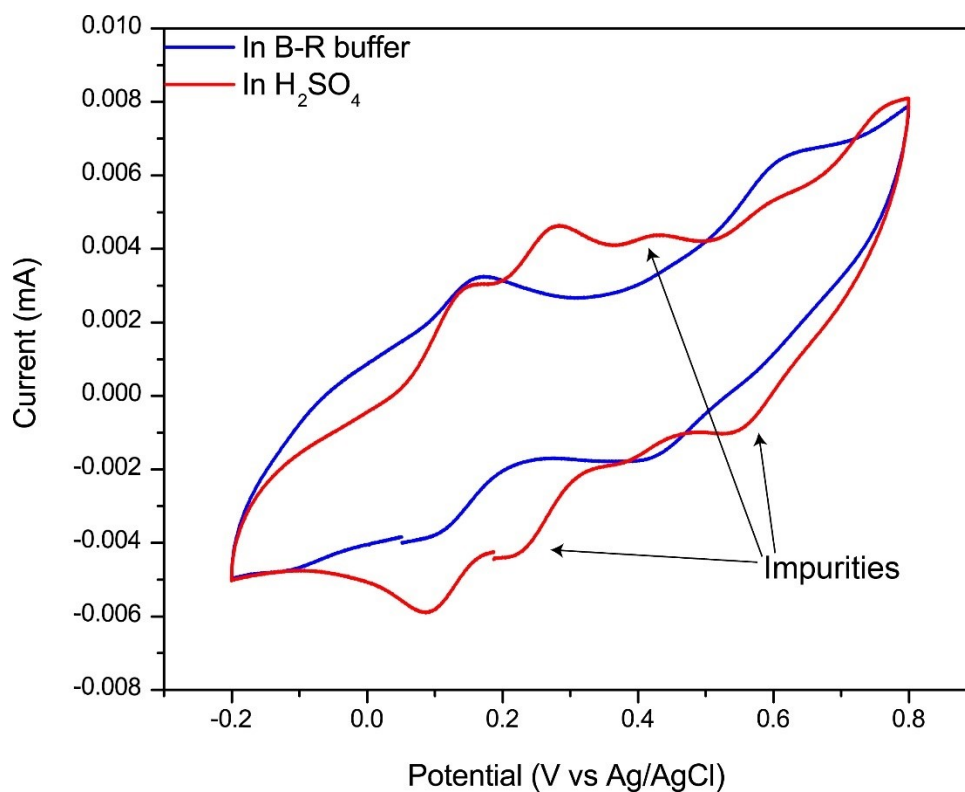


**Figure S15.** CVs traces of the product,  $[\text{Os}(\text{bpy})_2(\text{OH}_2)(\text{py})](\text{PF}_6)_2$  (py=pyridine), in B-R buffer (pH=5.50) made from different solvents systems: B-R buffer (pH=6.80) and 0.1 M  $\text{H}_2\text{SO}_4$  (pH=6.80 which was titrated with 0.1 M NaOH).

### S3.3 Choice of precipitation agents

We replaced  $\text{NH}_4\text{PF}_6$  with  $\text{NaPF}_6$  as the precipitation agent to avoid additional byproducts which we hypothesize to arise from  $\text{NH}_3$  coordination to the osmium center. At pH 6.8,  $\text{NH}_4^+$  and  $\text{NH}_3$  are in equilibrium ( $\text{NH}_4^+$   $pK_a = 9.24$ ) and ammonia complexes of osmium are precededented.<sup>4-6</sup>

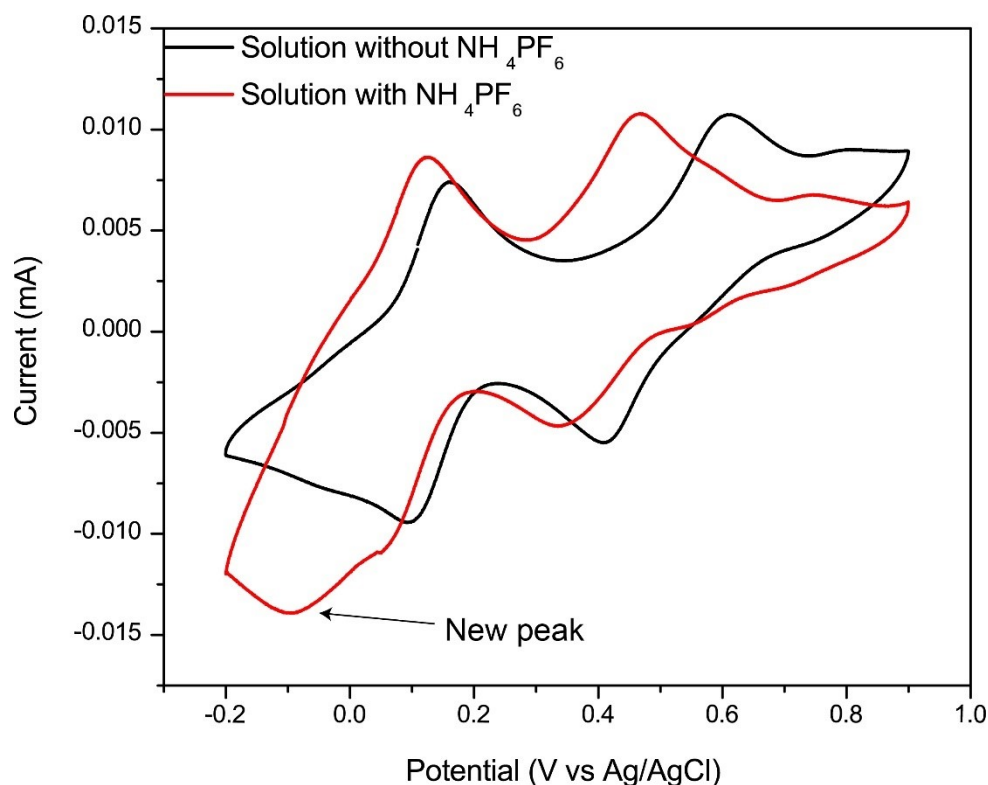


**Figure S16.** CV traces of  $[\text{Os}(\text{bpy})_2(\text{OH}_2)(\text{py})](\text{PF}_6)_2$  ( $\text{py}=\text{pyridine}$ ) in B-R buffer without and with  $\text{NH}_4\text{PF}_6$  (100 equiv). Concentration of  $[\text{Os}(\text{bpy})_2(\text{OH}_2)(\text{py})](\text{PF}_6)_2 = 1 \text{ mM}$ ; scan rate = 100 mV/s.

### S3.4 Synthesis of $[\text{Os}(\text{bpy})_2(\text{OH}_2)(\text{py}^L)](\text{PF}_6)_2$ ( $\text{py}^L=\text{pyridine}$ , 4-methoxypyridine, 4-methylpyridine)

General procedure for the synthesis of parent pyridine and electron-donating pyridine derivatives 4-methoxypyridine, 4-methylpyridine: In a 10 mL round-bottom flask, pH 3.5 B-R buffer (5 mL) was added to  $\text{Os}(\text{bpy})_2\text{CO}_3$  (47.9 mg, 0.0850 mmol, 1.00 equiv). Pyridine (around 23 equiv) was added to the mixture with stirring and the pH of the solution was adjusted to 6.8. After the solution stirred for 20 min, the pH was adjusted to 5.5 and solid  $\text{NaPF}_6$  (200 mg, 1.19 mmol, 7.00 equiv) was added, affording a black precipitate. The black precipitate aggregated to form a large black ball-like solid (consisting of the product, pyridinium hexafluorophosphate salt and residual pyridine). The ball-like solid was filtered, washed with cold water (5 mL) and dried under dynamic vacuum overnight (to remove residual pyridine). The dried ball-like solid was suspended in diethyl ether (25 mL) and vigorously stirred for 1 day to break down the material into smaller particles. The black solid was collected via vacuum filtration and washed with diethyl ether (25 mL). 2-Propanol (10 mL) was added to the solid and the suspension was sonicated for 10 min to remove the pyridinium hexafluorophosphate salt. The black-yellow solid was filtered, washed with 2-propanol (5 mL), diethyl ether (20 mL), and then dried at room temperature under dynamic vacuum overnight (yields: parent pyridine  $67\pm 11\%$ ; 4-methoxypyridine  $57\pm 5\%$ ; 4-methylpyridine  $36\pm 8\%$ ).

**Parent pyridine (4):**  $^1\text{H}$  NMR (400 MHz,  $\text{D}_2\text{O}$ , 298 K)  $\delta$  8.94 (ddd,  $J = 5.7, 1.5, 0.8$  Hz, 1H), 8.42 (dt,  $J = 8.2, 1.2$  Hz, 1H), 8.36 (ddd,  $J = 5.8, 1.5, 0.7$  Hz, 1H), 8.33 – 8.12 (m, 4H), 8.08 (ddd,  $J = 8.4, 1.5, 0.8$  Hz, 1H), 7.76 – 7.55 (m, 5H), 7.55 – 7.44 (m, 2H), 7.40 (ddd,  $J = 7.4, 5.8, 1.4$  Hz, 1H), 7.31 (ddd,  $J = 8.2, 7.6, 1.4$  Hz, 1H), 7.19 – 7.06 (m, 2H), 6.94 (ddd,  $J = 7.4, 5.8, 1.3$  Hz, 1H), 6.86 (ddd,  $J = 7.5, 5.9, 1.4$  Hz, 1H). Elemental analysis: found: C 33.85%, H 2.63%, N 6.85%; calcd. for  $\text{C}_{25}\text{H}_{23}\text{N}_5\text{OOSF}_{12}\text{P}_2$ , C 33.75%, H 2.61%, N 7.87%. FTIR:  $\nu_{\text{max}}$  3565  $\text{cm}^{-1}$ .

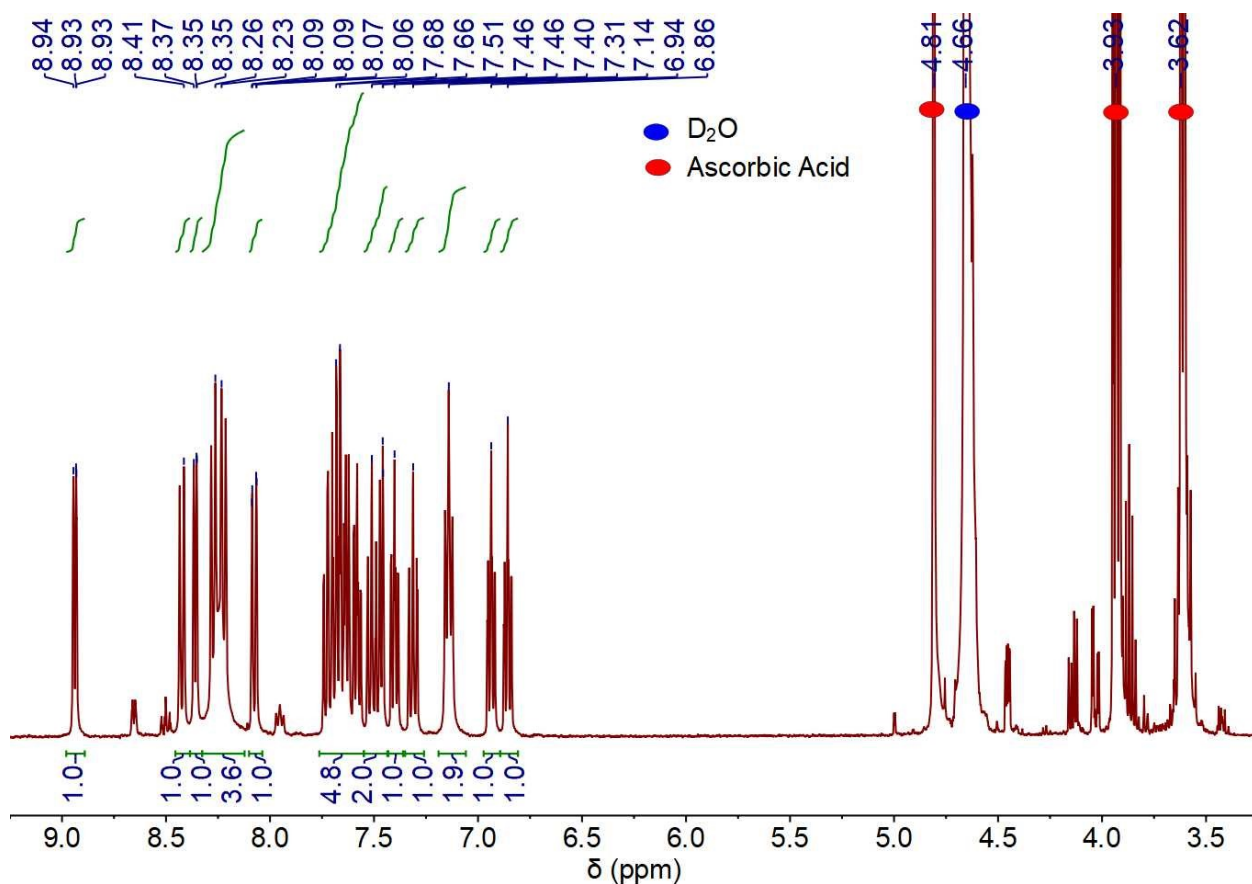


**Figure S17.**  $^1\text{H}$  NMR spectrum of  $[\text{Os}(\text{bpy})_2(\text{OH}_2)(\text{py})](\text{PF}_6)_2$  ( $\text{py}=\text{pyridine}$ ) (400 MHz,  $\text{D}_2\text{O}$ , 298 K). Ascorbic acid (around 5 equiv) was added to the NMR solvent to reduce paramagnetic Os(III) to Os(II) to improve the quality of the spectrum.

### S3.4.1 Oxidation of $[\text{Os}(\text{bpy})_2(\text{OH}_2)(\text{py})](\text{PF}_6)_2$

The product,  $[\text{Os}(\text{bpy})_2(\text{OH}_2)(\text{py})](\text{PF}_6)_2$ , was found to be slowly oxidized to higher Os oxidation states in the presence of air which was confirmed by UV-Vis monitoring and open circuit potential (OCV) measurements.<sup>7</sup>

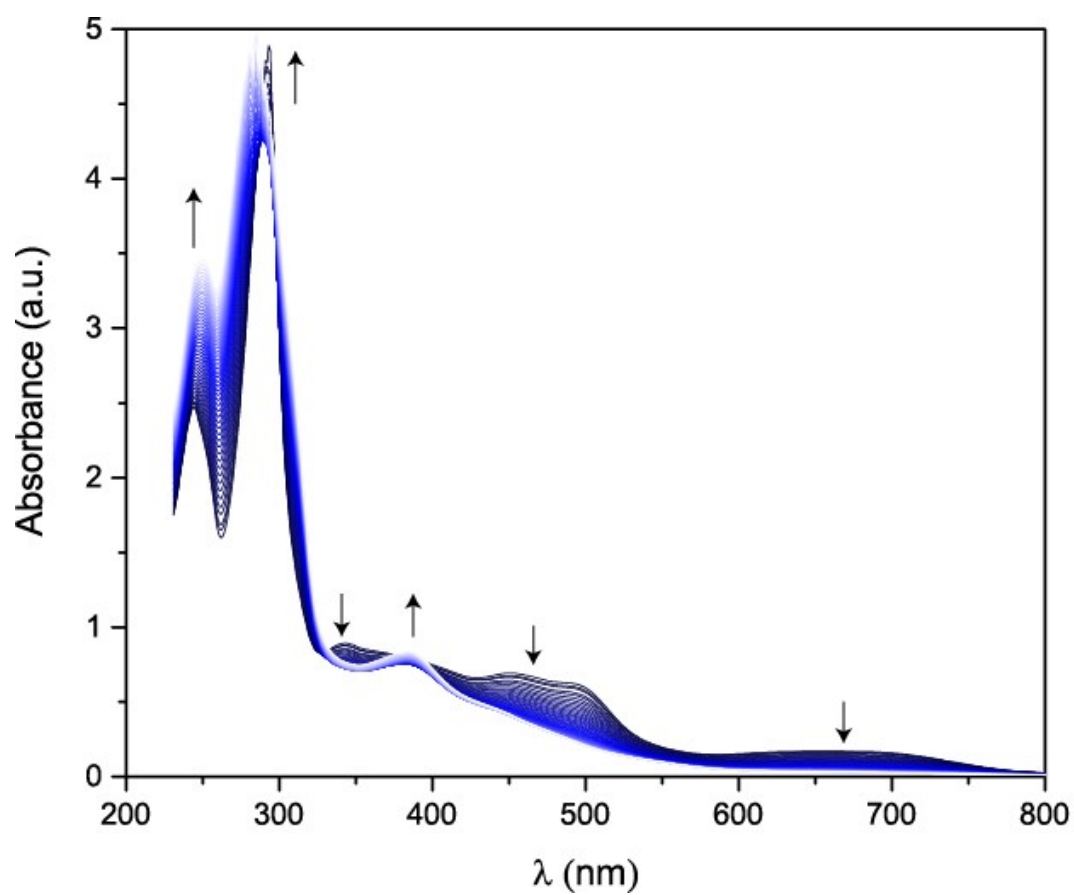


**Figure S18.** UV-Vis spectra of  $[\text{Os}(\text{bpy})_2(\text{OH}_2)(\text{py})](\text{PF}_6)_2$  (py=pyridine) in B-R buffer open to air at pH=6.80. Concentration of  $[\text{Os}(\text{bpy})_2(\text{OH}_2)(\text{py})](\text{PF}_6)_2 = 0.65$  mM; Each UV-Vis measurement was taken at half-hour intervals, with a total monitoring time of 24 hours.

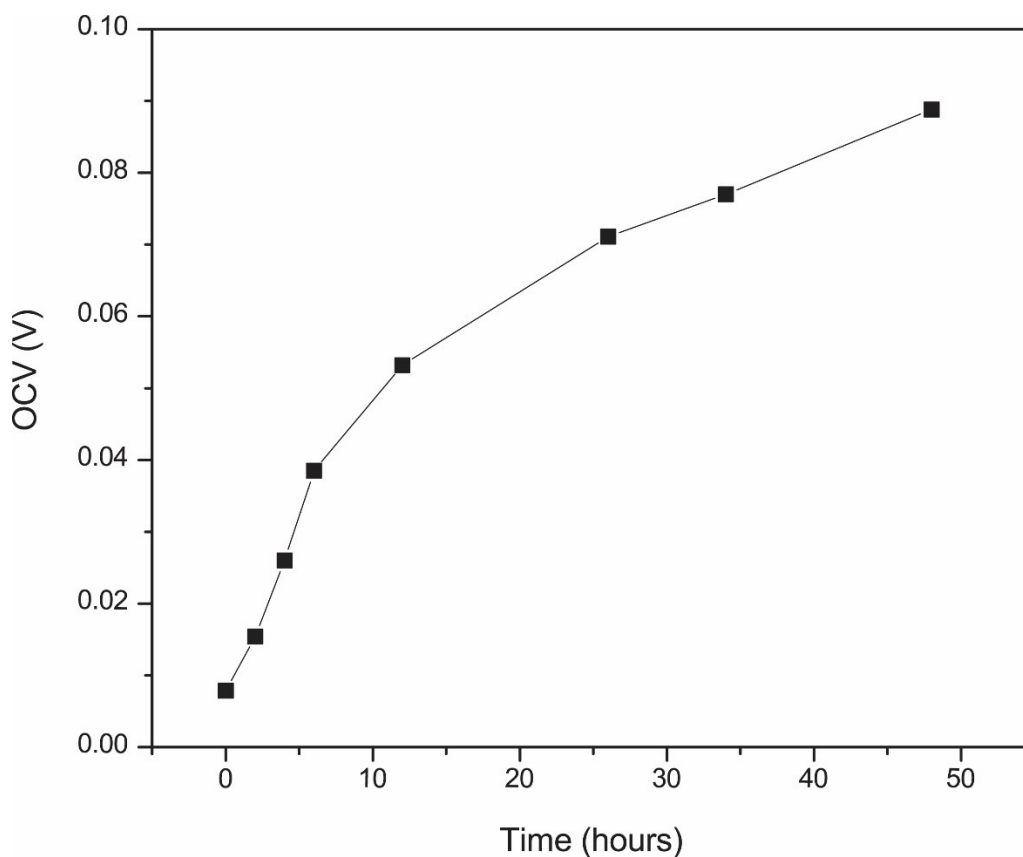


**Figure S19.** Open circuit voltage (OCV) measurements of  $[\text{Os}(\text{bpy})_2(\text{OH}_2)(\text{py})](\text{PF}_6)_2$  ( $\text{py}=\text{pyridine}$ ) in B-R buffer open to air at  $\text{pH}=6.80$ . Concentration = 2 mM.

Although Os(II) was found to be slowly be oxidized, the CV traces of the solution remain unchanged implying the oxidation of the complex by air is reversible.

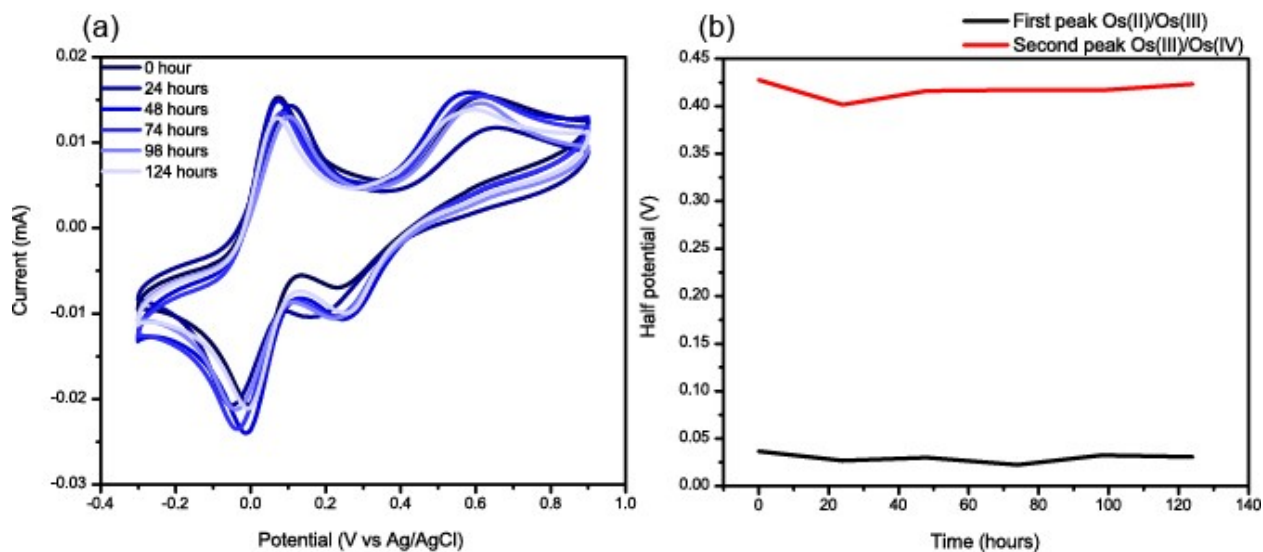


**Figure S20.** (a) CV traces of  $[\text{Os}(\text{bpy})_2(\text{OH}_2)(\text{py})](\text{PF}_6)_2$  ( $\text{py}=\text{pyridine}$ ) in B-R buffer open to air and monitored for a total of 124 h. Concentration of  $[\text{Os}(\text{bpy})_2(\text{OH}_2)(\text{py})](\text{PF}_6)_2 = 2$  mM; scan rate = 100 mV/s. (b) monitoring of the Os(II)/Os(III) and Os(III)/Os(IV) half peak potential as a function of time

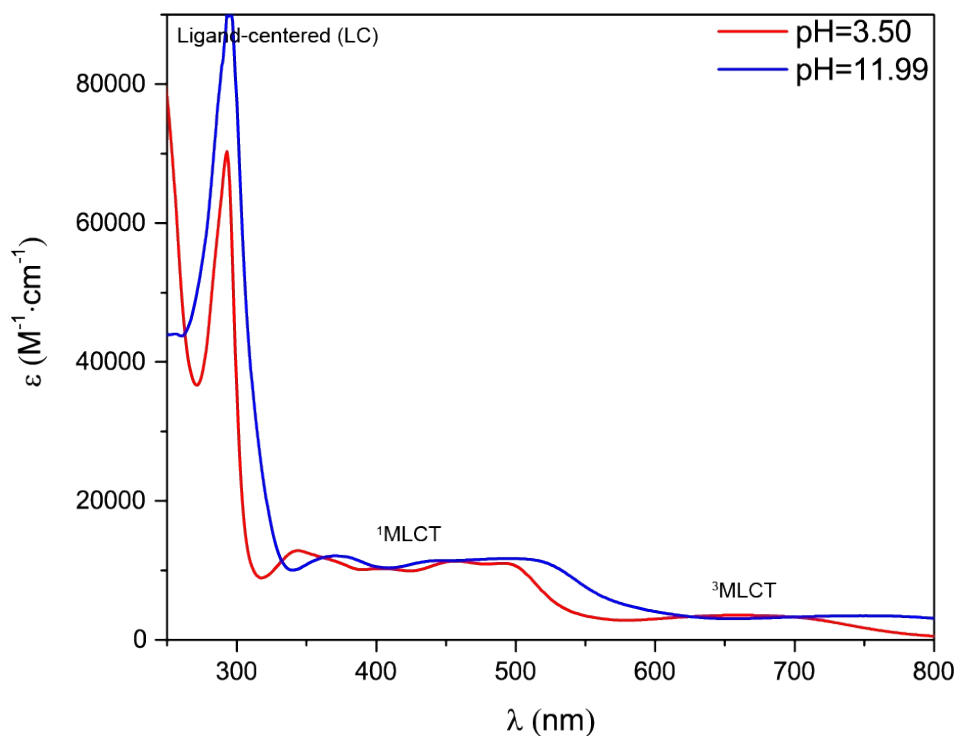


**Figure S21.** UV-Vis spectra of freshly prepared  $[\text{Os}(\text{bpy})_2(\text{OH}_2)(\text{py})](\text{PF}_6)_2$  (py=pyridine) in B-R buffer at different pH values. Concentration = 0.25 mM, ascorbic acid (around 5 equiv) was added to reduce excess Os(III) to Os(II); Tentative assignment at pH=3.50:  $\lambda_{\text{max}}$ : 659 nm ( $^3\text{MLCT}$ ,  $\epsilon=3534.3 \text{ M}^{-1} \text{ cm}^{-1}$ ); 491 nm ( $^1\text{MLCT}$ ,  $\epsilon=11029.1 \text{ M}^{-1} \text{ cm}^{-1}$ ); 456 nm ( $^1\text{MLCT}$ ,  $\epsilon=11317.5 \text{ M}^{-1} \text{ cm}^{-1}$ ); 405 nm ( $^1\text{MLCT}$ ,  $\epsilon=10239.6 \text{ M}^{-1} \text{ cm}^{-1}$ ); 344 nm ( $^1\text{MLCT}$ ,  $\epsilon=12840.2 \text{ M}^{-1} \text{ cm}^{-1}$ ); 293 nm (LC,  $\epsilon=70319.9 \text{ M}^{-1} \text{ cm}^{-1}$ ).<sup>8</sup>

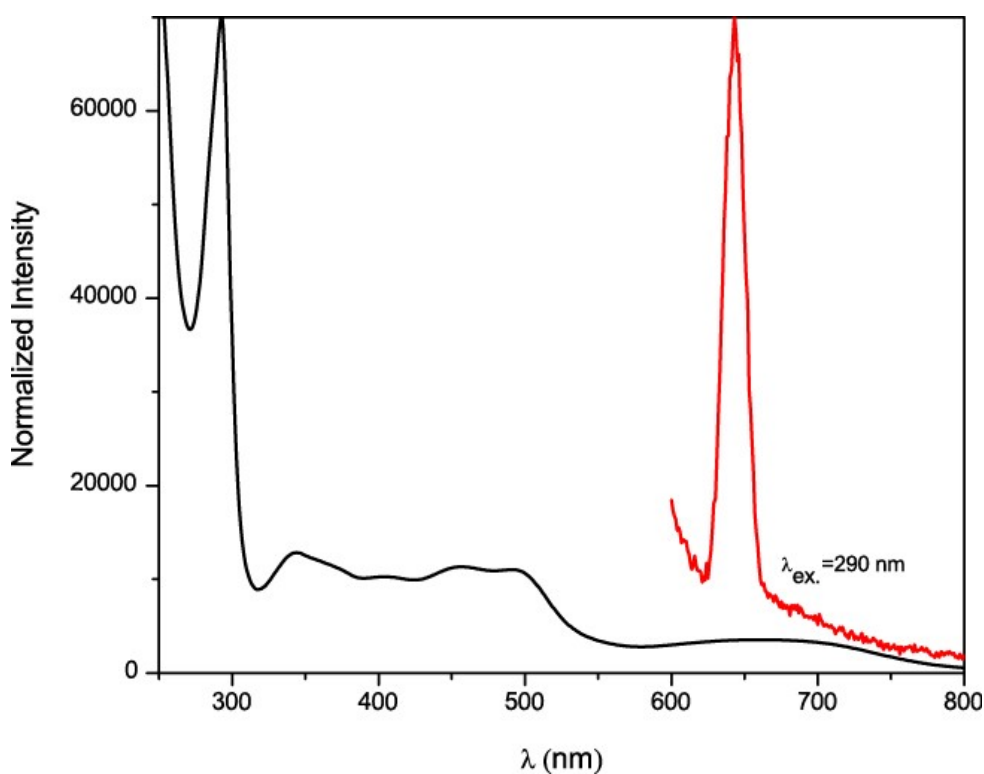


**Figure S22.** Emission spectrum (red) of  $[\text{Os}(\text{bpy})_2(\text{OH}_2)(\text{py})](\text{PF}_6)_2$  (py=pyridine) in B-R buffer (the black trace is the absorption spectrum) at pH 3.5.  $\lambda_{\text{em. max}} = 643 \text{ nm}$  at  $\lambda_{\text{exc.}} = 290 \text{ nm}$ .

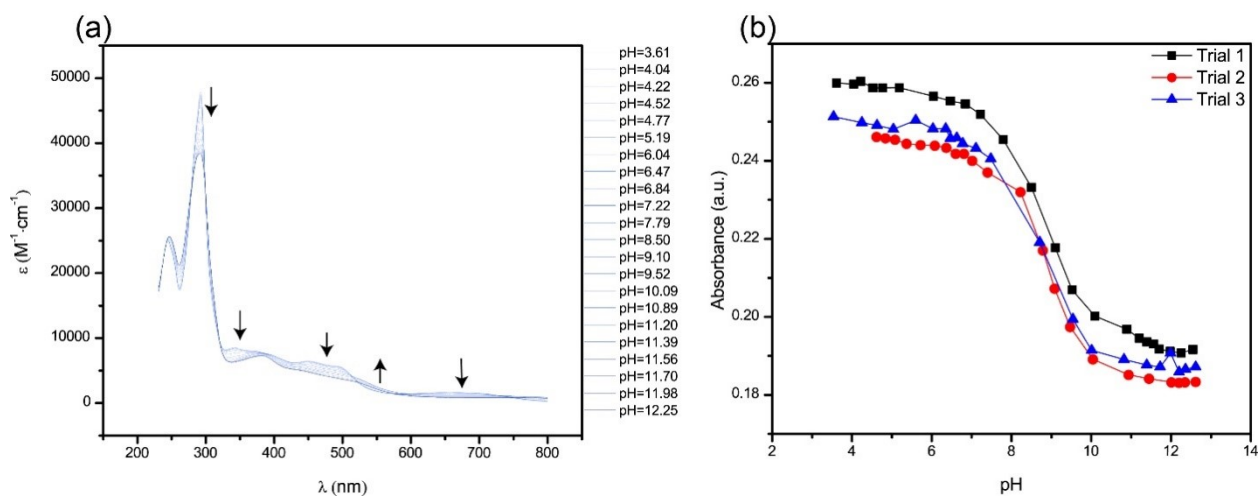


**Figure S23.** (a) UV-Vis spectra of  $[\text{Os}(\text{bpy})_2(\text{OH}_2)(\text{py})](\text{PF}_6)_2$  (py=pyridine) in B-R buffer at different pH values; (b) Spectrophotometric  $pK_a$  determination of the water ligand of  $[\text{Os}(\text{bpy})_2(\text{OH}_2)(\text{py})](\text{PF}_6)_2$  (py=pyridine) by measuring the absorbance values at  $\lambda_{\text{max}}=342 \text{ nm}$  by varying the solution pH ( $pK_a = 9.05 \pm 0.09$ ).

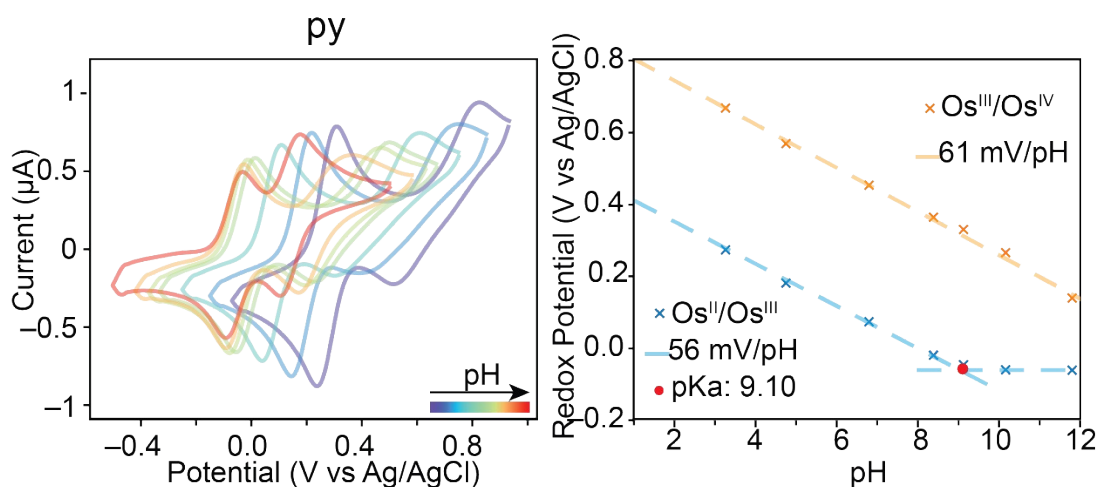


**Figure S24.** (a) CV traces of  $[\text{Os}(\text{bpy})_2(\text{OH}_2)(\text{py})](\text{PF}_6)_2$  (py=pyridine) in B-R buffer at different pH values; (b)  $pK_a$  determination of the water ligand of  $[\text{Os}(\text{bpy})_2(\text{OH}_2)(\text{py})](\text{PF}_6)_2$  (py=pyridine) by construction of a Pourbaix diagram ( $pK_a = 9.10$ ).

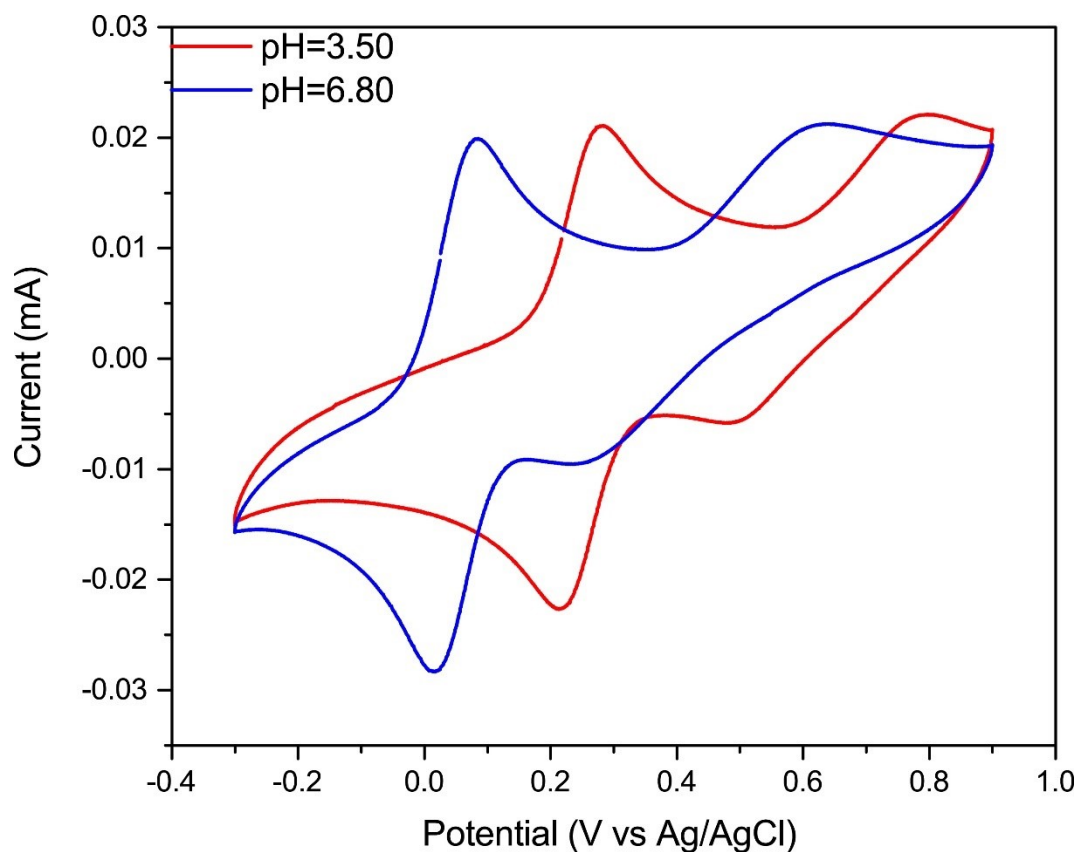


**Figure S25.** CV traces of  $[\text{Os}(\text{bpy})_2(\text{OH}_2)(\text{py})](\text{PF}_6)_2$  (py=pyridine) in B-R buffer at different pH values. Concentration of  $[\text{Os}(\text{bpy})_2(\text{OH}_2)(\text{py})](\text{PF}_6)_2 = 2 \text{ mM}$ ; scan rate = 100 mV/s. At pH 6.8: reversible waves at 0.073 V vs Ag/AgCl ( $\text{Os}^{\text{II/III}}$ ) and 0.433 V vs Ag/AgCl ( $\text{Os}^{\text{III/IV}}$ ).<sup>2</sup>

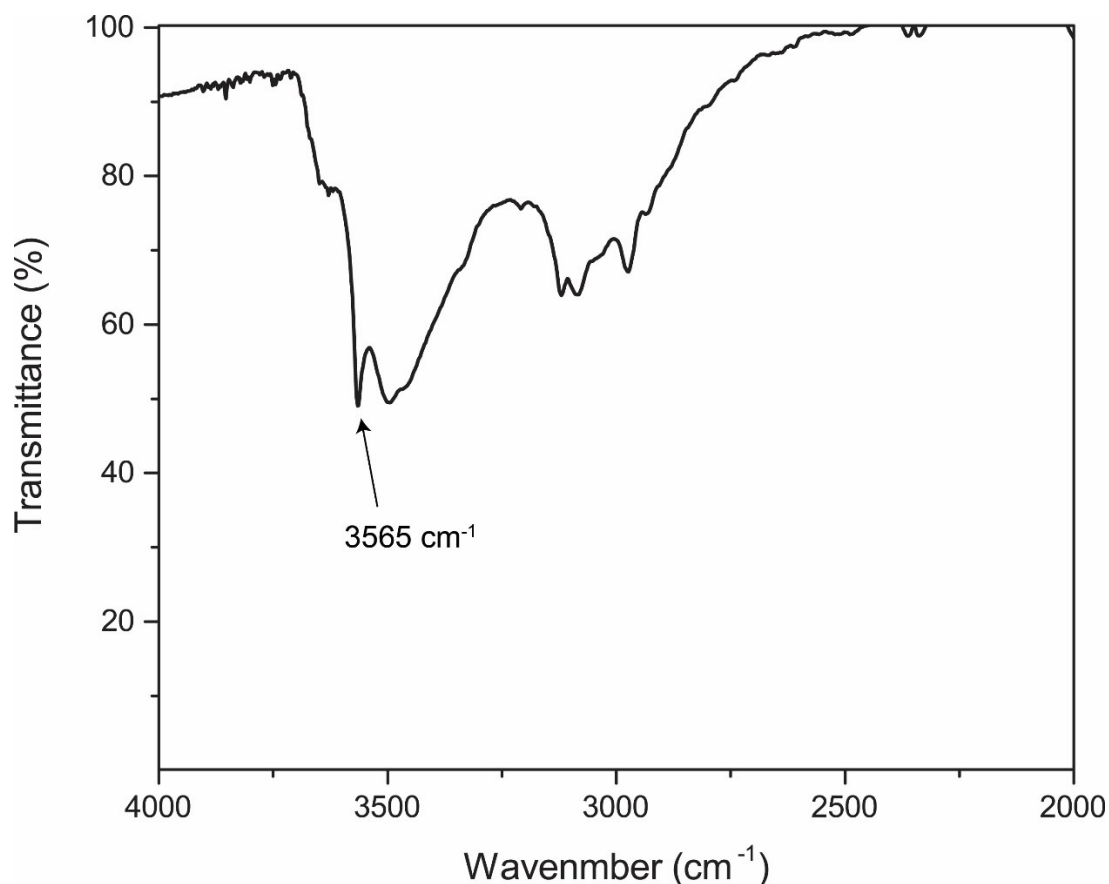


**Figure S26.** Transmission FTIR spectrum of  $[\text{Os}(\text{bpy})_2(\text{OH}_2)(\text{py})](\text{PF}_6)_2$  (py=pyridine); the O-H stretch of the coordinated water occurred at  $3565 \text{ cm}^{-1}$ .

### S3.4.2 Diffusion coefficient measurement of $[\text{Os}(\text{bpy})_2(\text{OH}_2)(\text{py})](\text{PF}_6)_2$ (py=pyridine)

The diffusion coefficient of  $[\text{Os}(\text{bpy})_2(\text{OH}_2)(\text{py})](\text{PF}_6)_2$  (py=pyridine) was measured by Randles-Ševčík equation at  $25 \text{ }^\circ\text{C}$  in B-R buffer (pH = 3.50, 6.80 and 8.15) to assess the structure (mononuclear vs dinuclear) in the solution state:

$$i_p = 2.69 \times 10^5 n^{\frac{3}{2}} AC\sqrt{Dv}$$

Where  $i_p$  is the current maximum in amps,  $n$  is the number of electrons transferred in the redox event ( $n = 1$ ),  $A$  is the electrode area in  $\text{cm}^2$ ,  $C$  is the concentration in  $\text{mol}/\text{cm}^3$ ,  $D$  is the diffusion coefficient in  $\text{cm}^2/\text{s}$  and  $v$  is the scan rate in  $\text{V}/\text{s}$ . A plot of  $i_p$  versus  $v^{0.5}$  would yield the slope of

$$2.69 \times 10^5 n^{\frac{3}{2}} AC\sqrt{v}$$

To prepare the sample for the diffusion coefficient test, a bulk recrystallization of the solid was performed:  $[\text{Os}(\text{bpy})_2(\text{OH}_2)(\text{py})](\text{PF}_6)_2$  (py=pyridine) (100 mg) was suspended in ethanol (10 mL). Diethyl ether (100 mL) was added to the mixture with stirring, and the resulting solid was collected by filtration and dried under dynamic vacuum.

At 0.531 mM of  $[\text{Os}(\text{bpy})_2(\text{OH}_2)(\text{py})](\text{PF}_6)_2$  (py=pyridine):

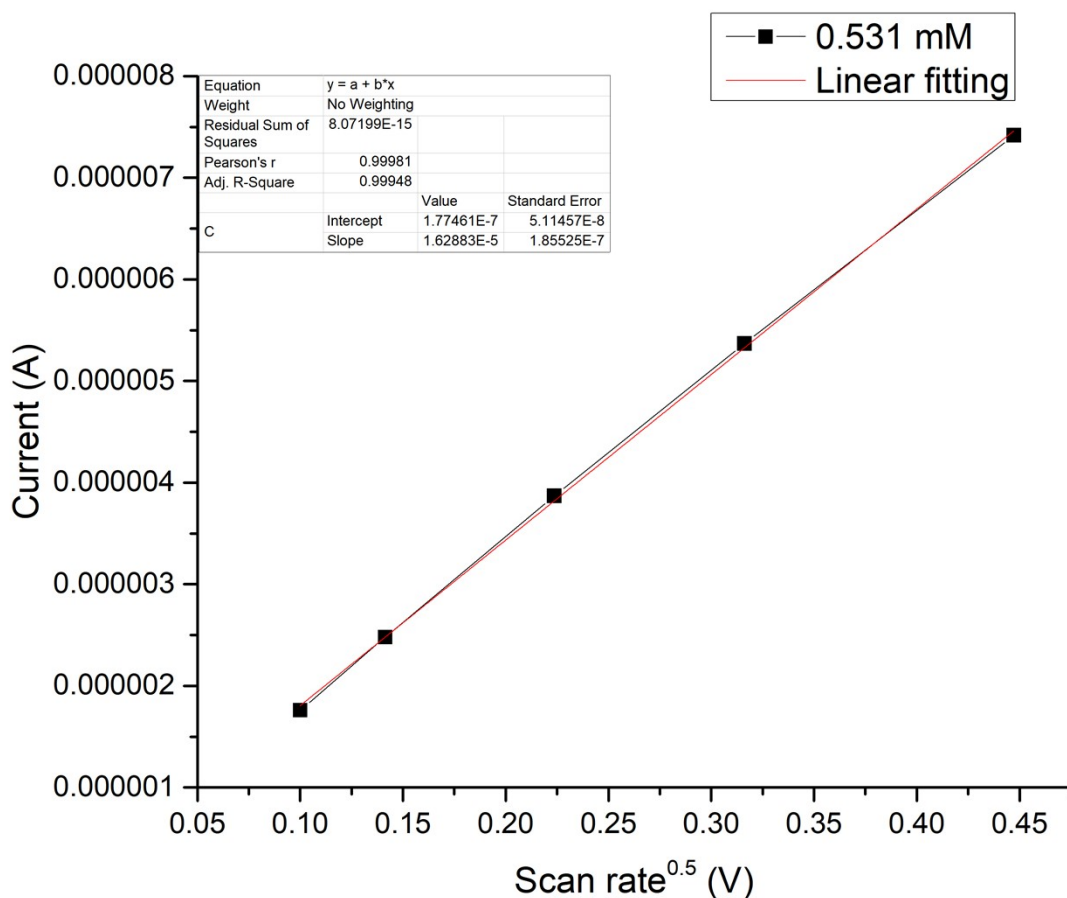


**Figure S27.** Plot of scan rate<sup>0.5</sup> versus current of  $[\text{Os}(\text{bpy})_2(\text{OH}_2)(\text{py})](\text{PF}_6)_2$  (py=pyridine) at 0.531 mM and pH 3.5. The slope derived from the plot was used to determine the diffusion coefficient of the complex using the Randles–Ševčík equation.

**Table S1.** Summary of the diffusion coefficients obtained using electrochemical methods of  $[\text{Os}(\text{bpy})_2(\text{OH}_2)(\text{py})](\text{PF}_6)_2$  (py=pyridine) at various concentrations.

pH	Concentration (mM)	Diffusion coefficient ( $10^{-6}$ cm <sup>2</sup> /s)
3.50	1.010	3.5
3.50	0.758	2.5
3.50	0.531	2.6
3.50	0.347	3
3.50	0.255	2.4
6.80	0.330	3.1

8.15	0.374	3.0
------	-------	-----

The diffusion coefficient was calculated to be  $(2.9 \pm 0.6) \times 10^{-6} \text{ cm}^2/\text{s}$ . According to the Stokes-Einstein law, the diffusion coefficient of a molecule is inversely proportional to its radius. Therefore, if the dinuclear structure were present in the solution state, there should be a relationship between the concentration of the solute and the diffusion coefficient. Specifically, at low concentrations, the mononuclear structure should dominate, resulting in higher diffusion coefficients, and vice versa. Since we did not observe this trend, we conclude that the dinuclear structure is not present in the solution state. The complex remained mononuclear, as confirmed by testing the diffusion coefficient at various pH values (pH = 6.80 and 8.15, Table S1), which yielded similar results. Further support for this conclusion comes from DOSY experiments (Figure S28), which also showed consistent results at a 1 mM solution concentration.

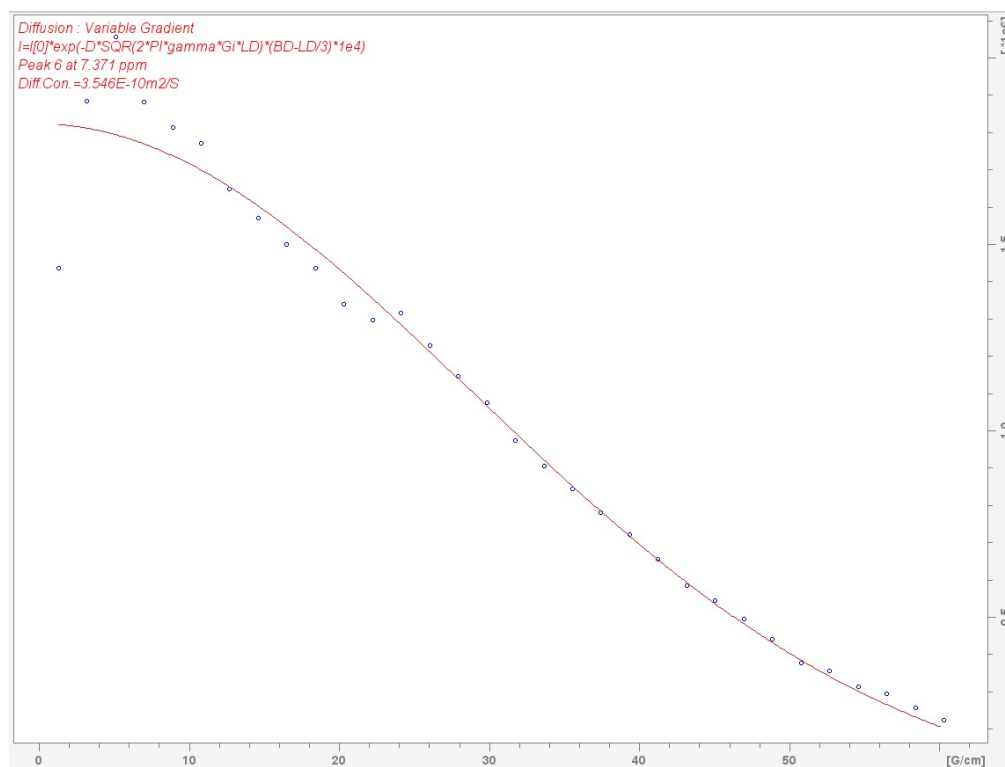


**Figure S28.** Signal attenuation curves for  $^1\text{H}$  DOSY data of  $[\text{Os}(\text{bpy})_2(\text{OH}_2)(\text{py})](\text{PF}_6)_2$  (py=pyridine) in deuterated B-R buffer (40 mM) with ascorbic acid (10 equiv, pH = 6.80); the diffusion coefficient was measured to be  $3.5 \times 10^{-6} \text{ cm}^2/\text{s}$ .

**4-methoxypyridine derivative (5):**  $^1\text{H}$  NMR (400 MHz,  $\text{D}_2\text{O}$ , 298 K)  $\delta$  8.93 (d,  $J = 5.7$  Hz, 1H), 8.38 (dd,  $J = 13.3, 7.0$  Hz, 2H), 8.22 (dd,  $J = 15.9, 8.2$  Hz, 2H), 8.09 – 7.90 (m, 3H), 7.74 – 7.51 (m, 4H), 7.47 (t,  $J = 7.6$  Hz, 2H), 7.39 (t,  $J = 6.8$  Hz, 1H), 7.28 (t,  $J = 7.9$  Hz, 1H), 6.89 (t,  $J = 6.7$  Hz, 1H), 6.81 (t,  $J = 6.9$  Hz, 1H), 6.70 (d,  $J = 6.5$  Hz, 2H), 3.68 (s, 3H). Elemental analysis: found: C 33.83%,

H 2.87%, N 6.80%; calcd. for  $C_{26}H_{25}N_5O_2OsF_{12}P_2$ , C 33.96%, H 2.74%, N 7.62%. FTIR:  $\nu_{\max}$  3553  $cm^{-1}$ .

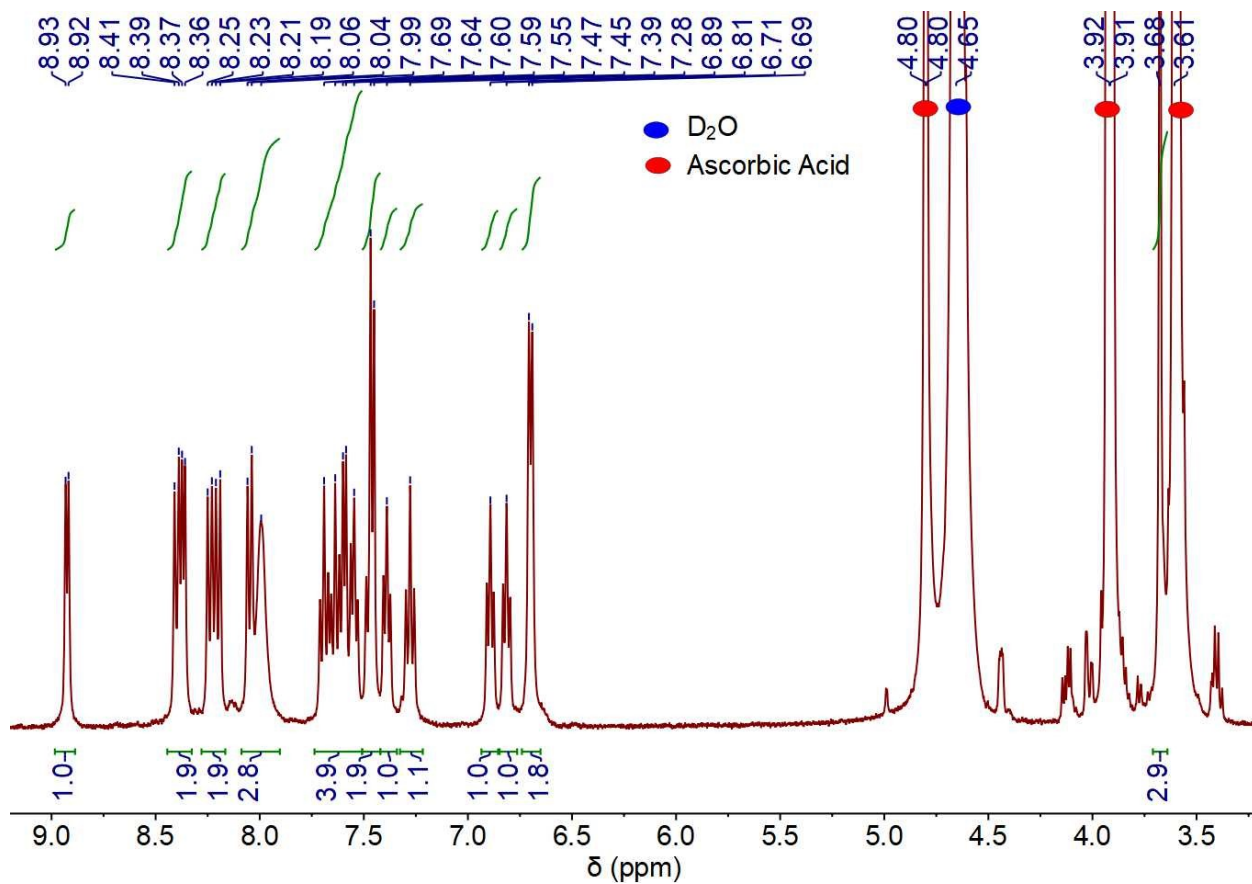


**Figure S29.**  $^1H$  NMR spectrum of  $[Os(bpy)_2(OH_2)(py^L)](PF_6)_2$  ( $py^L=4$ -methoxypyridine) (400 MHz,  $D_2O$ , 298 K). Ascorbic acid (around 5 equiv) was added to the NMR solvent to reduce paramagnetic Os(III) to Os(II) to improve the quality of the spectrum.

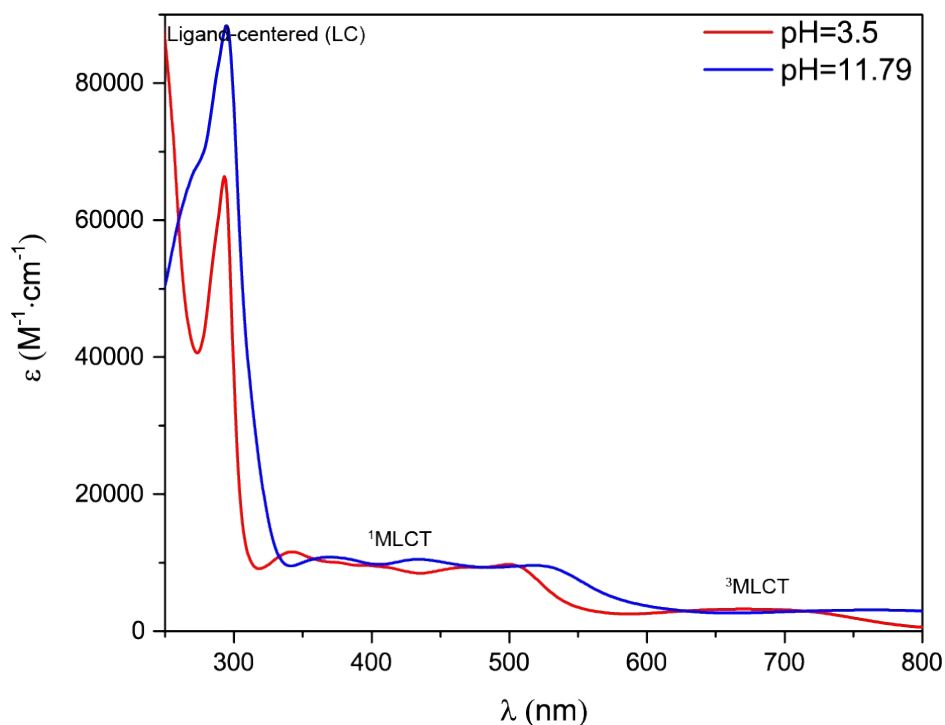


**Figure S30.** UV-Vis spectra of freshly prepared  $[\text{Os}(\text{bpy})_2(\text{OH}_2)(\text{py}^L)](\text{PF}_6)_2$  ( $\text{py}^L=4\text{-methoxypyridine}$ ) in B-R buffer at different pH values. Concentration = 0.25 mM, ascorbic acid (around 5 equiv) was added to reduce excess Os(III) to Os(II); Tentative assignment at pH=3.50:  $\lambda_{\text{max}}$ : 666 nm ( $^3\text{MLCT}$ ,  $\epsilon=3227.0 \text{ M}^{-1} \text{ cm}^{-1}$ ); 499 nm ( $^1\text{MLCT}$ ,  $\epsilon=9741.4 \text{ M}^{-1} \text{ cm}^{-1}$ ); 471 nm ( $^1\text{MLCT}$ ,  $\epsilon=9315.4 \text{ M}^{-1} \text{ cm}^{-1}$ ); 343 nm ( $^1\text{MLCT}$ ,  $\epsilon=11563.6 \text{ M}^{-1} \text{ cm}^{-1}$ ); 293 nm (LC,  $\epsilon=66388.6 \text{ M}^{-1} \text{ cm}^{-1}$ ).<sup>8</sup>

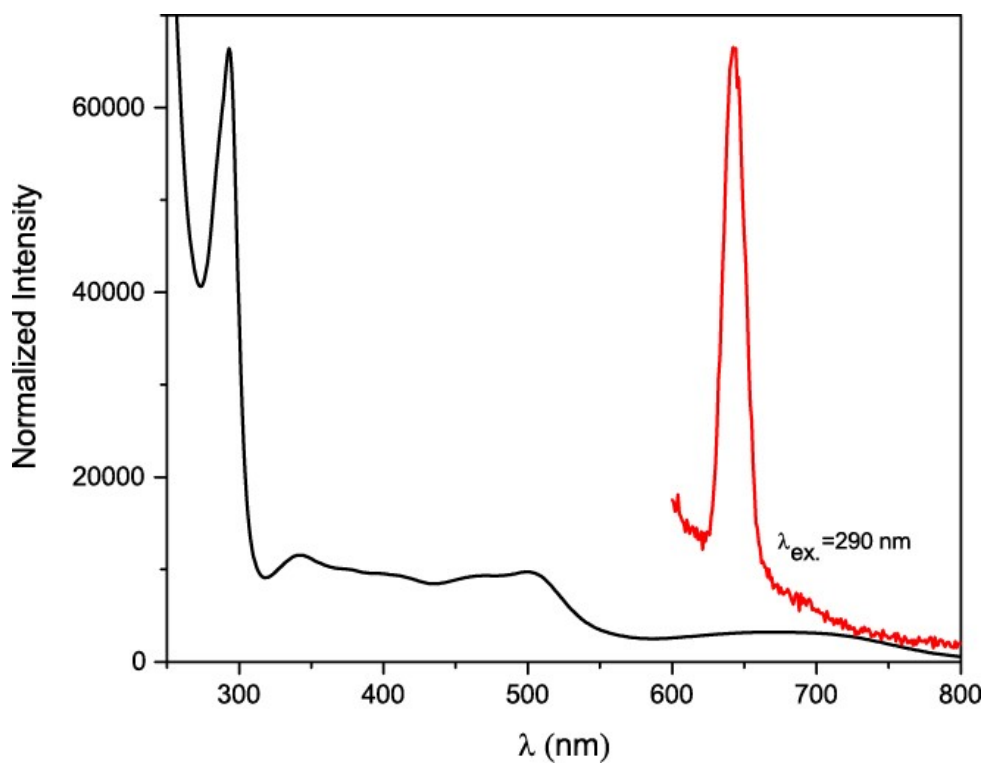


**Figure S31.** Emission spectrum (red) of  $[\text{Os}(\text{bpy})_2(\text{OH}_2)(\text{py}^L)](\text{PF}_6)_2$  ( $\text{py}^L=4\text{-methoxypyridine}$ ) in B-R buffer (the black trace is the UV-Vis spectrum) at pH 3.5.  $\lambda_{\text{em. max}} = 644 \text{ nm}$  at  $\lambda_{\text{exc.}} = 290 \text{ nm}$ .

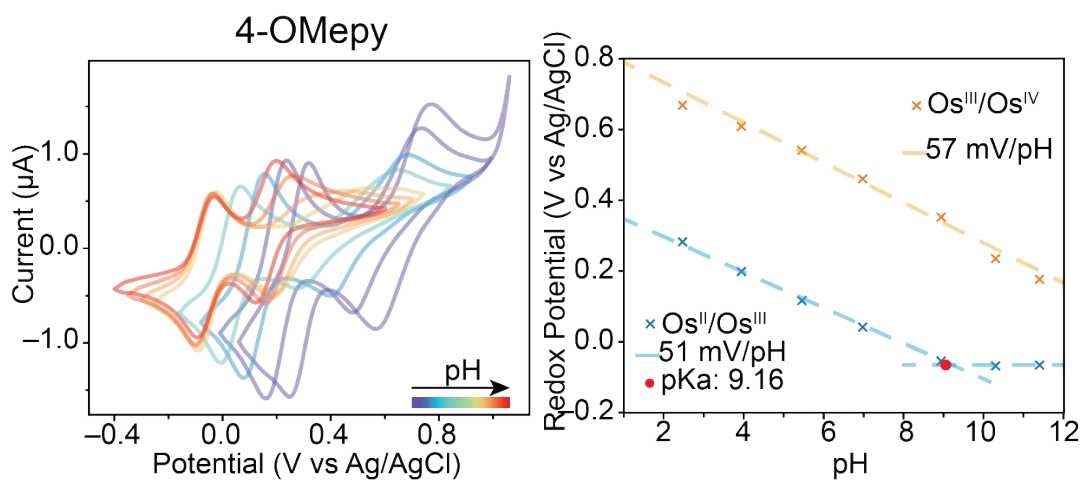


**Figure S32.** (a) CV traces of  $[\text{Os}(\text{bpy})_2(\text{OH}_2)(\text{py}^L)](\text{PF}_6)_2$  ( $\text{py}^L=4\text{-methoxypyridine}$ ) in B-R buffer at different pH values; (b)  $\text{pK}_a$  determination of the water ligand of  $[\text{Os}(\text{bpy})_2(\text{OH}_2)(\text{py}^L)](\text{PF}_6)_2$  ( $\text{py}^L=4\text{-methoxypyridine}$ ) construction of a Pourbaix diagram ( $\text{pK}_a = 9.16$ ).

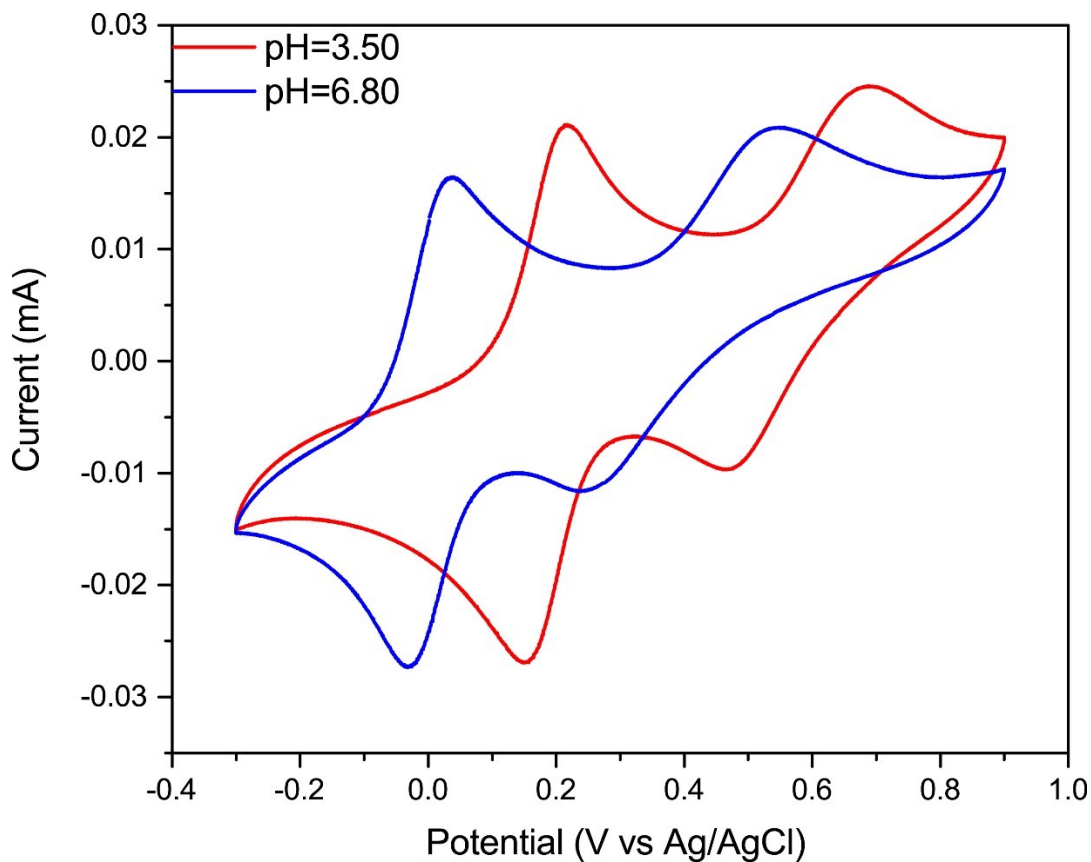


**Figure S33.** CV traces of  $[\text{Os}(\text{bpy})_2(\text{OH}_2)(\text{py}^L)](\text{PF}_6)_2$  ( $\text{py}^L=4\text{-methoxypyridine}$ ) in B-R buffer at different pH values. Concentration of  $[\text{Os}(\text{bpy})_2(\text{OH}_2)(\text{py}^L)](\text{PF}_6)_2 = 2 \text{ mM}$ ; scan rate = 100 mV/s. At pH 6.8: reversible waves at 0.033 V vs Ag/AgCl ( $\text{Os}^{\text{II/III}}$ ) and 0.393 V vs Ag/AgCl ( $\text{Os}^{\text{III/IV}}$ ).

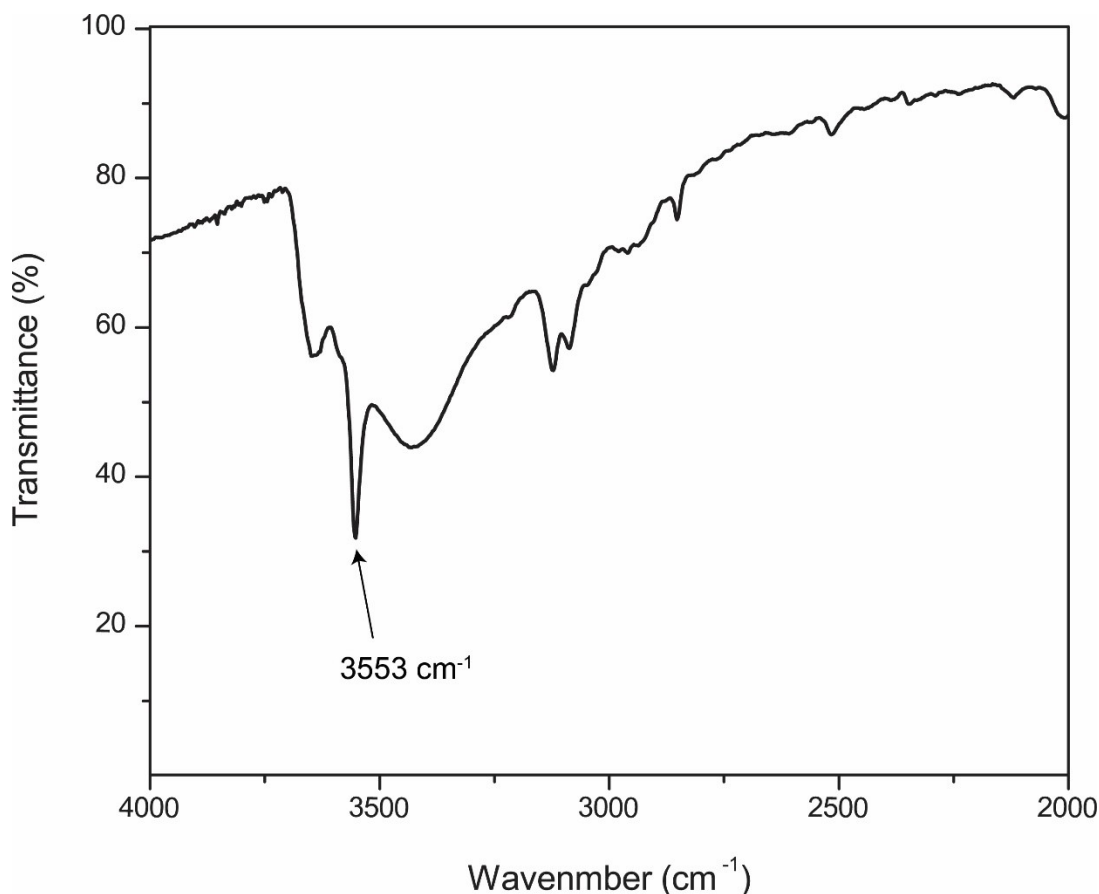


**Figure S34.** Transmission FTIR spectrum of  $[\text{Os}(\text{bpy})_2(\text{OH}_2)(\text{py}^L)](\text{PF}_6)_2$  ( $\text{py}^L=4\text{-methoxypyridine}$ ); the O-H stretch of the coordinated water occurred at  $3553 \text{ cm}^{-1}$ .

**4-methylpyridine derivative (6):**  $^1\text{H NMR}$  (400 MHz,  $\text{D}_2\text{O}$ , 298 K)  $\delta$  8.93 (dt,  $J = 5.6, 1.1 \text{ Hz}$ , 1H), 8.42 (dd,  $J = 8.2, 1.2 \text{ Hz}$ , 1H), 8.35 (dt,  $J = 5.8, 1.2 \text{ Hz}$ , 1H), 8.26 (dt,  $J = 8.3, 1.1 \text{ Hz}$ , 1H), 8.21 (dt,  $J = 8.3, 1.2 \text{ Hz}$ , 1H), 8.13 – 7.92 (m, 3H), 7.75 – 7.54 (m, 4H), 7.53 – 7.43 (m, 2H), 7.40 (ddd,  $J = 7.5, 5.8, 1.4 \text{ Hz}$ , 1H), 7.30 (td,  $J = 7.9, 1.4 \text{ Hz}$ , 1H), 6.98 (d,  $J = 6.1 \text{ Hz}$ , 2H), 6.93 (ddd,  $J = 7.4, 5.8, 1.4 \text{ Hz}$ , 1H), 6.85 (ddd,  $J = 7.5, 5.9, 1.4 \text{ Hz}$ , 1H), 2.15 (s, 3H). Elemental analysis: found: C 34.56%, H 2.79%, N 7.75%; calcd. for  $\text{C}_{26}\text{H}_{25}\text{N}_5\text{O}_5\text{F}_{12}\text{P}_2$ , C 34.79%, H 3.03%, N 7.67%. IR (ATR):  $\nu_{\text{max}} 3551 \text{ cm}^{-1}$ .

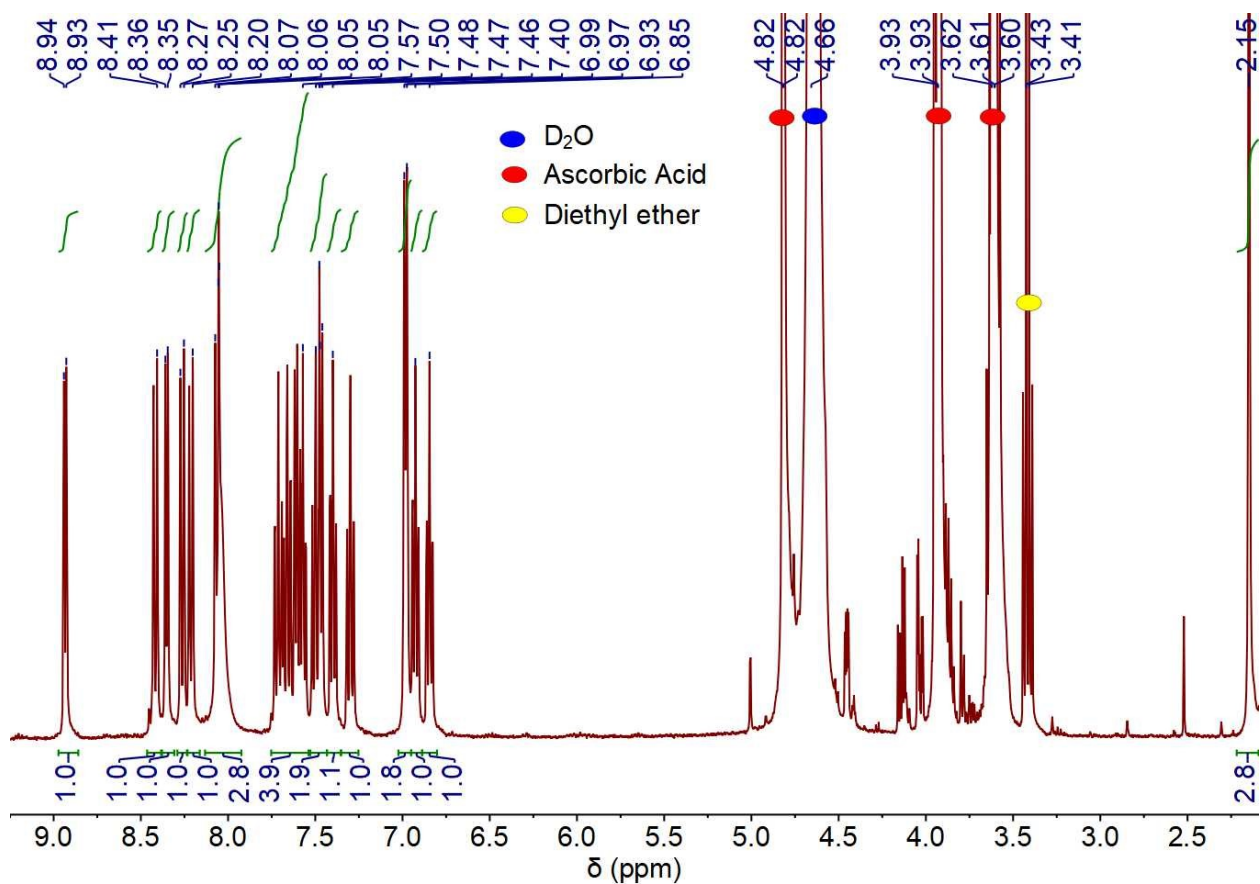


**Figure S35.** <sup>1</sup>H NMR spectrum of [Os(bpy)<sub>2</sub>(OH<sub>2</sub>)(py<sup>L</sup>)](PF<sub>6</sub>)<sub>2</sub> (py<sup>L</sup>=4-methylpyridine) (400 MHz, D<sub>2</sub>O, 298 K). Ascorbic acid (around 5 equiv) was added to the NMR solvent to reduce paramagnetic Os(III) to Os(II) to improve the quality of the spectrum.

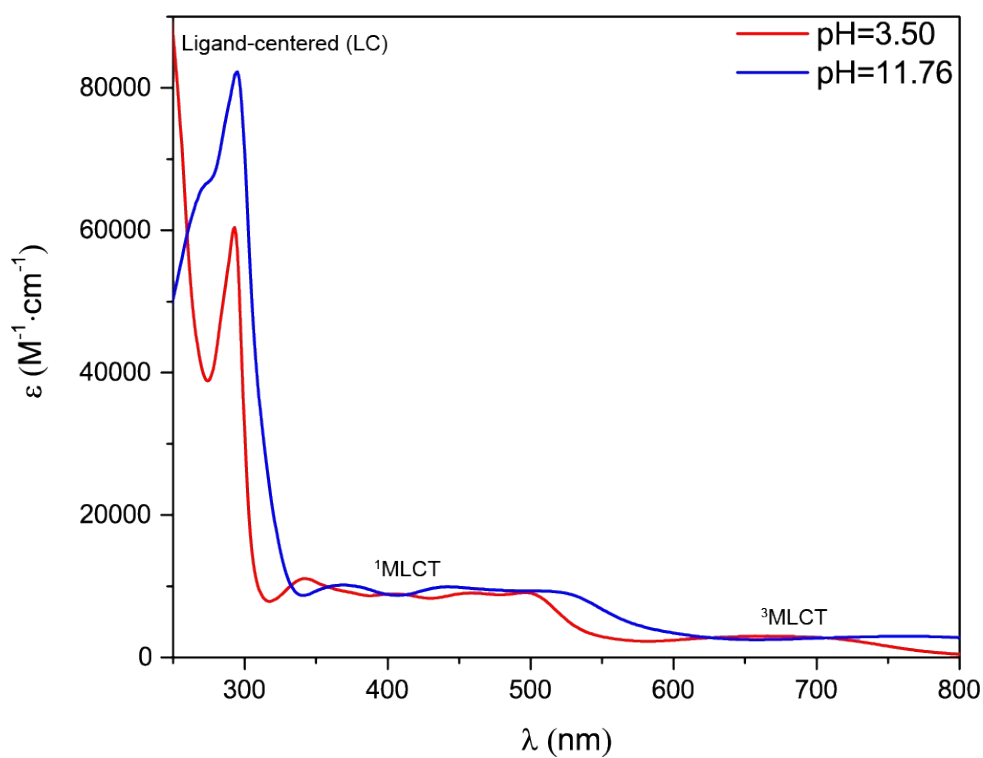


**Figure S36.** UV-Vis spectra of a freshly prepared  $[\text{Os}(\text{bpy})_2(\text{OH}_2)(\text{py}^L)](\text{PF}_6)_2$  ( $\text{py}^L=4\text{-methylpyridine}$ ) in B-R buffer at different pH values. Concentration = 0.5 mM, ascorbic acid (around 5 equiv) was added to reduce excess Os(III) to Os(II); Tentative assignment at pH=3.50:  $\lambda_{\text{max}}$ : 665 nm ( $^3\text{MLCT}$ ,  $\epsilon=2976.2 \text{ M}^{-1} \text{ cm}^{-1}$ ); 496 nm ( $^1\text{MLCT}$ ,  $\epsilon=9098.0 \text{ M}^{-1} \text{ cm}^{-1}$ ); 458 nm ( $^1\text{MLCT}$ ,  $\epsilon=9025.7 \text{ M}^{-1} \text{ cm}^{-1}$ ); 405 nm ( $^1\text{MLCT}$ ,  $\epsilon=8891.8 \text{ M}^{-1} \text{ cm}^{-1}$ ); 342 nm ( $^1\text{MLCT}$ ,  $\epsilon=11071.0 \text{ M}^{-1} \text{ cm}^{-1}$ ); 293 nm (LC,  $\epsilon=60426 \text{ M}^{-1} \text{ cm}^{-1}$ ).<sup>8</sup>

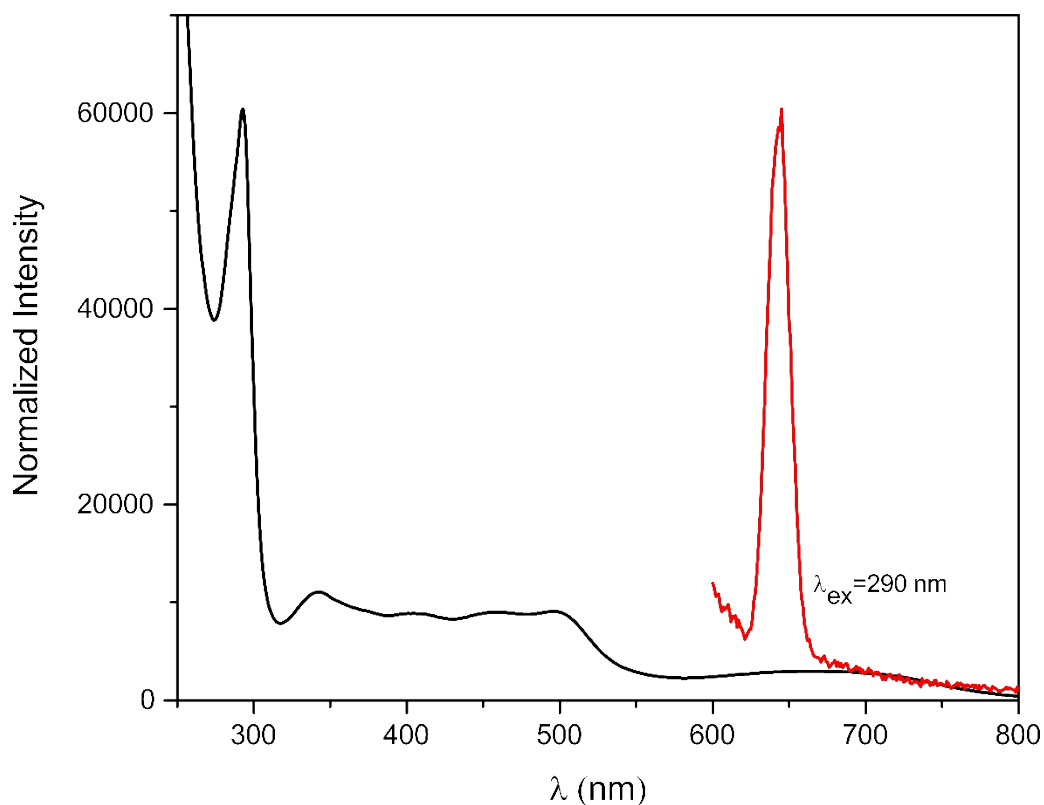


**Figure S37.** Emission spectrum (red) of  $[\text{Os}(\text{bpy})_2(\text{OH}_2)(\text{py}^L)](\text{PF}_6)_2$  ( $\text{py}^L=4\text{-methylpyridine}$ ) in B-R buffer (the black trace is the UV-Vis spectrum) at pH 3.5.  $\lambda_{\text{em. max}} = 643 \text{ nm}$  at  $\lambda_{\text{exc.}} = 290 \text{ nm}$ .

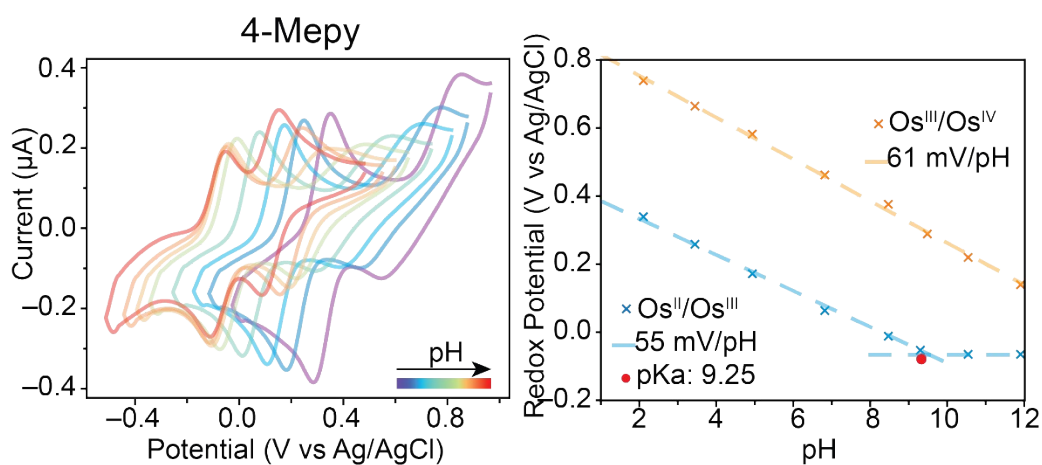


**Figure S38.** (a) CV traces of  $[\text{Os}(\text{bpy})_2(\text{OH}_2)(\text{py}^L)](\text{PF}_6)_2$  ( $\text{py}^L=4\text{-methylpyridine}$ ) in B-R buffer at different pH values; (b)  $\text{p}K_a$  determination of the water ligand of  $[\text{Os}(\text{bpy})_2(\text{OH}_2)(\text{py}^L)](\text{PF}_6)_2$  ( $\text{py}^L=4\text{-methylpyridine}$ ) by construction of a Pourbaix diagram ( $\text{p}K_a=9.25$ ).

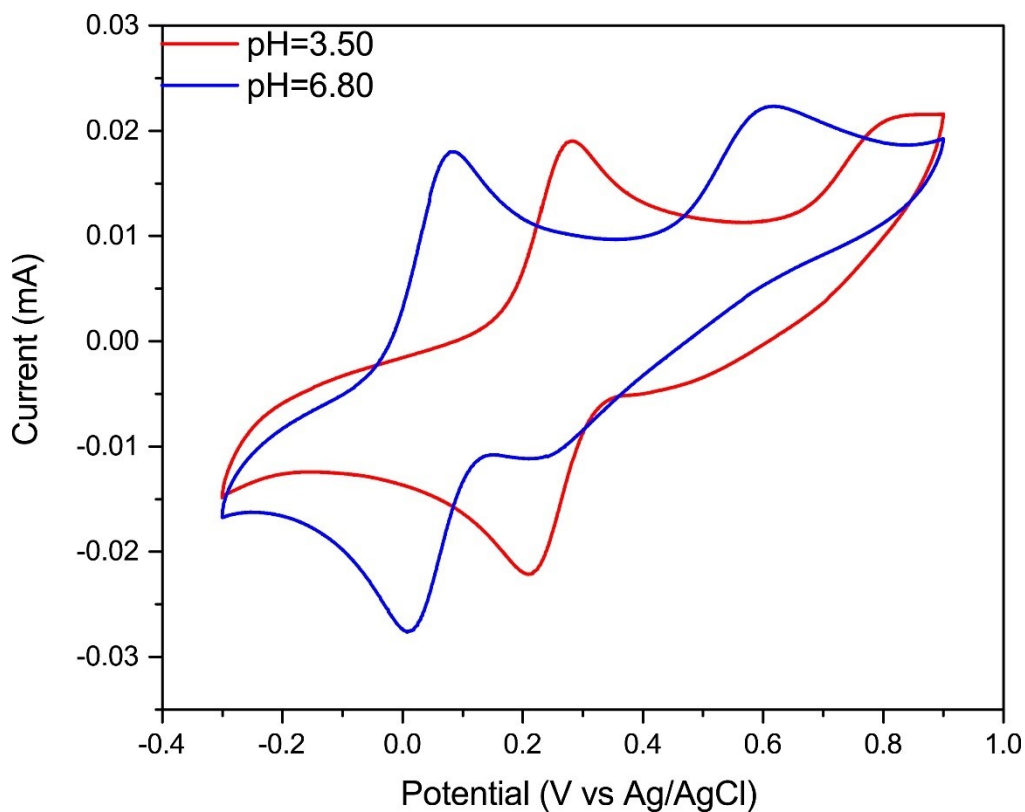


**Figure S39.** CV traces of  $[\text{Os}(\text{bpy})_2(\text{OH}_2)(\text{py}^L)](\text{PF}_6)_2$  ( $\text{py}^L=4\text{-methylpyridine}$ ) in B-R buffer at different pH values. Concentration of  $[\text{Os}(\text{bpy})_2(\text{OH}_2)(\text{py}^L)](\text{PF}_6)_2 = 2 \text{ mM}$ ; scan rate = 100 mV/s. At pH 6.8: reversible waves at 0.054 V vs Ag/AgCl ( $\text{Os}^{\text{III/III}}$ ) and 0.413 V vs Ag/AgCl ( $\text{Os}^{\text{III/IV}}$ ).

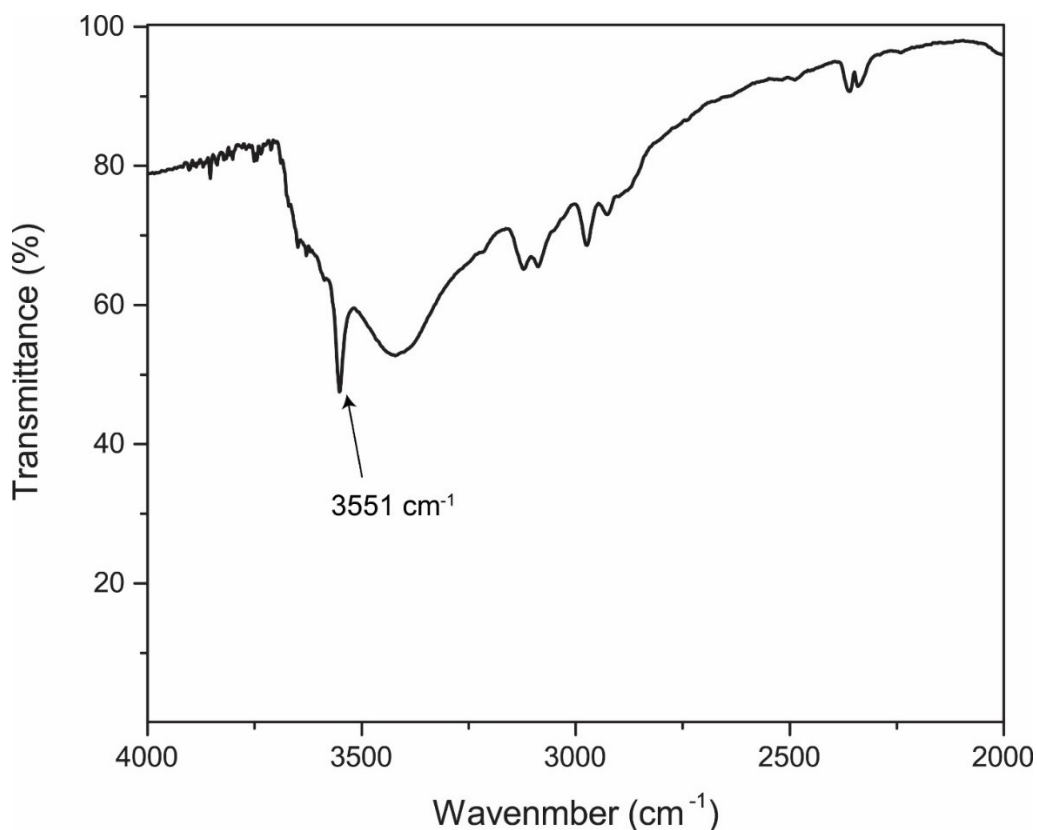


**Figure S40.** Transmission FTIR spectrum of  $[\text{Os}(\text{bpy})_2(\text{OH}_2)(\text{py}^L)](\text{PF}_6)_2$  ( $\text{py}^L=4\text{-methylpyridine}$ ); the O-H stretch of the coordinated water occurred at  $3551\text{ cm}^{-1}$ .

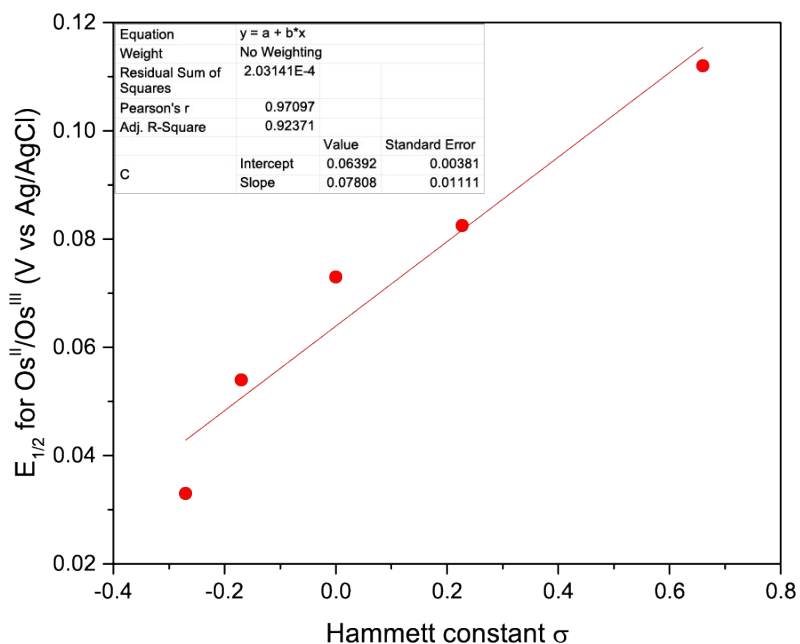


**Figure S41.** Plot of the Hammett constant ( $\sigma$ ) of the *para*-substituent on the pyridine versus  $E_{1/2}$  of the  $\text{Os}^{\text{II}}/\text{Os}^{\text{III}}$  couples for compounds **4-8** ( $R^2 = 0.924$ , slope =  $+0.078$ ).

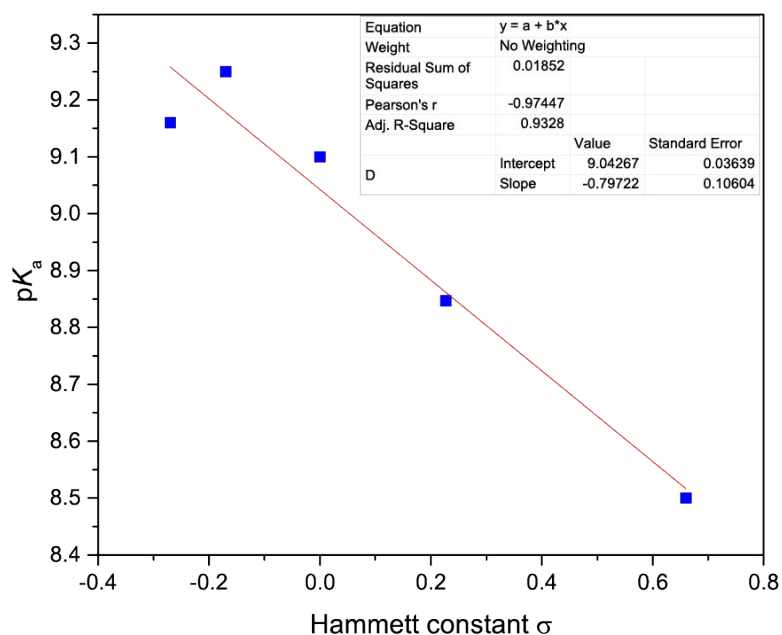


**Figure S42.** Plot of the Hammett constant ( $\sigma$ ) of the *para*-substituent on the pyridine versus  $pK_a$  values for compounds **4-8** ( $R^2 = 0.933$ , slope =  $-0.7972$ ).

### S3.4.3 ICP-MS analysis of the Chloride content in $[\text{Os}(\text{bpy})_2(\text{OH}_2)(\text{py}^L)](\text{PF}_6)_2$ ( $\text{py}^L=4\text{-methylpyridine}$ )

Chloride as a counter ion was also observed in the lattice structure, likely originating from the Cl ligand in precursor **1**. However, the crystal structure does not necessarily reflect the bulk composition of the solid. Based on the ICP-MS analysis, only trace amounts of Cl are present.

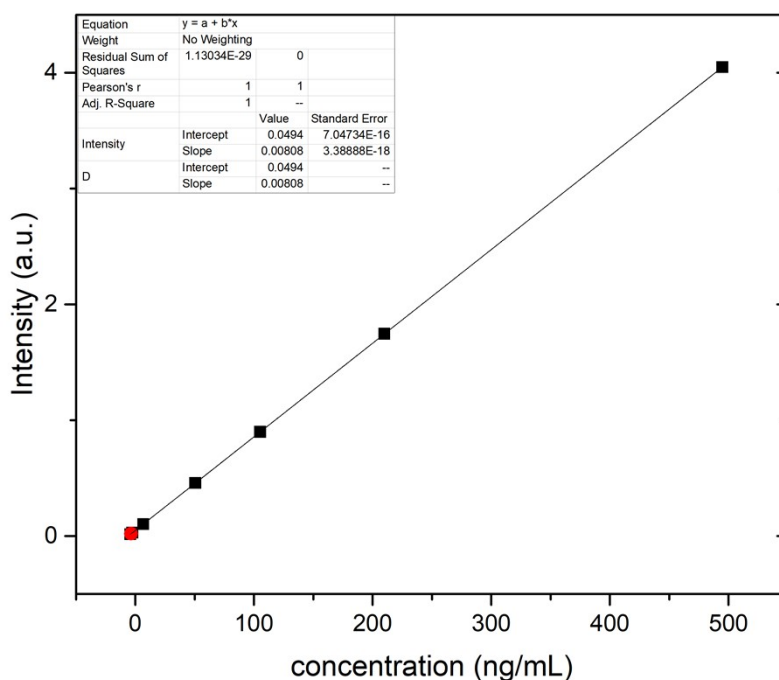


**Figure S43.** ICP-MS analysis of the chloride content of  $[\text{Os}(\text{bpy})_2(\text{OH}_2)(\text{py}^L)](\text{PF}_6)_2$  ( $\text{py}^L=4$ -methylpyridine). The concentration of the unknown concentration samples (red dots) was found to be around 0 ng/mL, equivalent to around 0 wt% of the sample based on the calibration line (black line). Therefore, only trace amounts of Cl are present in the solid mixture.

### S3.5 Synthesis of $[\text{Os}(\text{bpy})_2(\text{OH}_2)(\text{py}^L)](\text{PF}_6)_2$ ( $\text{py}^L=4$ -cyanopyridine, 4-chloropyridine)

General procedure for synthesis of electron-withdrawing pyridine derivative 4-cyanopyridine and 4-chloropyridine: In a 10 mL round-bottom flask, pH 3.5 B-R buffer (5 mL) was added to  $\text{Os}(\text{bpy})_2\text{CO}_3$  (47.9 mg, 0.0850 mmol, 1.00 equiv). Pyridine (around 18 equiv for 4-cyanopyridine and around 10 equiv for 4-chloropyridine) was added to the mixture with stirring and the pH of the solution was adjusted to 6.8. The solution was rigorously stirred. CV of the solution was monitored in situ until the current of the peak  $E_{1/2}=0.112$  V (for 4-cyanopyridine) and  $E_{1/2}=0.083$  V (for 4-chloropyridine) reached a plateau (normally 30-40 minutes will be adequate). The undissolved 4-cyanopyridine was filtered off while 4-chloropyridine was completely soluble in water (no need to filter). Solid  $\text{NaPF}_6$  (200 mg, 1.19 mmol, 7.00 equiv) was added to the (filtered) solution affording a black precipitate. The black precipitate aggregated to form a large black ball-like solid (consisting of the product, pyridinium hexafluorophosphate salt, residual pyridine). The ball-like solid was collected via vacuum filtration, washed with cold water (5 mL) and dried at room temperature under dynamic vacuum overnight. The dried ball-like solid was suspended in diethyl ether (25 mL) and vigorously stirred for 1 day to break down the material into smaller particles. The black solid was collected via vacuum filtration and dried at room temperature under dynamic vacuum overnight (yields: 4-cyanopyridine

45±23%; 4-chloropyridine 59±4%). Since 4-cyanopyridinium salt and 4-chloropyridinium salt are both soluble in diethyl ether, no further purification was performed.

**4-cyanopyridine derivative (7):**  $^1\text{H}$  NMR (400 MHz,  $\text{D}_2\text{O}$ , 298 K)  $\delta$  8.87 (dd,  $J = 5.6, 1.2$  Hz, 1H), 8.50 (dd,  $J = 34.3, 7.3$  Hz, 3H), 8.31 (td,  $J = 8.5, 5.1$  Hz, 3H), 8.15 (dd,  $J = 7.7, 6.4$  Hz, 1H), 7.83 – 7.72 (m, 2H), 7.66 – 7.55 (m, 3H), 7.50 – 7.34 (m, 5H), 7.01 (ddd,  $J = 7.3, 5.7, 1.3$  Hz, 1H), 6.91 (ddd,  $J = 7.5, 5.9, 1.4$  Hz, 1H). Elemental analysis: found: C 33.42%, H 2.48%, N 8.36%; calcd for  $\text{C}_{26}\text{H}_{22}\text{N}_6\text{O}_6\text{S}_2\text{F}_{12}\text{P}_2$ , C 34.14%, H 2.42%, N 9.19%. IR (ATR):  $\nu_{\text{max}}$  3546, 2235, 2202  $\text{cm}^{-1}$ .

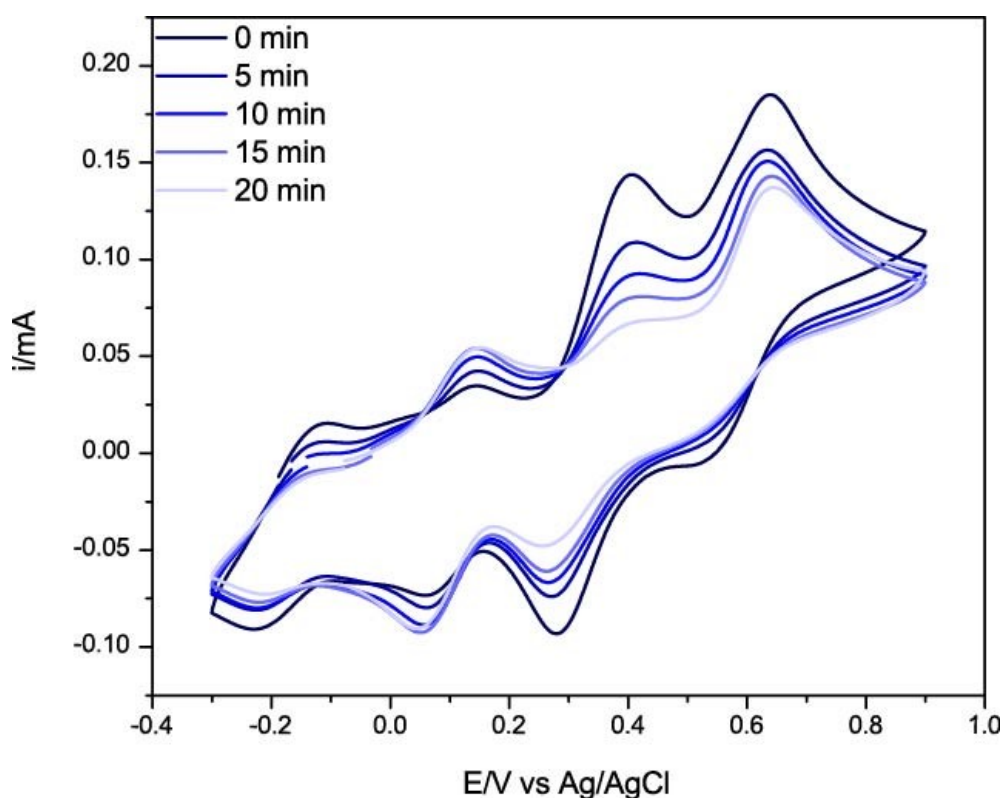


**Figure S44.** In situ CV traces of  $[\text{Os}(\text{bpy})_2(\text{OH}_2)(\text{py}^L)](\text{PF}_6)_2$  ( $\text{py}^L=4\text{-cyanopyridine}$ ) in pH=6.8 B-R buffer; Concentration of  $[\text{Os}(\text{bpy})_2(\text{OH}_2)(\text{py}^L)](\text{PF}_6)_2 = 17$  mM; scan rate = 100 mV/s.

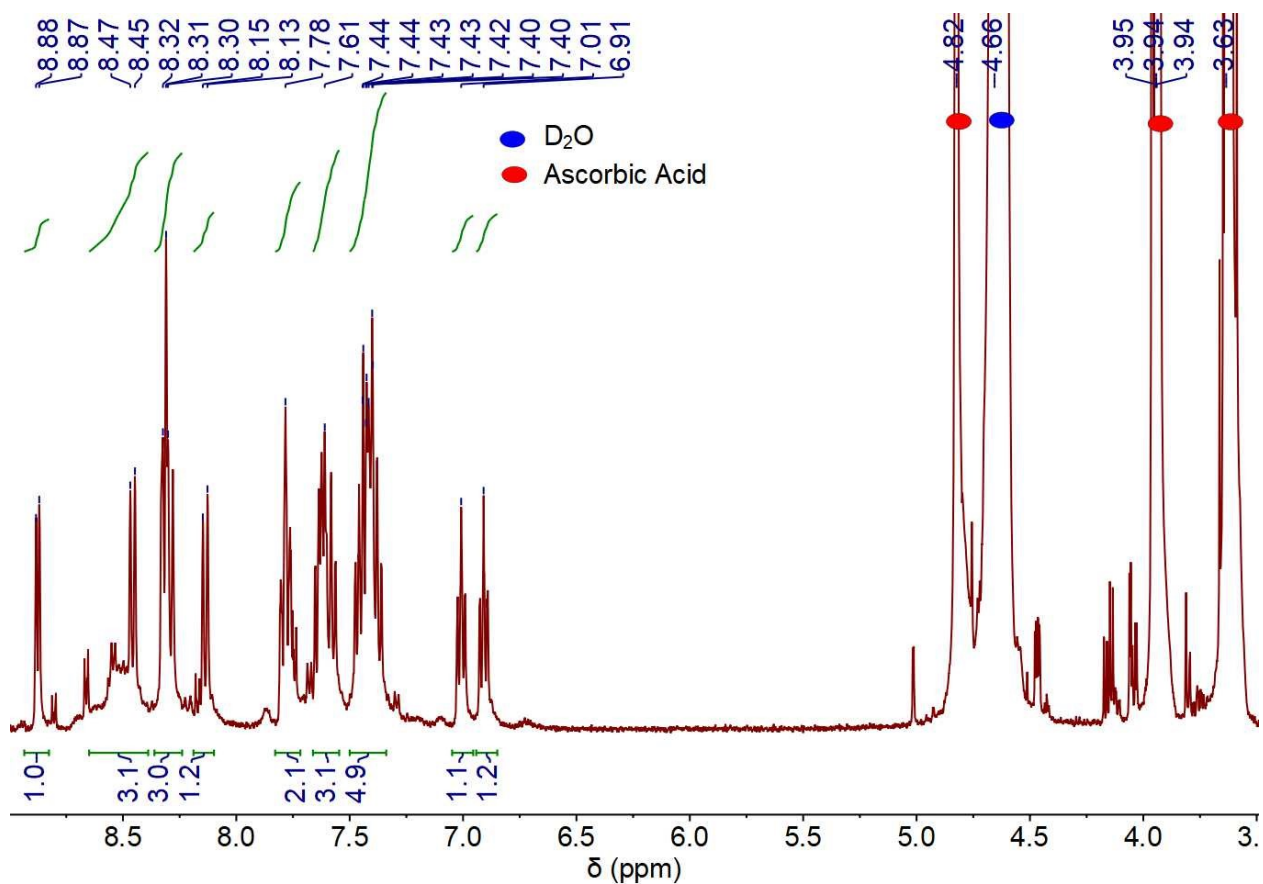


**Figure S45.** <sup>1</sup>H NMR spectrum of [Os(bpy)<sub>2</sub>(OH<sub>2</sub>)(py<sup>L</sup>)](PF<sub>6</sub>)<sub>2</sub> (py<sup>L</sup>=4-cyanopyridine) (400 MHz, D<sub>2</sub>O, 298 K). Ascorbic acid (around 5 equiv) was added to the NMR solvent to reduce paramagnetic Os(III) to Os(II) to improve the quality of the spectrum.

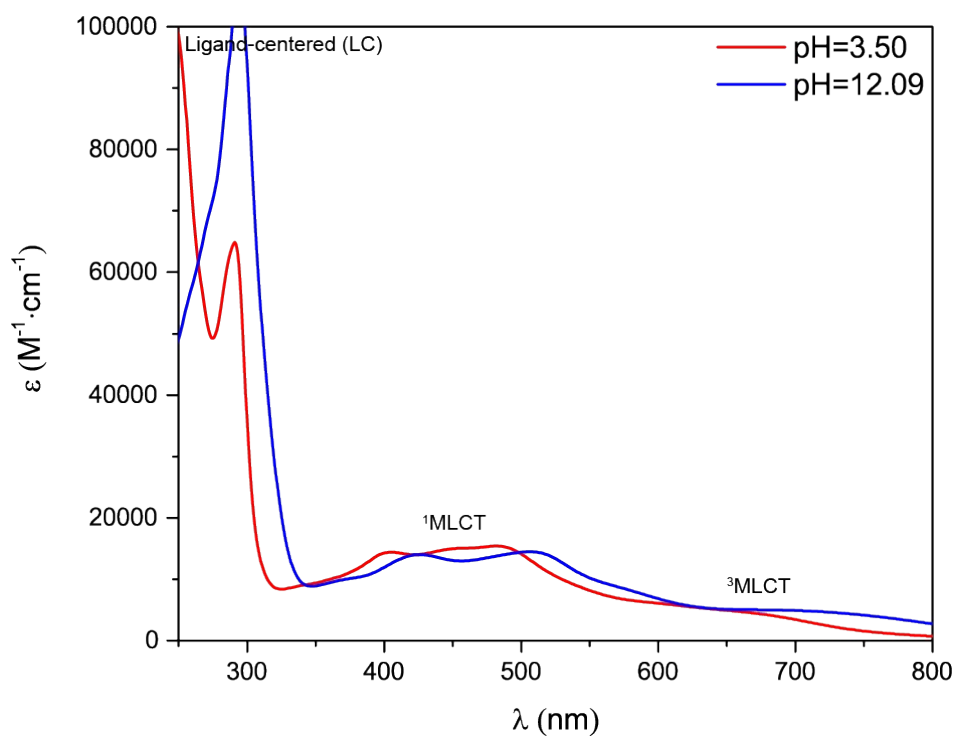


**Figure S46.** UV-Vis spectra of freshly prepared  $[\text{Os}(\text{bpy})_2(\text{OH}_2)(\text{py}^L)](\text{PF}_6)_2$  ( $\text{py}^L=4\text{-cyanopyridine}$ ) in B-R buffer at different pH values. Concentration = 0.5 mM, ascorbic acid (around 5 equiv) was added to reduce excess Os(III) to Os(II); Tentative assignment at pH=3.50:  $\lambda_{\text{max}}$ : 482 nm ( ${}^1\text{MLCT}$ ,  $\epsilon=15383.9 \text{ M}^{-1} \text{ cm}^{-1}$ ); 405 nm ( ${}^1\text{MLCT}$ ,  $\epsilon=14377.1 \text{ M}^{-1} \text{ cm}^{-1}$ ); 405 nm ( ${}^1\text{MLCT}$ ,  $\epsilon=8891.8 \text{ M}^{-1} \text{ cm}^{-1}$ ); 291 nm (LC,  $\epsilon=60892 \text{ M}^{-1} \text{ cm}^{-1}$ ).<sup>8</sup>

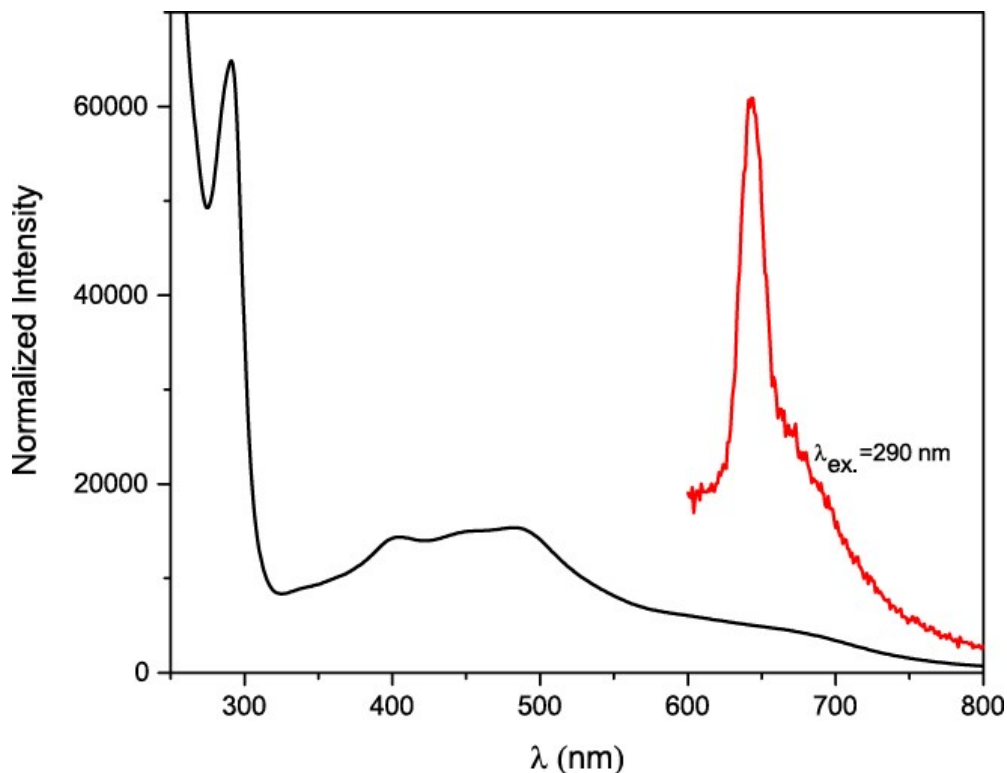


**Figure S47.** Emission spectrum (red) of  $[\text{Os}(\text{bpy})_2(\text{OH}_2)(\text{py}^L)](\text{PF}_6)_2$  ( $\text{py}^L=4\text{-cyanopyridine}$ ) in B-R buffer (the black trace is the UV-Vis spectrum) at pH 3.5.  $\lambda_{\text{em. max}} = 643 \text{ nm}$  at  $\lambda_{\text{exc.}} = 290 \text{ nm}$ .

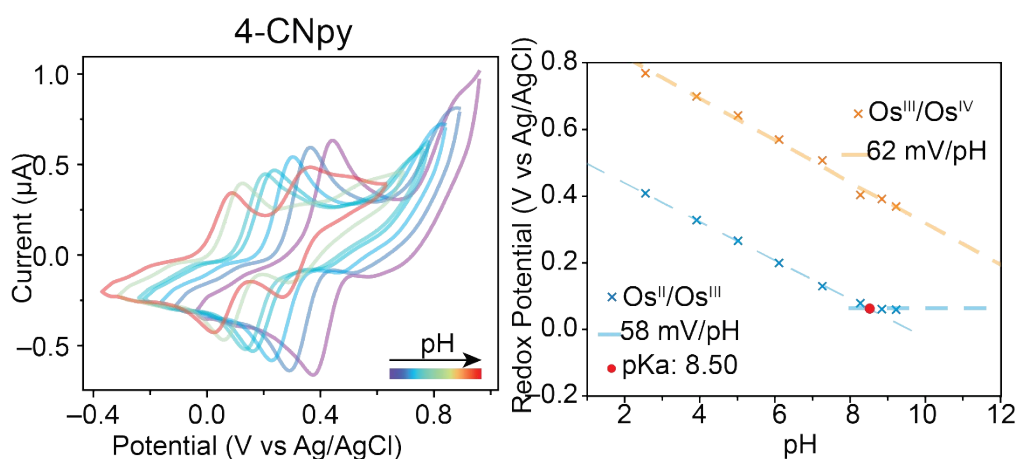


**Figure S48.** (a) CV traces of  $[\text{Os}(\text{bpy})_2(\text{OH}_2)(\text{py}^L)](\text{PF}_6)_2$  ( $\text{py}^L=4\text{-cyanopyridine}$ ) in B-R buffer at different pH values; (b)  $\text{pK}_a$  determination of the water ligand of  $[\text{Os}(\text{bpy})_2(\text{OH}_2)(\text{py}^L)](\text{PF}_6)_2$  ( $\text{py}^L=4\text{-cyanopyridine}$ ) by construction of a Pourbaix diagram ( $\text{pK}_a = 8.50$ ).

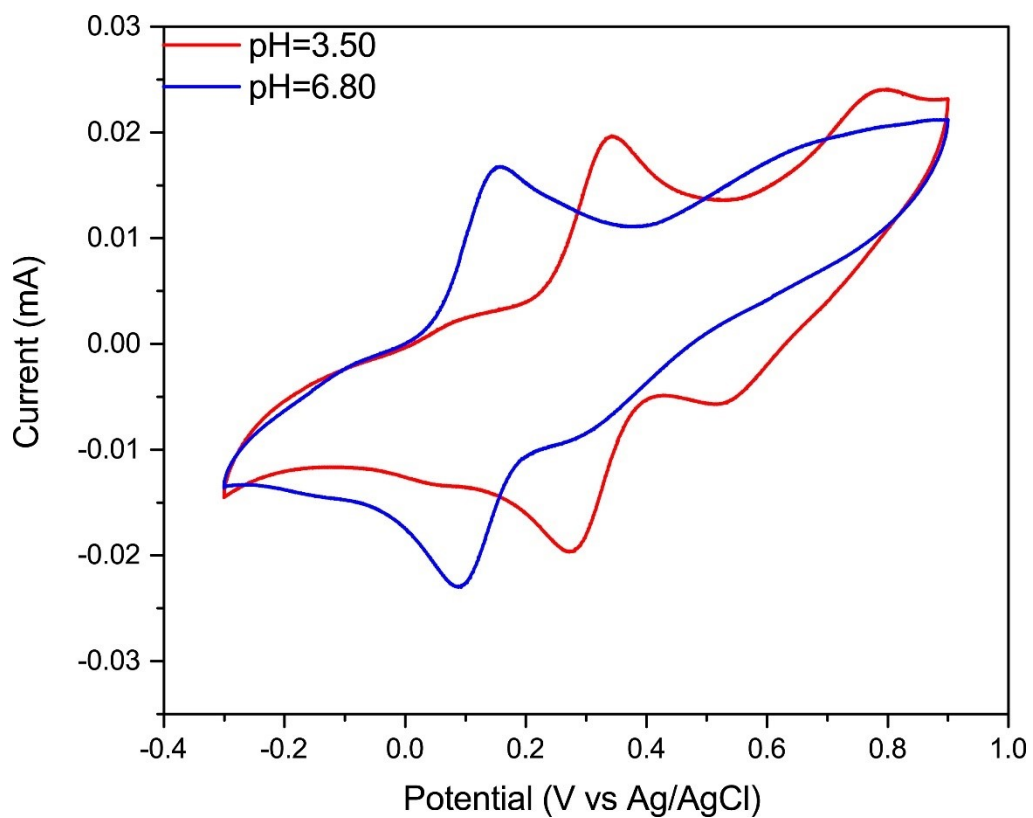


**Figure S49.** CV traces of  $[\text{Os}(\text{bpy})_2(\text{OH}_2)(\text{py}^L)](\text{PF}_6)_2$  ( $\text{py}^L=4\text{-cyanopyridine}$ ) in B-R buffer at different pH values. Concentration of  $[\text{Os}(\text{bpy})_2(\text{OH}_2)(\text{py}^L)](\text{PF}_6)_2 = 2 \text{ mM}$ ; scan rate = 100 mV/s. At pH 6.8: reversible waves at 0.112 V vs Ag/AgCl ( $\text{Os}^{\text{II/III}}$ ) and 0.482 V vs Ag/AgCl ( $\text{Os}^{\text{III/IV}}$ ).

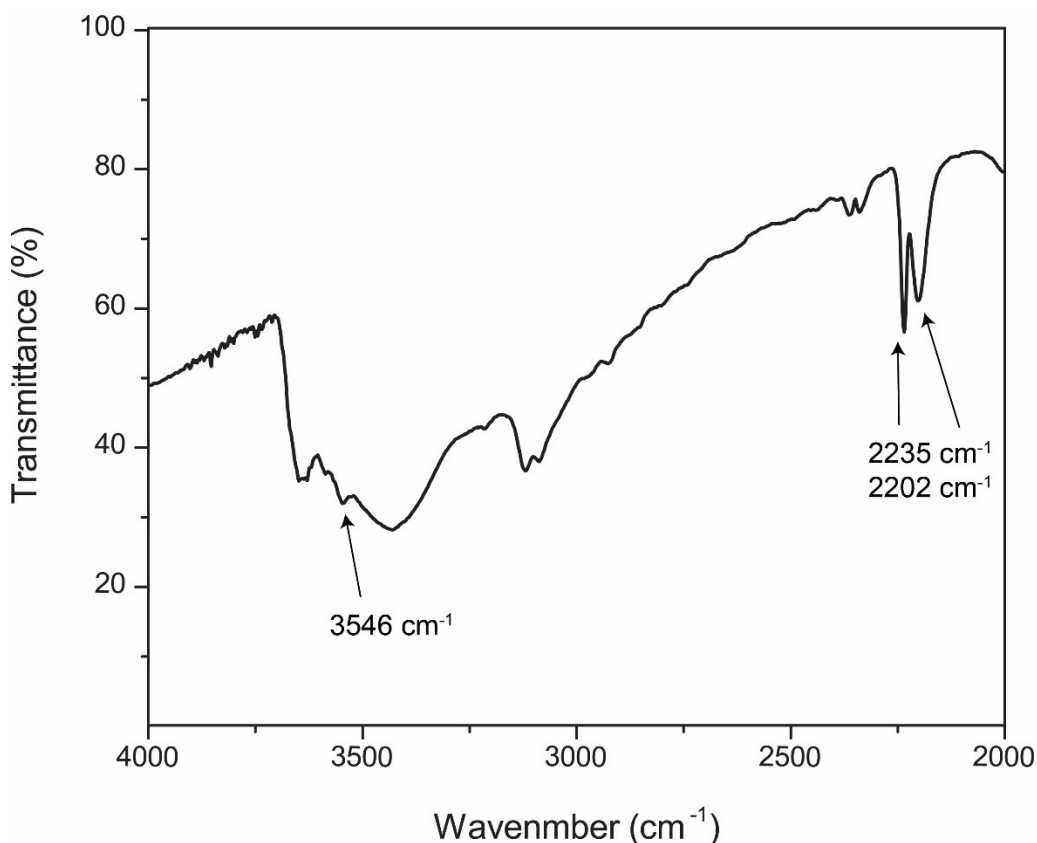


**Figure S50.** Transmission FTIR spectrum of  $[\text{Os}(\text{bpy})_2(\text{OH}_2)(\text{py}^L)](\text{PF}_6)_2$  ( $\text{py}^L=4\text{-cyanopyridine}$ ); the O-H stretch of the coordinated water occurred at  $3546\text{ cm}^{-1}$  and the C-N stretch of the coordinated cyanopyridine occurred at  $2235$  and  $2202\text{ cm}^{-1}$ .

**4-chloropyridine derivative (8):**  $^1\text{H NMR}$  (400 MHz,  $\text{D}_2\text{O}$ , 298 K)  $\delta$  8.92 (d,  $J = 5.7\text{ Hz}$ , 1H), 8.44 (d,  $J = 8.3\text{ Hz}$ , 1H), 8.37 (d,  $J = 5.8\text{ Hz}$ , 1H), 8.27 (dd,  $J = 13.1, 8.3\text{ Hz}$ , 2H), 8.19 (s, 2H), 8.11 (d,  $J = 8.2\text{ Hz}$ , 1H), 7.85 – 7.67 (m, 2H), 7.61 (dd,  $J = 9.6, 6.1\text{ Hz}$ , 2H), 7.57 – 7.50 (m, 1H), 7.50 – 7.39 (m, 2H), 7.34 (t,  $J = 7.8\text{ Hz}$ , 1H), 7.21 (d,  $J = 6.2\text{ Hz}$ , 2H), 6.96 (t,  $J = 6.7\text{ Hz}$ , 1H), 6.88 (t,  $J = 6.7\text{ Hz}$ , 1H). Elemental analysis: found: C 32.02%, H 2.40%, N 7.31%; calcd for  $\text{C}_{26}\text{H}_{22}\text{N}_6\text{OOSF}_{12}\text{P}_2$ , C 32.49%, H 2.40%, N 7.58%. IR (ATR):  $\nu_{\text{max}} 3545\text{ cm}^{-1}$ .

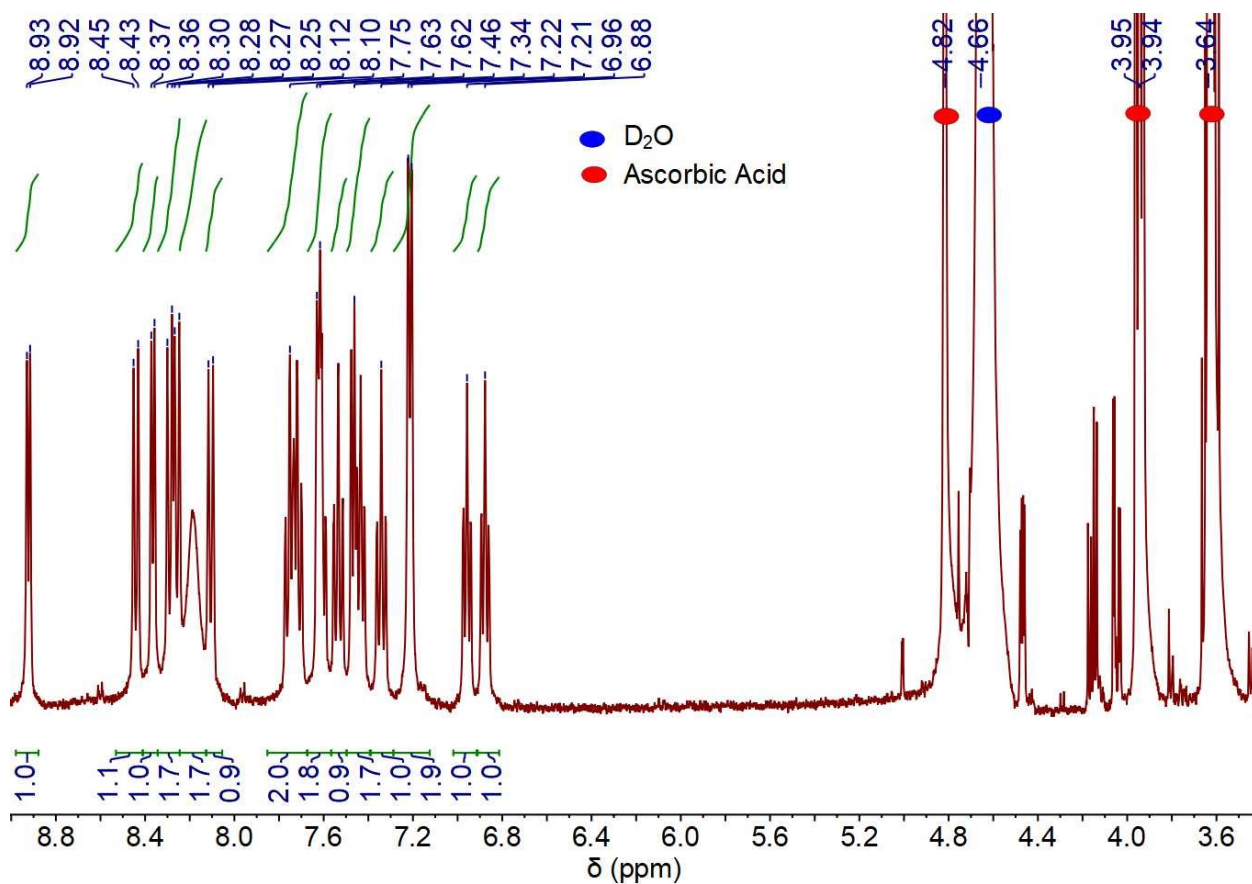


**Figure S51.** <sup>1</sup>H NMR spectrum of [Os(bpy)<sub>2</sub>(OH<sub>2</sub>)(py<sup>L</sup>)](PF<sub>6</sub>)<sub>2</sub> (py<sup>L</sup>=4-chloropyridine) (400 MHz, DMSO-*d*<sub>6</sub>, 298 K). Ascorbic acid (around 5 equiv) was added to the NMR solvent to reduce paramagnetic Os(III) to Os(II) to improve the quality of the spectrum.

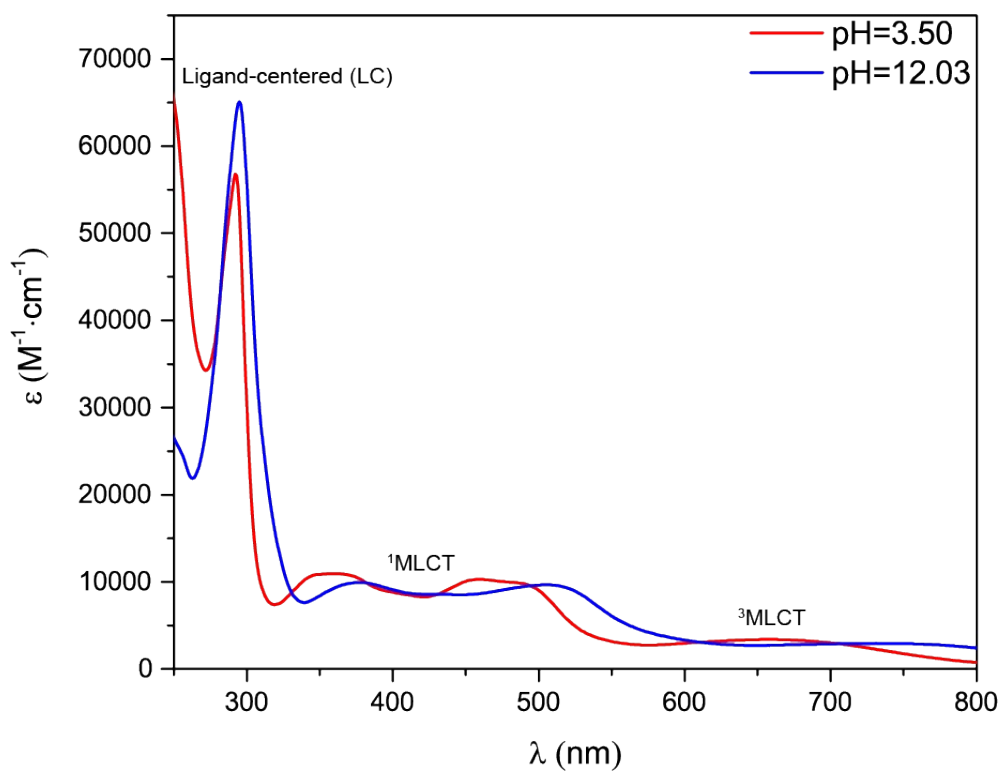


**Figure S52.** UV-Vis spectra of freshly prepared  $[\text{Os}(\text{bpy})_2(\text{OH}_2)(\text{py}^L)](\text{PF}_6)_2$  ( $\text{py}^L=4\text{-chloropyridine}$ ) in B-R buffer at different pH values. Concentration = 0.5 mM, ascorbic acid (around 5 equiv) was added to reduce excess Os(III) to Os(II); Tentative assignment at pH=3.50:  $\lambda_{\text{max}}$ : 657 nm ( ${}^3\text{MLCT}$ ,  $\epsilon=3386.8 \text{ M}^{-1} \text{ cm}^{-1}$ ); 460 nm ( ${}^1\text{MLCT}$ ,  $\epsilon=10285.02 \text{ M}^{-1} \text{ cm}^{-1}$ ); 362 nm ( ${}^1\text{MLCT}$ ,  $\epsilon=10940.5 \text{ M}^{-1} \text{ cm}^{-1}$ ); 292 nm (LC,  $\epsilon=56802.7 \text{ M}^{-1} \text{ cm}^{-1}$ ).<sup>8</sup>

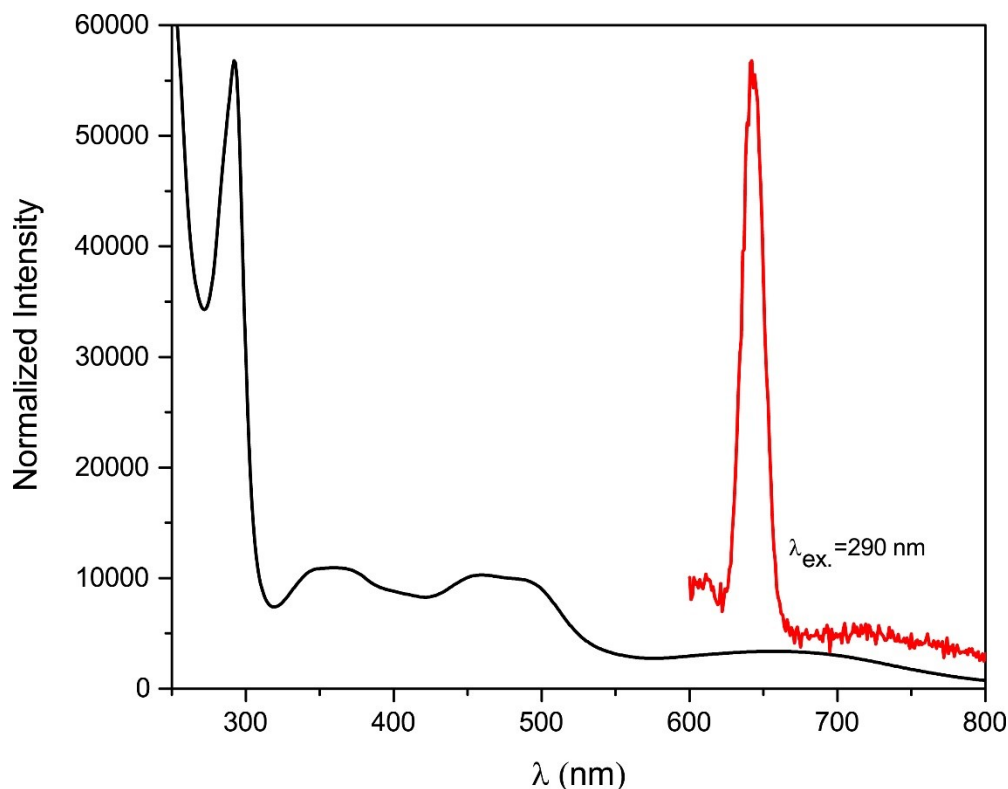


**Figure S53.** Emission spectrum (red) of  $[\text{Os}(\text{bpy})_2(\text{OH}_2)(\text{py}^L)](\text{PF}_6)_2$  ( $\text{py}^L=4\text{-chloropyridine}$ ) in B-R buffer (the black trace is the UV-Vis spectrum) at pH 3.5.  $\lambda_{\text{em. max}} = 642 \text{ nm}$  at  $\lambda_{\text{exc.}} = 290 \text{ nm}$ .

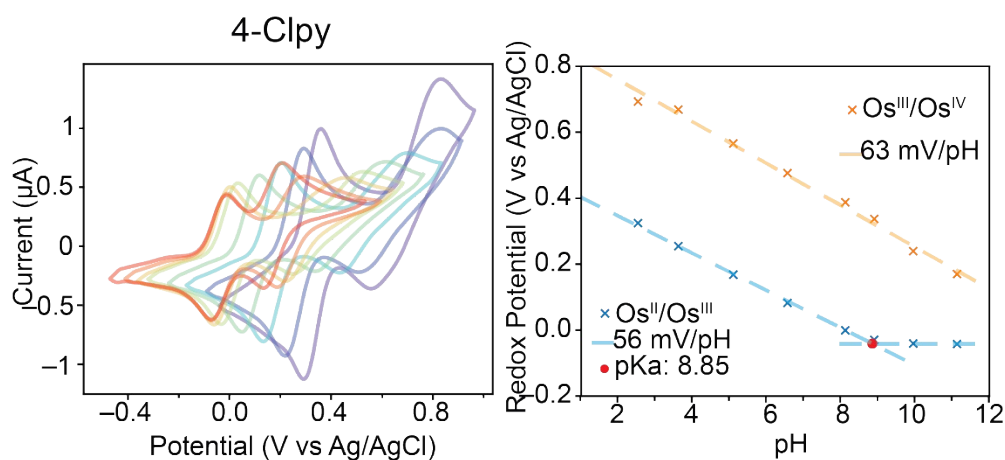


**Figure S54.** (a) CV traces of  $[\text{Os}(\text{bpy})_2(\text{OH}_2)(\text{py}^L)](\text{PF}_6)_2$  ( $\text{py}^L=4\text{-chloropyridine}$ ) in B-R buffer at different pH values; (b)  $\text{pK}_a$  determination of the water ligand of  $[\text{Os}(\text{bpy})_2(\text{OH}_2)(\text{py}^L)](\text{PF}_6)_2$  ( $\text{py}^L=4\text{-chloropyridine}$ ) by construction of a Pourbaix diagram ( $\text{pK}_a = 8.85$ ).

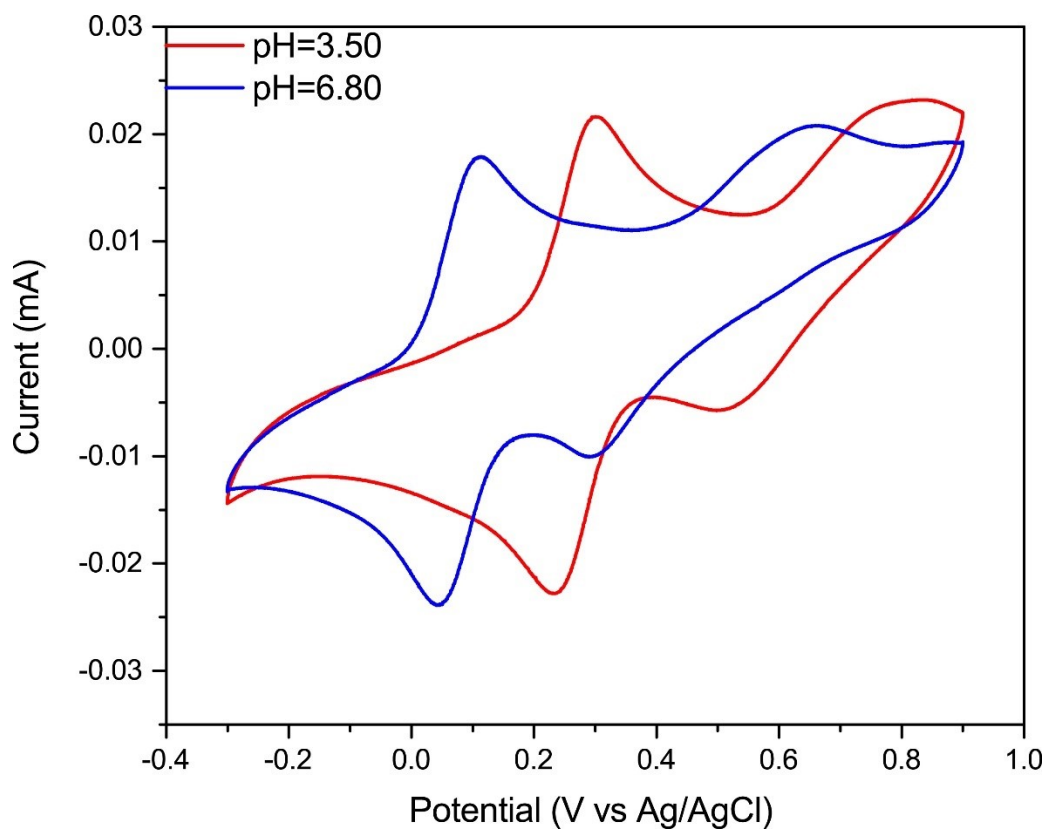


**Figure S55.** CV traces of  $[\text{Os}(\text{bpy})_2(\text{OH}_2)(\text{py}^L)](\text{PF}_6)_2$  ( $\text{py}^L=4\text{-chloropyridine}$ ) in B-R buffer at different pH values. Concentration of  $[\text{Os}(\text{bpy})_2(\text{OH}_2)(\text{py}^L)](\text{PF}_6)_2 = 2 \text{ mM}$ ; scan rate = 100 mV/s. At pH 6.8: reversible waves at 0.083 V vs Ag/AgCl ( $\text{Os}^{\text{II/III}}$ ) and 0.474 V vs Ag/AgCl ( $\text{Os}^{\text{III/IV}}$ ).

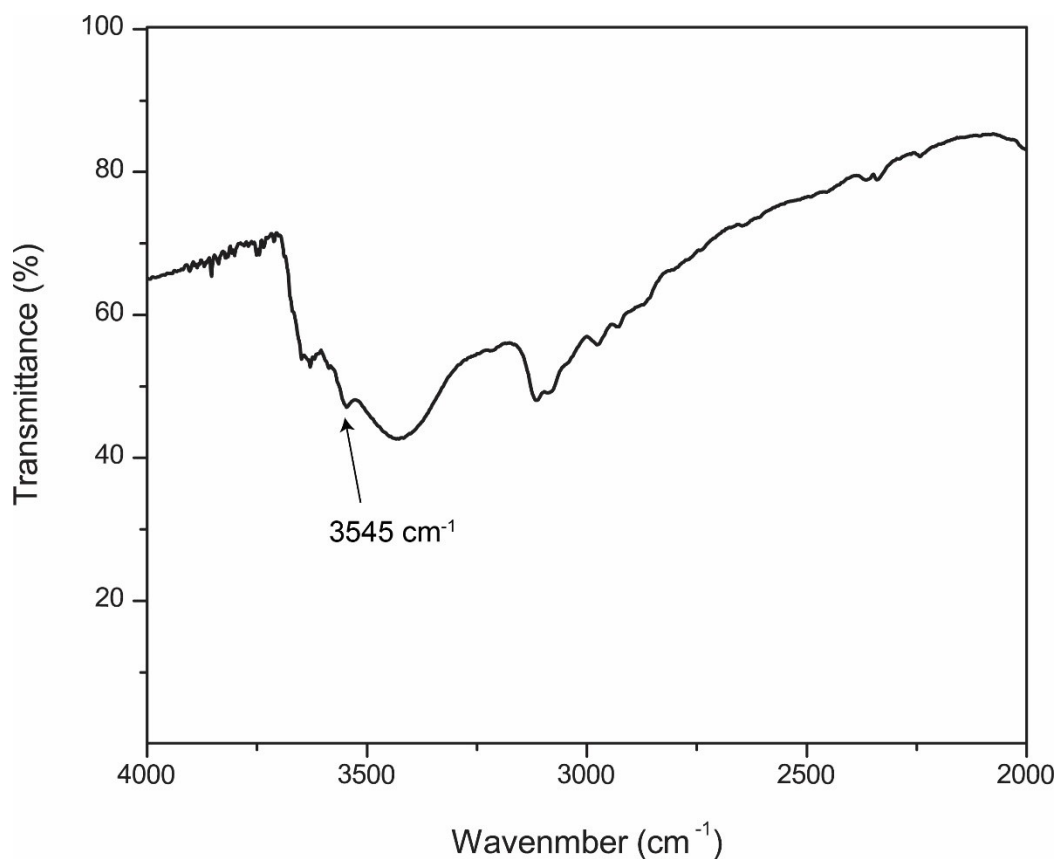
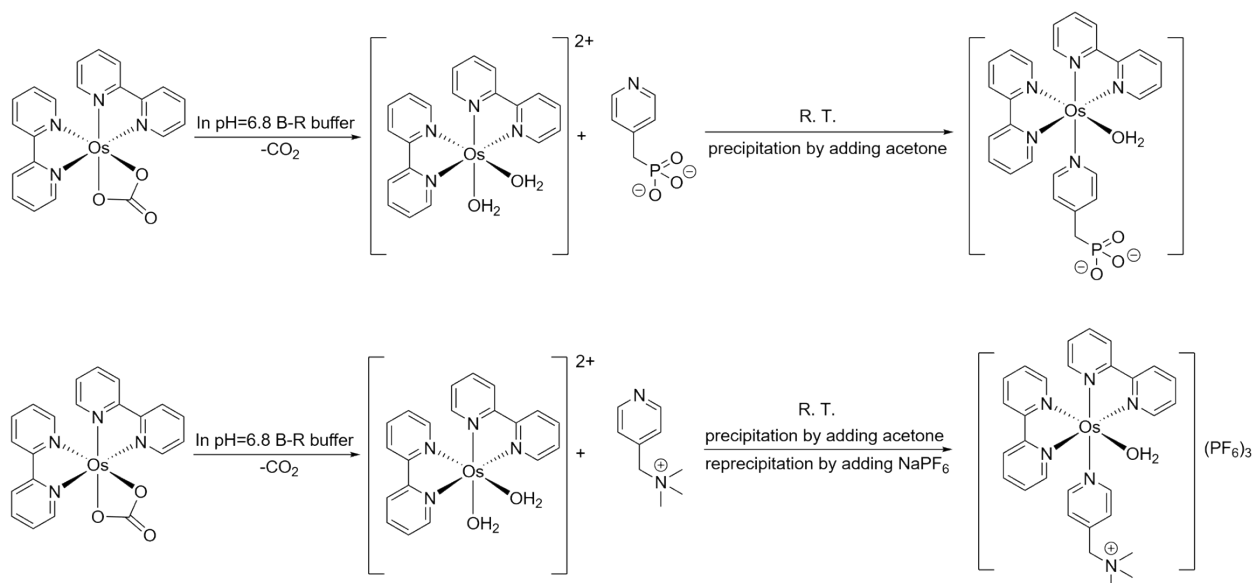


**Figure S56.** Transmission FTIR spectrum of  $[\text{Os}(\text{bpy})_2(\text{OH}_2)(\text{py}^L)](\text{PF}_6)_2$  ( $\text{py}^L=4\text{-chloropyridine}$ ); the O-H stretch of the coordinated water occurred at  $3545\text{ cm}^{-1}$ .

### S3.6 Synthesis of $[\text{Os}(\text{bpy})_2(\text{OH}_2)(\text{py}^L)](\text{PF}_6)_x$ ( $\text{py}^L=4\text{-pyridylmethylphosphonic acid}$ , $4\text{-N}$ - $(\text{pyridin-4-ylmethyl})\text{-N,N,N}$ -trimethylammonium)



General procedure for synthesis of ionic pyridine derivative 4-pyridylmethylphosphonic acid, 4-*N*-(pyridin-4-ylmethyl)-*N,N,N*-trimethylammonium: In a 10 mL round-bottom flask, pH 3.5 B-R buffer (5 mL) was added to  $\text{Os}(\text{bpy})_2\text{CO}_3$  (47.9 mg, 0.0850 mmol, 1.00 equiv). Pyridine (around 23 equiv)

added to the mixture with stirring and the pH of the solution was adjusted to 6.8. CV of the solution was monitored in situ until the current of the peak  $E_{1/2}=0.033$  V (for 4-pyridylmethylphosphonic acid, 20 minutes will be adequate) and  $E_{1/2}=0.103$  V (for 4-*N*-(pyridin-4-ylmethyl)-*N,N,N*-trimethylammonium, 30 minutes will be adequate) reached a plateau.

For 4-pyridylmethylphosphonic acid derivative: Acetone (250 mL) was added to the 5 mL aqueous mixture, and the mixture was allowed to stay steady at room temperature for 30 minutes affording a black precipitate. The precipitate consisting of the product and the starting material 4-pyridylmethylphosphonic acid derivative was redissolved in DI water (10 mL), and the aqueous solution was dried in a lyophilizer. The crude product could be purified by both HiTrap Q HP (Cytiva brand) and HiTrap SP HP (Cytiva brand) ion exchange columns to remove the starting material 4-pyridylmethylphosphonic acid. For the ion exchange column, the crude product (10 mg) was dissolved in DI water (0.3 mL), and the eluent is DI water. The yellow-colored fraction was collected and dried by a lyophilizer (column yield 9.1 mg, 91%, mixed with exchanged salt which does not have electrochemical signals).

For 4-*N*-(pyridin-4-ylmethyl)-*N,N,N*-trimethylammonium derivative (the precursor 4-*N*-(pyridin-4-ylmethyl)-*N,N,N*-trimethylammonium was synthesized from a reported procedure.<sup>9</sup>): Acetone (400 mL) was added to the 5 mL aqueous mixture, and the mixture was allowed to stay steady under room temperature for 2 hours affording a red-black precipitate. The purple precipitate was collected by vacuum filtration and redissolved in DI water (5 mL). Solid NaPF<sub>6</sub> (200 mg, 1.19 mmol, 7.00 equiv) was added to the aqueous solution affording a yellow-black precipitate which was collected by vacuum filtration, washed with cold water (5 mL) and diethyl ether (20 mL), and dried at room temperature under dynamic vacuum overnight.

(yields: 4-pyridylmethylphosphonic acid 91% mixed with exchanged salt; 4-*N*-(pyridin-4-ylmethyl)-*N,N,N*-trimethylammonium 40±22%)

**4-pyridylmethylphosphonic acid derivative after ion exchange column (9):** <sup>1</sup>H NMR (400 MHz, D<sub>2</sub>O, 298 K) δ 8.94 (dt, *J* = 5.6, 1.3 Hz, 1H), 8.47 – 8.35 (m, 2H), 8.26 (dd, *J* = 8.4, 1.3 Hz, 1H), 8.22 (dd, *J* = 8.2, 1.3 Hz, 1H), 8.18 – 8.00 (m, 3H), 7.71 (td, *J* = 7.9, 1.4 Hz, 1H), 7.69 – 7.64 (m, 1H), 7.62 (d, *J* = 6.0 Hz, 1H), 7.58 (ddd, *J* = 7.5, 5.7, 1.4 Hz, 1H), 7.50 (td, *J* = 7.9, 1.4 Hz, 1H), 7.47 (d, *J* = 5.7 Hz, 1H), 7.40 (ddd, *J* = 7.4, 5.8, 1.3 Hz, 1H), 7.31 (td, *J* = 7.9, 1.3 Hz, 1H), 7.04 (d, *J* = 5.8 Hz, 2H), 6.93 (ddd, *J* = 7.4, 5.9, 1.3 Hz, 1H), 6.85 (ddd, *J* = 7.4, 5.9, 1.4 Hz, 1H), 2.86 (d, *J* = 21.4 Hz, 2H); <sup>31</sup>P NMR (162 MHz, D<sub>2</sub>O, 298 K) δ 16.95.

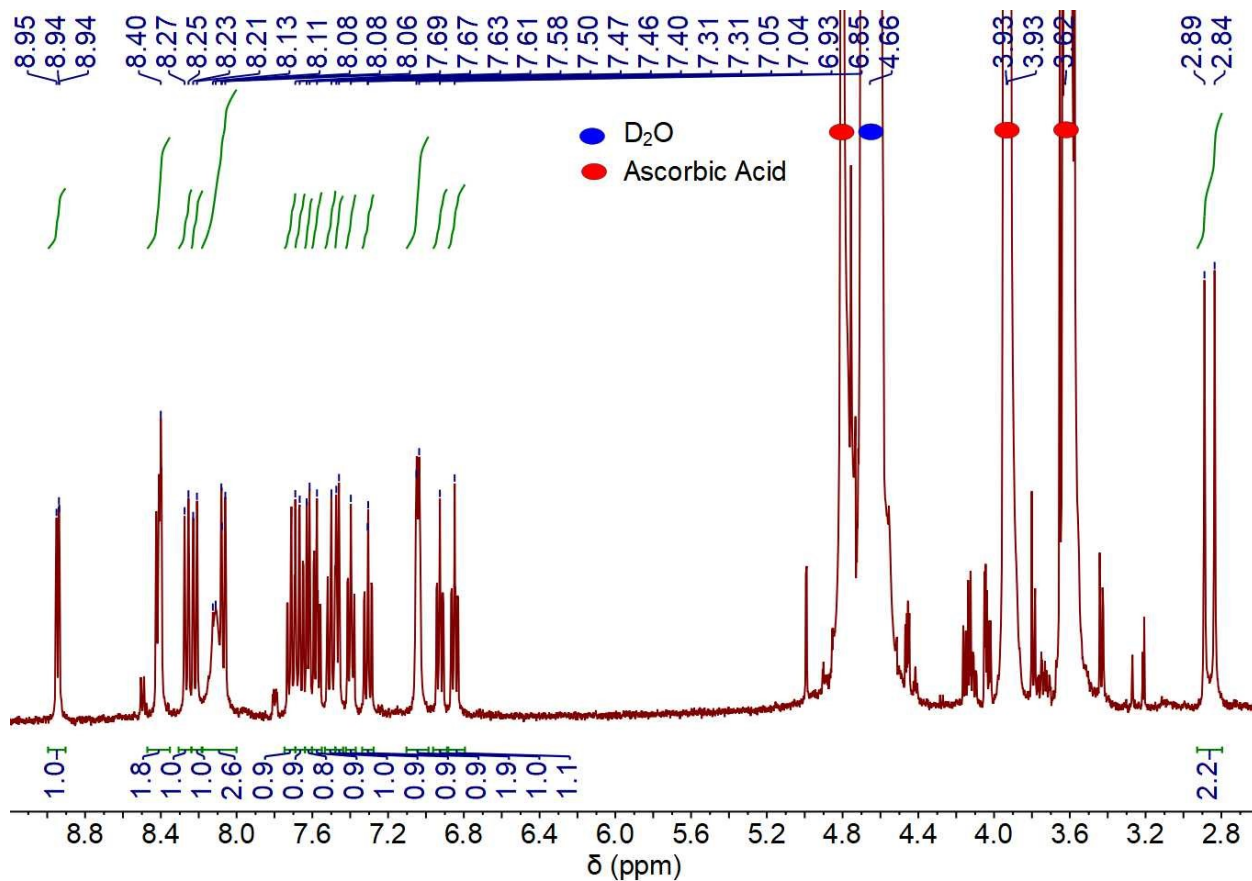


**Figure S57.** <sup>1</sup>H NMR spectrum of [Os(bpy)<sub>2</sub>(OH<sub>2</sub>)(py<sup>L</sup>)] (py<sup>L</sup>=4-pyridylmethylphosphonic acid) (400 MHz, D<sub>2</sub>O, 298 K). Ascorbic acid (around 5 equiv) was added to the NMR solvent to reduce paramagnetic Os(III) to Os(II) to improve the quality of the spectrum.

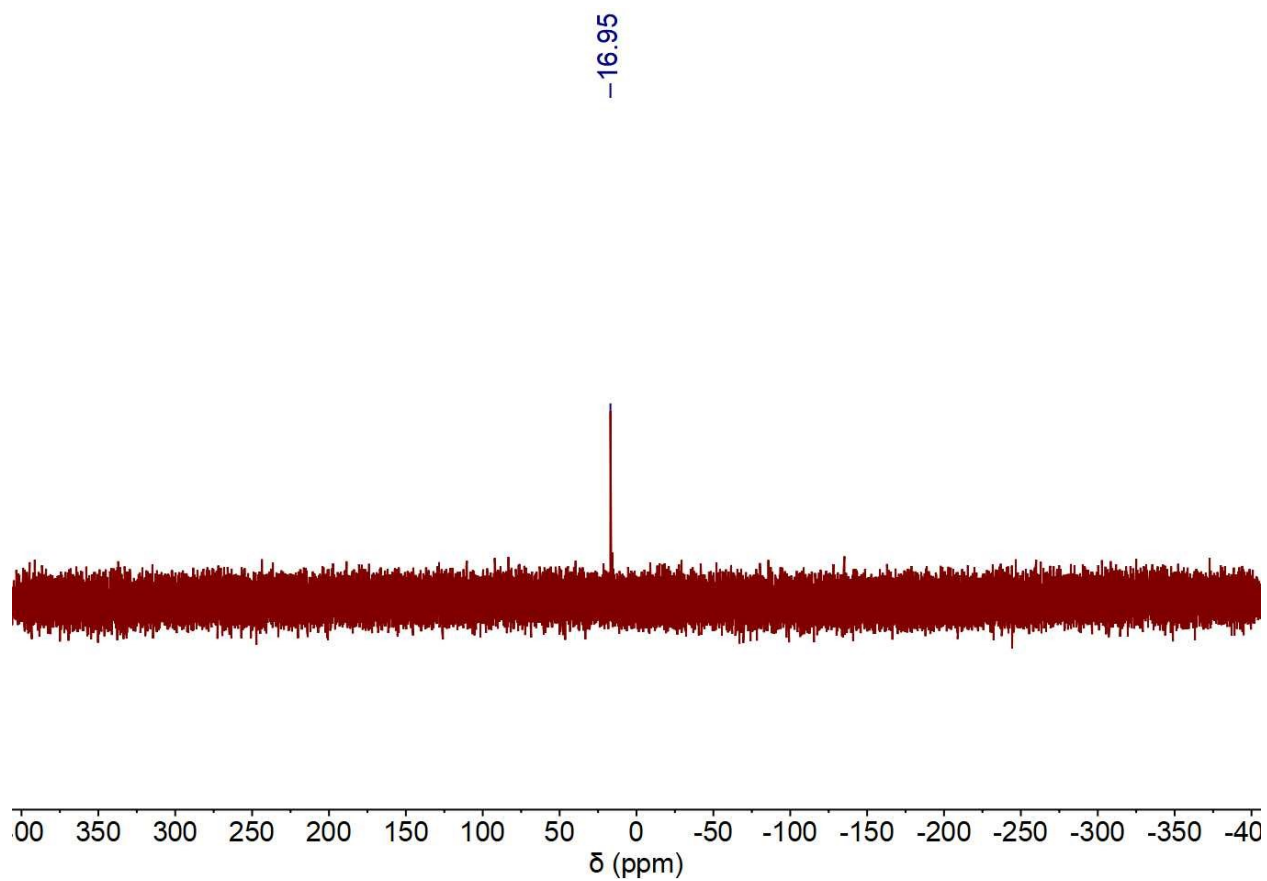


**Figure S58.**  $^{31}\text{P}$  NMR spectrum of  $[\text{Os}(\text{bpy})_2(\text{OH}_2)(\text{py}^L)]$  ( $\text{py}^L=4$ -pyridylmethylphosphonic acid) (162 MHz,  $\text{D}_2\text{O}$ , 298 K). Ascorbic acid (around 5 equiv) was added to the NMR solvent to reduce paramagnetic Os(III) to Os(II) to improve the quality of the spectrum.

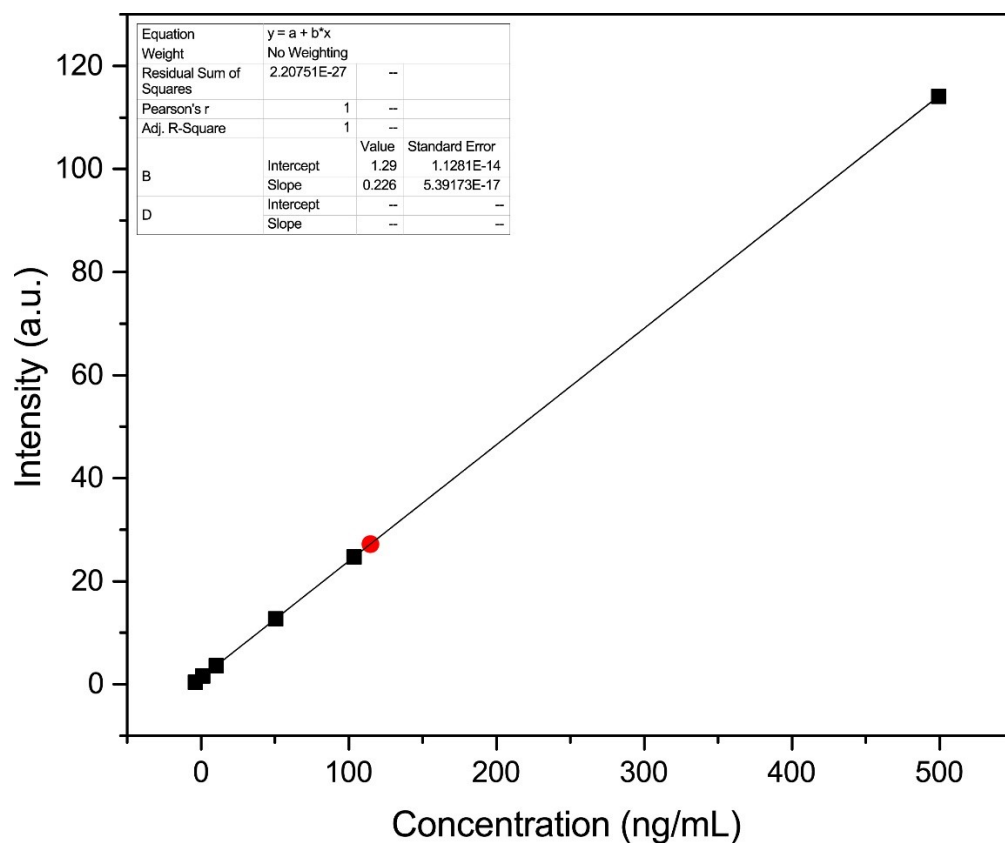


**Figure S59.** ICP-MS analysis of the osmium content to check the bulk purity for  $[\text{Os}(\text{bpy})_2(\text{OH}_2)(\text{py}^L)]$  ( $\text{py}^L=4$ -pyridylmethylphosphonic acid). The osmium concentration of the unknown sample (red dot) was found to be 114.73 ng/mL; therefore, the bulk purity of the sample is 8.69 wt% based on the calibration line (black line).

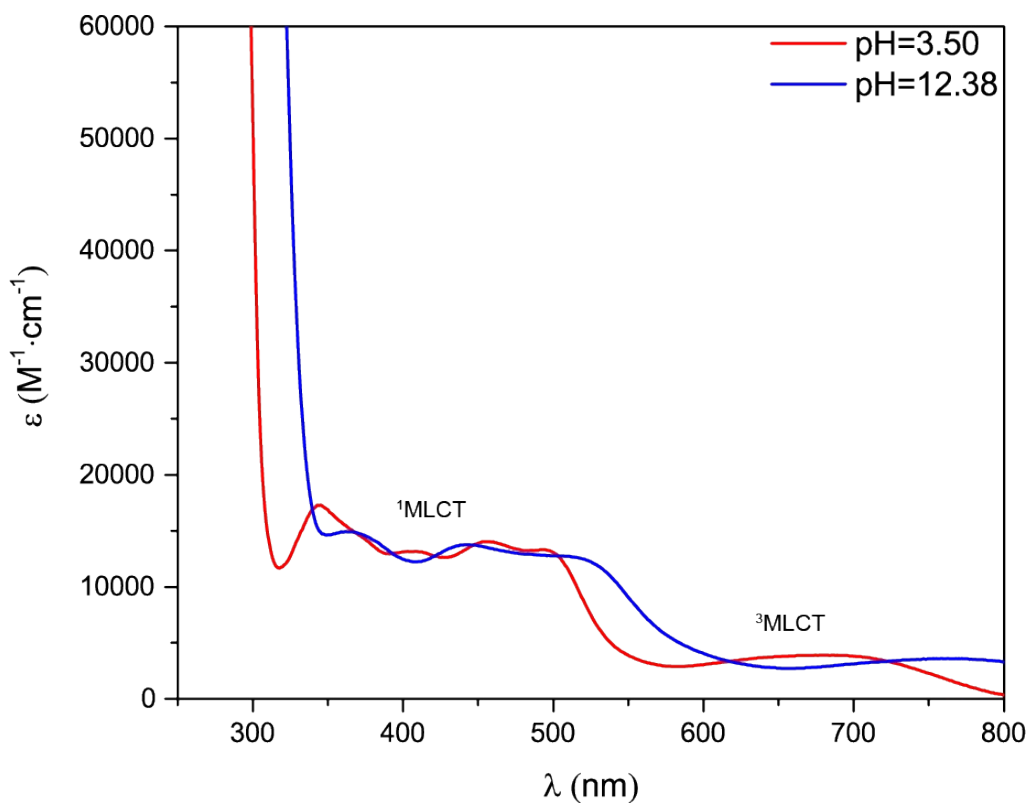


**Figure S60.** UV-Vis spectra of freshly prepared  $[\text{Os}(\text{bpy})_2(\text{OH}_2)(\text{py}^L)]$  ( $\text{py}^L=4$ -pyridylmethylphosphonic acid) in B-R buffer at different pH values. Concentration = 2 mM, ascorbic acid (around 5 equiv) was added to reduce excess Os(III) to Os(II); Tentative assignment at pH=3.50:  $\lambda_{\text{max}}$ : 685 nm ( $^3\text{MLCT}$ ,  $\epsilon=3898.0 \text{ M}^{-1} \text{ cm}^{-1}$ ); 493 nm ( $^1\text{MLCT}$ ,  $\epsilon=13311.3 \text{ M}^{-1} \text{ cm}^{-1}$ ); 455 nm ( $^1\text{MLCT}$ ,  $\epsilon=14034.6 \text{ M}^{-1} \text{ cm}^{-1}$ ); 403 nm ( $^1\text{MLCT}$ ,  $\epsilon=13174.2 \text{ M}^{-1} \text{ cm}^{-1}$ ); 345 nm ( $^1\text{MLCT}$ ,  $\epsilon=17310.2 \text{ M}^{-1} \text{ cm}^{-1}$ ).<sup>8</sup>

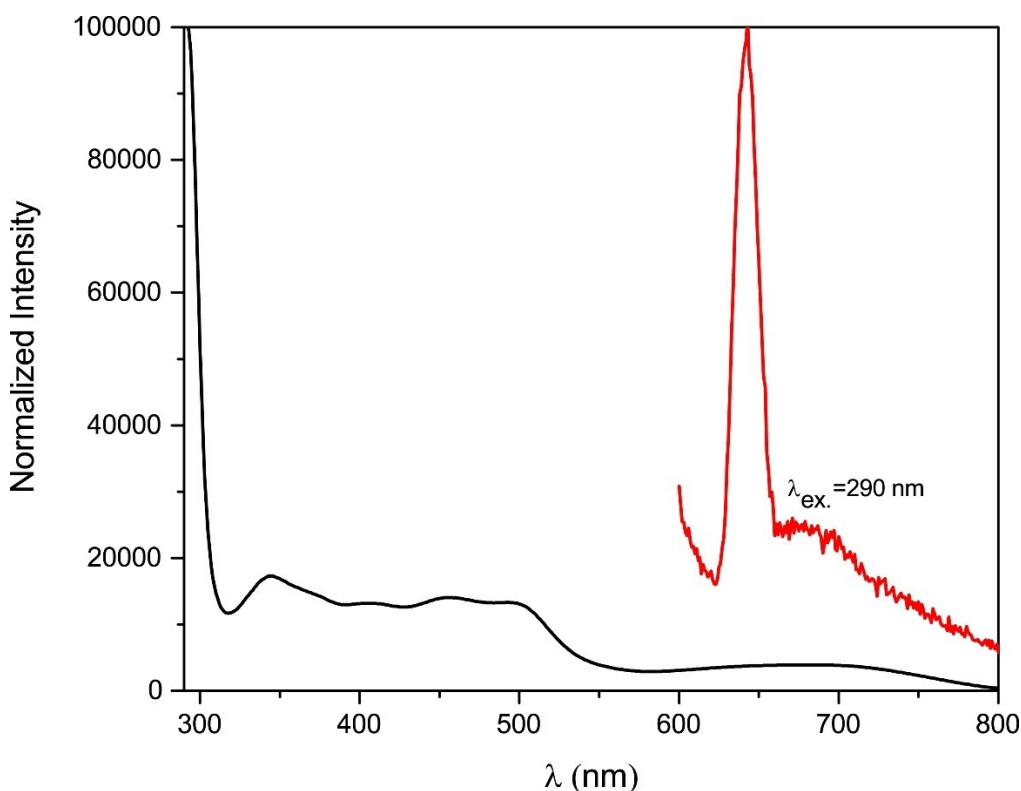


**Figure S61.** Emission spectrum (red) of  $[\text{Os}(\text{bpy})_2(\text{OH}_2)(\text{py}^L)]$  ( $\text{py}^L=4$ -pyridylmethylphosphonic acid) in B-R buffer (the black trace is the UV-Vis spectrum) at pH 3.5.  $\lambda_{\text{em. max}} = 643 \text{ nm}$  at  $\lambda_{\text{exc.}} = 290 \text{ nm}$ .

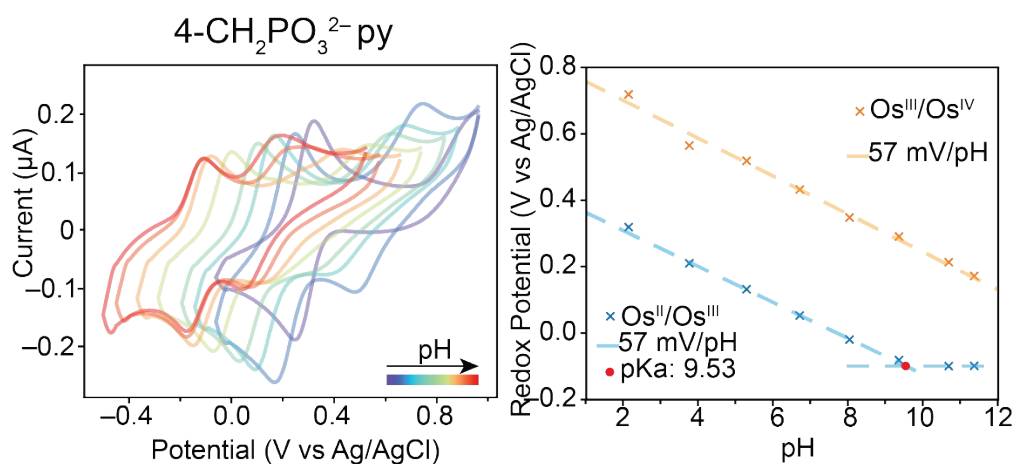


**Figure S62.** (a) CV traces of  $[\text{Os}(\text{bpy})_2(\text{OH}_2)(\text{py}^L)]$  ( $\text{py}^L=4$ -pyridylmethylphosphonic acid) in B-R buffer at different pH values; (b)  $\text{p}K_a$  determination of the water ligand of  $[\text{Os}(\text{bpy})_2(\text{OH}_2)(\text{py}^L)]$  ( $\text{py}^L=4$ -pyridylmethylphosphonic acid) by construction of a Pourbaix diagram ( $\text{p}K_a = 9.53$ ).

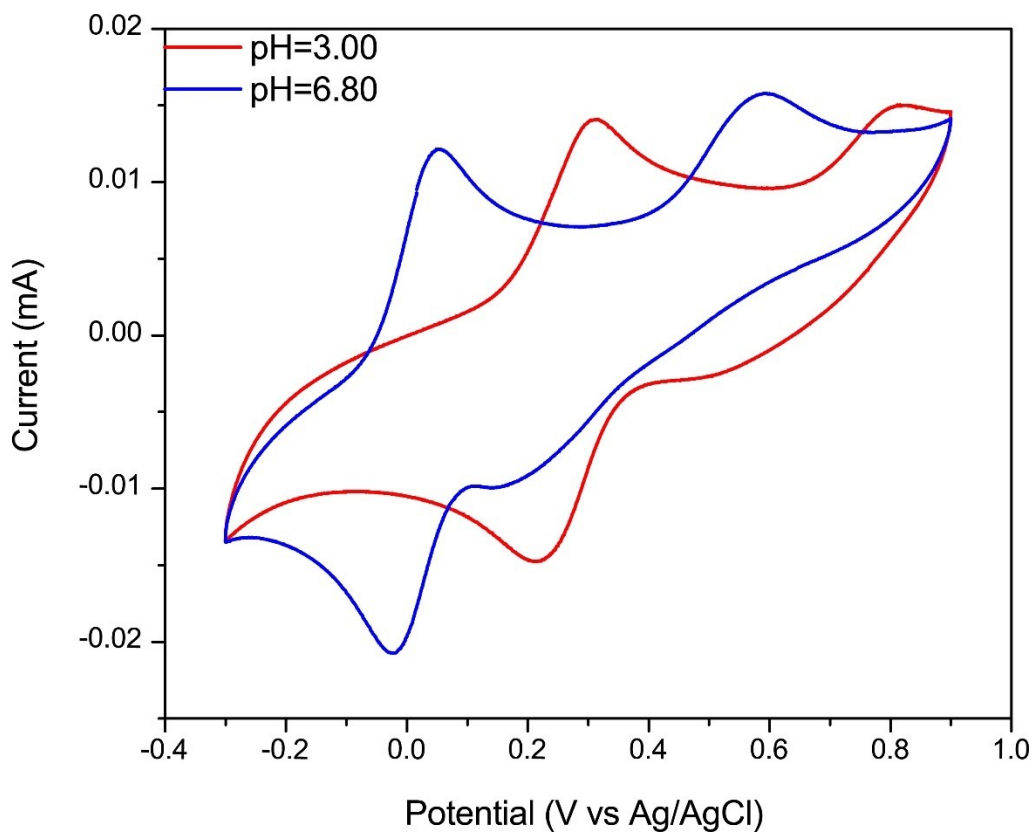


**Figure S63.** CV traces of  $[\text{Os}(\text{bpy})_2(\text{OH}_2)(\text{py}^L)]$  ( $\text{py}^L=4$ -pyridylmethylphosphonic acid) in B-R buffer at different pH values. Concentration of  $[\text{Os}(\text{bpy})_2(\text{OH}_2)(\text{py}^L)] = 2 \text{ mM}$ ; scan rate =  $100 \text{ mV/s}$ . At pH 6.8: reversible waves at  $0.033 \text{ V vs Ag/AgCl}$  ( $\text{Os}^{\text{III/II}}$ ) and  $0.404 \text{ V vs Ag/AgCl}$  ( $\text{Os}^{\text{III/IV}}$ ).

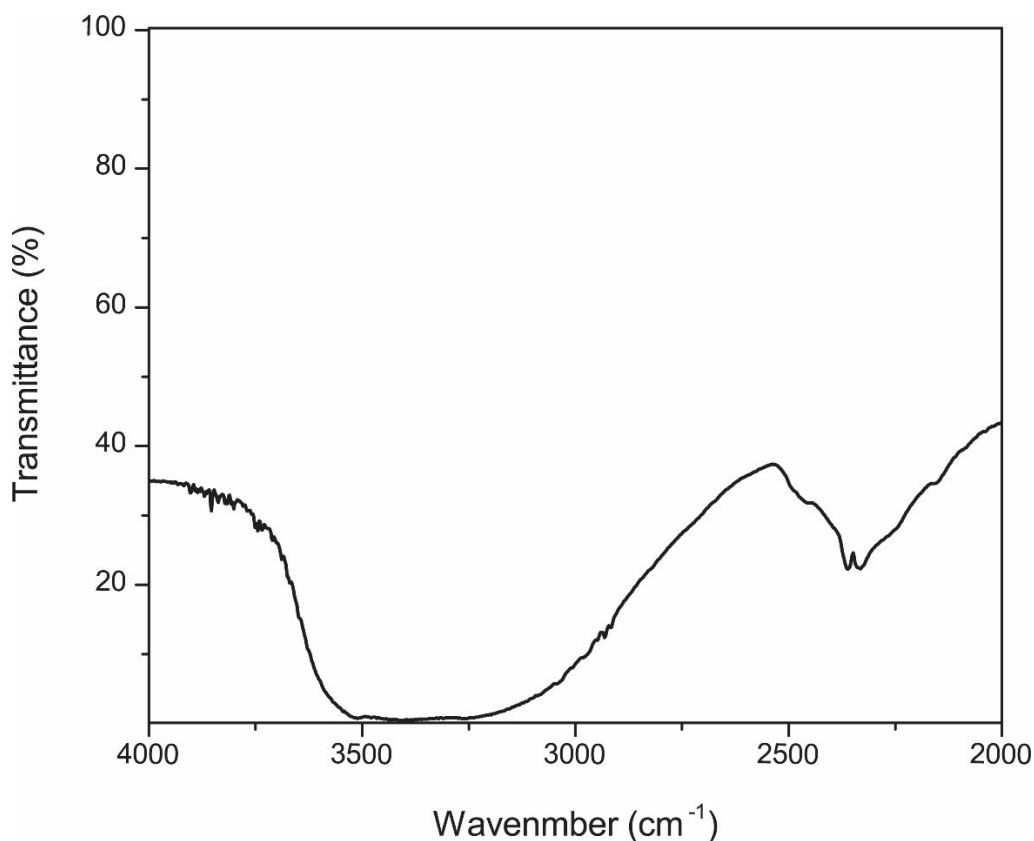


**Figure S64.** Transmission FTIR spectrum of  $[\text{Os}(\text{bpy})_2(\text{OH}_2)(\text{py}^L)]$  ( $\text{py}^L=4$ -pyridylmethylphosphonic acid).

**4-*N*-(pyridin-4-ylmethyl)-*N,N,N*-trimethylammonium derivative (10):**  $^1\text{H}$  NMR (400 MHz,  $\text{D}_2\text{O}$ , 298 K)  $\delta$  8.89 (dd,  $J = 5.6, 1.3$  Hz, 1H), 8.43 (d,  $J = 8.2$  Hz, 3H), 8.33 – 8.22 (m, 3H), 8.14 – 8.07 (m, 1H), 7.73 (dtd,  $J = 9.5, 7.9, 1.4$  Hz, 2H), 7.65 – 7.56 (m, 2H), 7.53 (td,  $J = 7.9, 1.4$  Hz, 1H), 7.45 – 7.39 (m, 2H), 7.33 (td,  $J = 7.8, 1.4$  Hz, 1H), 7.28 (d,  $J = 5.9$  Hz, 2H), 6.96 (ddd,  $J = 7.4, 5.8, 1.4$  Hz, 1H), 6.88 (ddd,  $J = 7.5, 5.9, 1.4$  Hz, 1H), 4.32 (s, 2H), 2.94 (s, 9H).

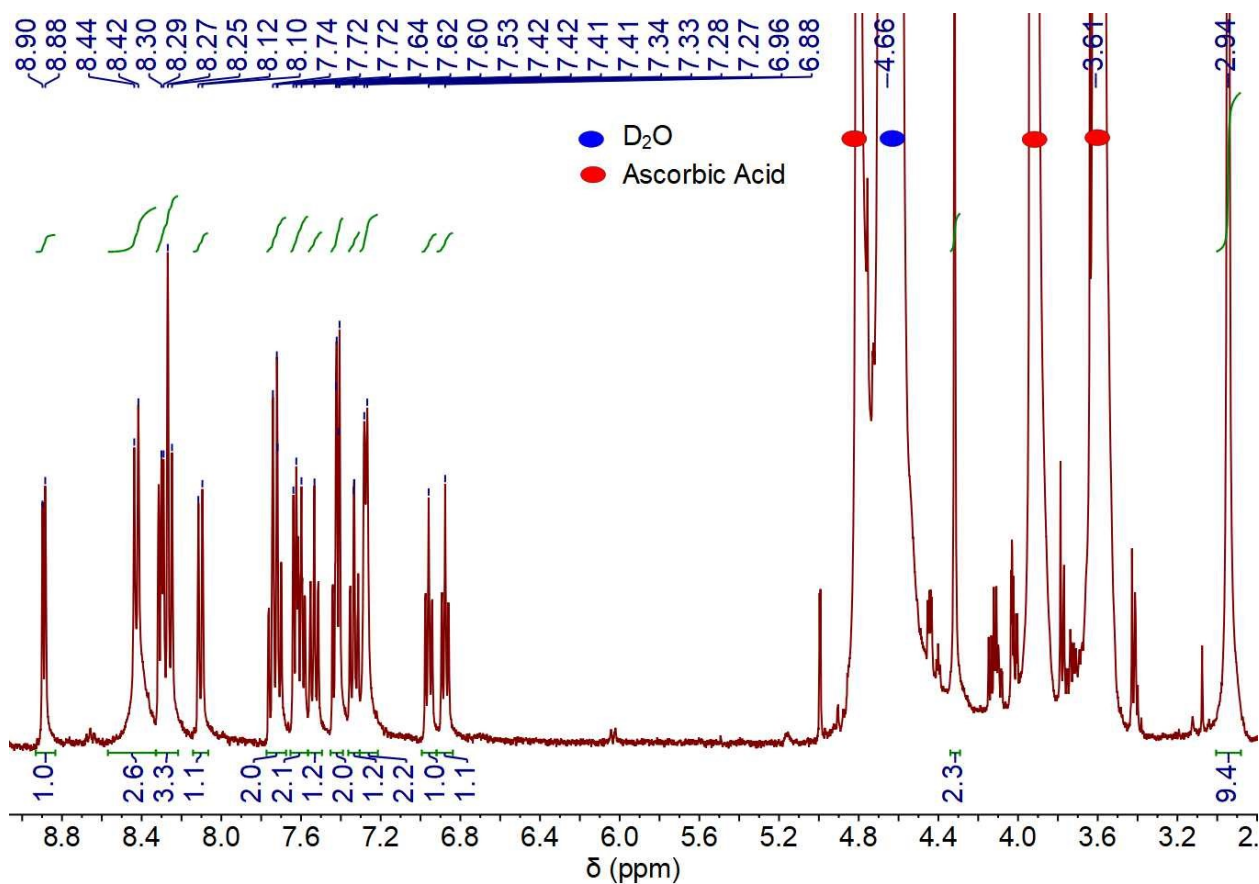


**Figure S65.** <sup>1</sup>H NMR spectrum of [Os(bpy)<sub>2</sub>(OH<sub>2</sub>)(py<sup>L</sup>)](PF<sub>6</sub>)<sub>3</sub> (py<sup>L</sup>=4-*N*-(pyridin-4-ylmethyl)-*N,N,N*-trimethylammonium) (400 MHz, D<sub>2</sub>O, 298 K). Ascorbic acid (around 5 equiv) was added to the NMR solvent to reduce paramagnetic Os(III) to Os(II) to improve the quality of the spectrum.

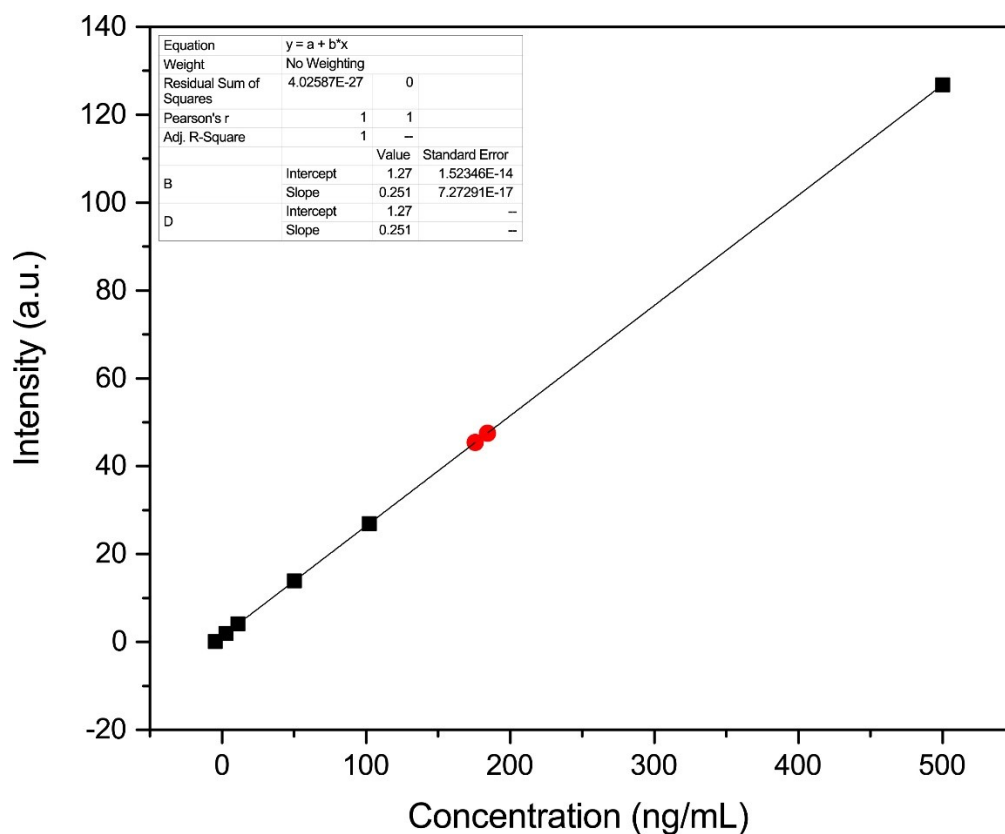


**Figure S66.** ICP-MS analysis of the osmium content to check the bulk purity for  $[\text{Os}(\text{bpy})_2(\text{OH}_2)(\text{py}^+)](\text{PF}_6)_3$  ( $\text{py}^+ = 4\text{-}N\text{-}(\text{pyridin-4-ylmethyl})\text{-}N,N,N\text{-trimethylammonium}$ ). The osmium concentration of the unknown samples (red dots) was found to be  $180.1 \pm 4.2$  ng/mL; therefore, the bulk purity of the sample is  $99.0 \pm 2.4$  wt% based on the calibration line (black line).

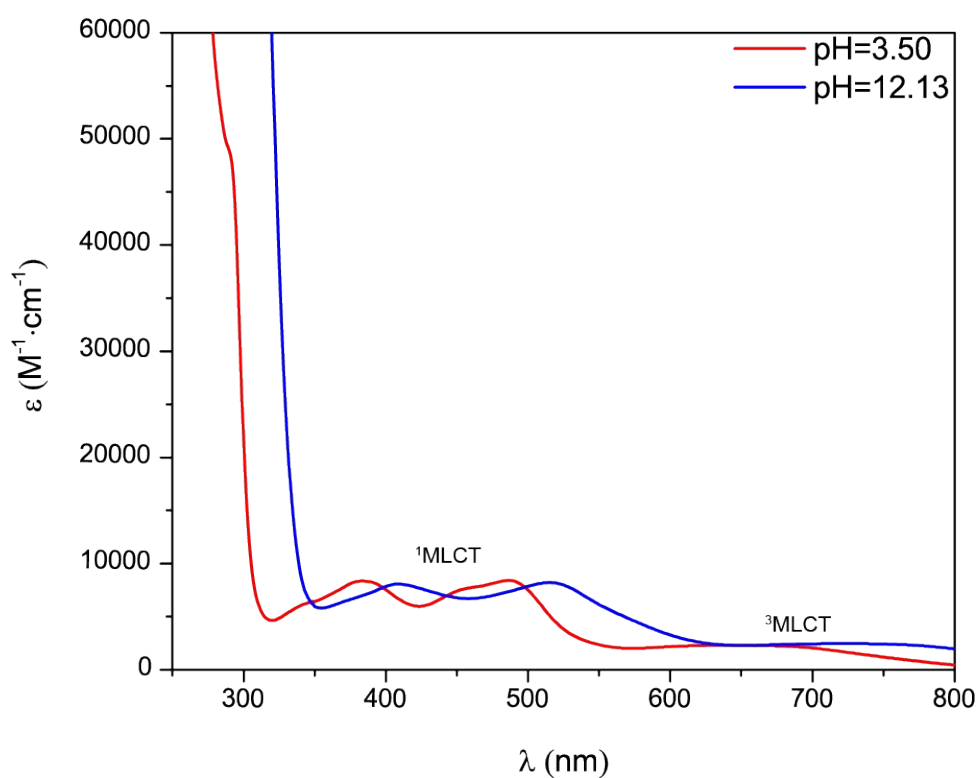


**Figure S67.** UV-Vis spectra of freshly prepared  $[\text{Os}(\text{bpy})_2(\text{OH}_2)(\text{py}^L)](\text{PF}_6)_3$  ( $\text{py}^L=4\text{-}N\text{-}(\text{pyridin-4-ylmethyl})\text{-}N,N,N\text{-trimethylammonium}$ ) in B-R buffer at different pH values. Concentration = 2 mM, ascorbic acid (around 5 equiv) was added to reduce excess Os(III) to Os(II); Tentative assignment at pH=3.50:  $\lambda_{\text{max}}$ : 645 nm ( ${}^3\text{MLCT}$ ,  $\epsilon=2291.9 \text{ M}^{-1} \text{ cm}^{-1}$ ); 486 nm ( ${}^1\text{MLCT}$ ,  $\epsilon=8408.2 \text{ M}^{-1} \text{ cm}^{-1}$ ); 384 nm ( ${}^1\text{MLCT}$ ,  $\epsilon=8353.5 \text{ M}^{-1} \text{ cm}^{-1}$ ).<sup>8</sup>

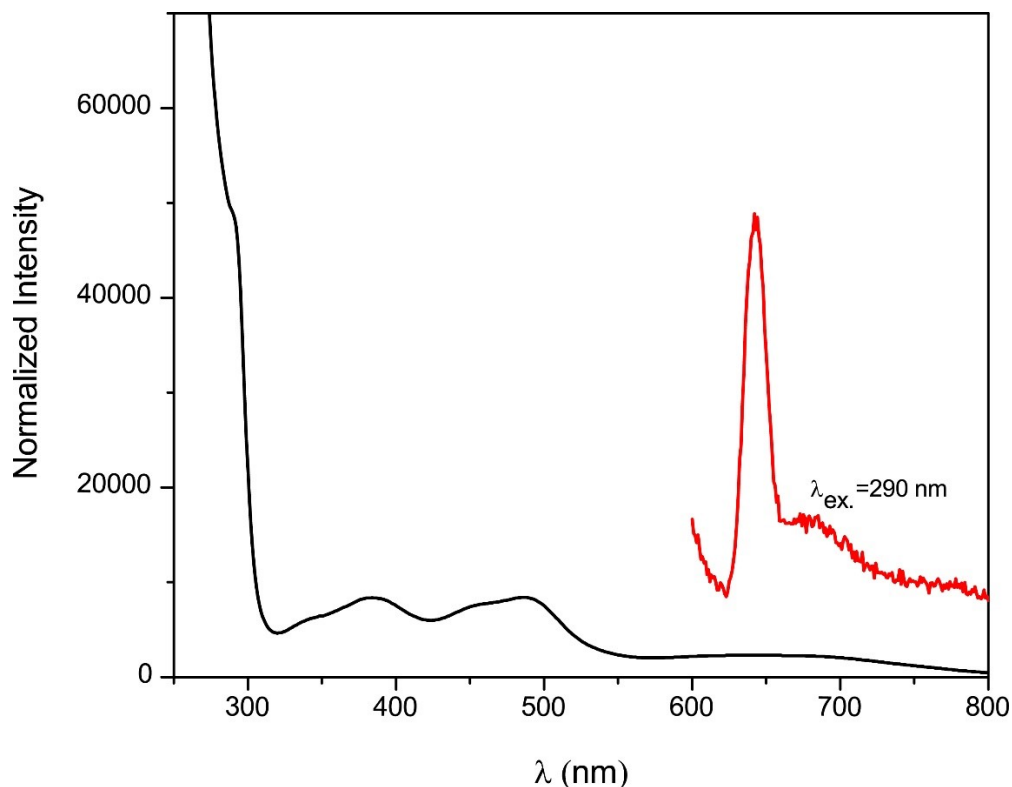


**Figure S68.** Emission spectrum (red) of  $[\text{Os}(\text{bpy})_2(\text{OH}_2)(\text{py}^L)](\text{PF}_6)_3$  ( $\text{py}^L=4\text{-}N\text{-}(\text{pyridin-4-ylmethyl})\text{-}N,N,N\text{-trimethylammonium}$ ) in B-R buffer (the black trace is the UV-Vis spectrum) at pH 3.5.  $\lambda_{\text{em. max}} = 643 \text{ nm}$  at  $\lambda_{\text{exc.}} = 290 \text{ nm}$ .

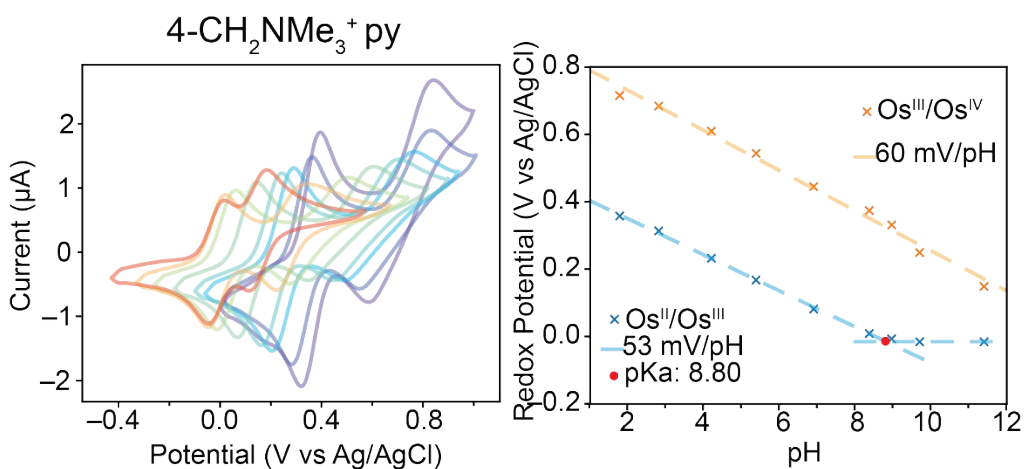


**Figure S69.** (a) CV traces of  $[\text{Os}(\text{bpy})_2(\text{OH}_2)(\text{py}^L)](\text{PF}_6)_3$  ( $\text{py}^L=4\text{-}N\text{-}(\text{pyridin-4-ylmethyl})\text{-}N,N,N\text{-trimethylammonium}$ ) in B-R buffer at different pH values; (b)  $\text{p}K_a$  determination of the water ligand of  $[\text{Os}(\text{bpy})_2(\text{OH}_2)(\text{py}^L)](\text{PF}_6)_3$  ( $\text{py}^L=4\text{-}N\text{-}(\text{pyridin-4-ylmethyl})\text{-}N,N,N\text{-trimethylammonium}$ ) by construction of a Pourbaix diagram ( $\text{p}K_a = 8.80$ ).

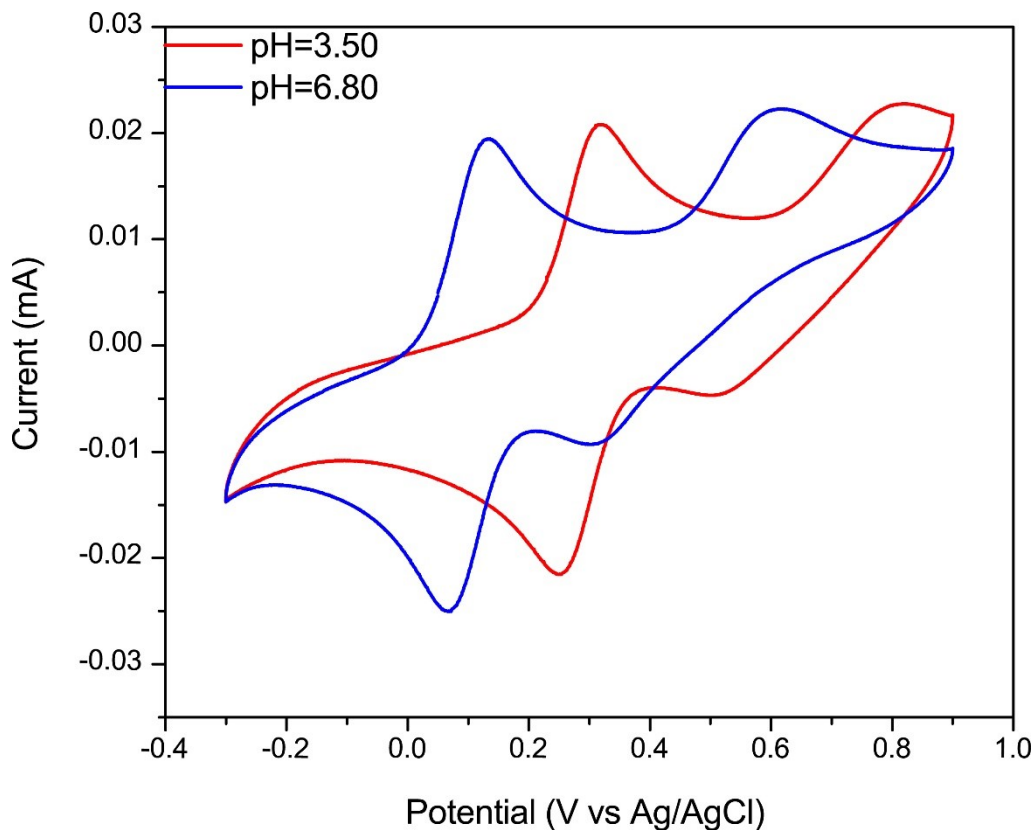


**Figure S70.** CV traces of  $[\text{Os}(\text{bpy})_2(\text{OH}_2)(\text{py}^L)](\text{PF}_6)_3$  ( $\text{py}^L=4\text{-}N\text{-}(\text{pyridin-4-ylmethyl})\text{-}N,N,N\text{-trimethylammonium}$ ) in B-R buffer at different pH values. Concentration of  $[\text{Os}(\text{bpy})_2(\text{OH}_2)(\text{py}^L)](\text{PF}_6)_2 = 2 \text{ mM}$ ; scan rate = 100 mV/s. At pH 6.8: reversible waves at 0.103 V vs Ag/AgCl ( $\text{Os}^{\text{III/IV}}$ ) and 0.458 V vs Ag/AgCl ( $\text{Os}^{\text{III/IV}}$ ).

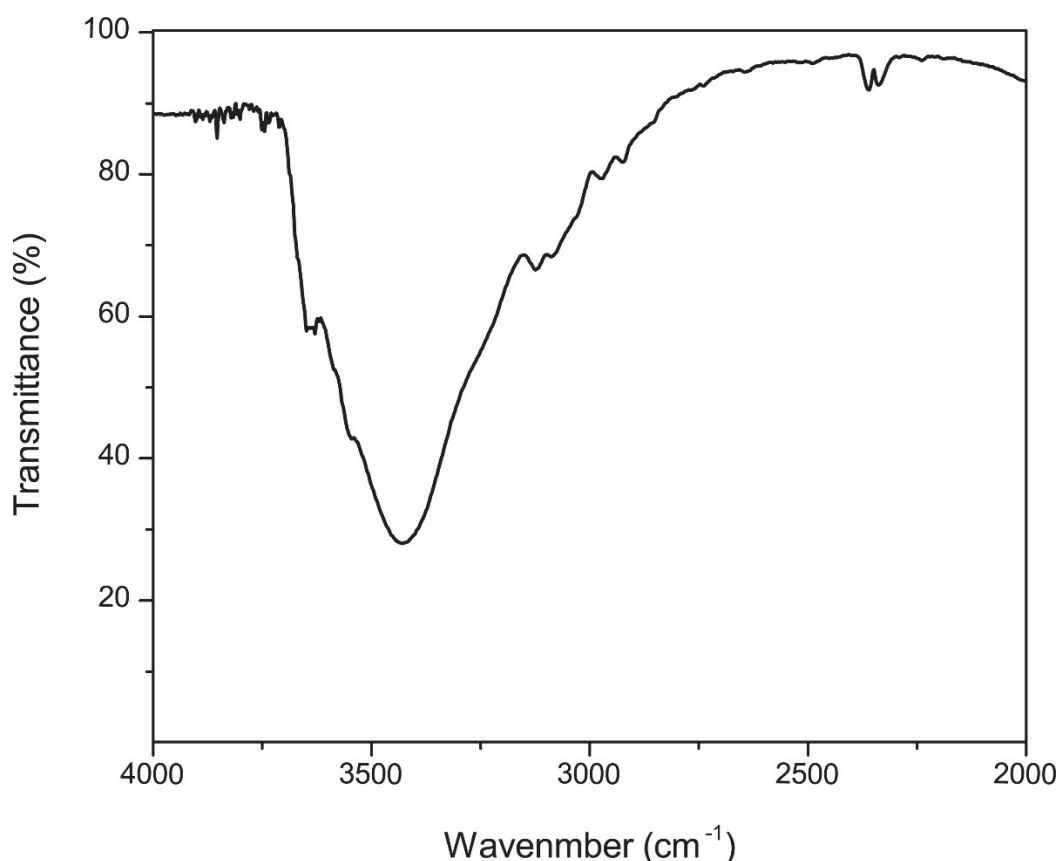


**Figure S71.** Transmission FTIR spectrum of  $[\text{Os}(\text{bpy})_2(\text{OH}_2)(\text{py}^L)](\text{PF}_6)_3$  (4-*N*-(pyridin-4-ylmethyl)-*N,N,N*-trimethylammonium).

### S3.6.1 Diffusion coefficient measurement of $[\text{Os}(\text{bpy})_2(\text{OH}_2)(\text{py})](\text{PF}_6)_2$ (py = 4-*N*-(pyridin-4-ylmethyl)-*N,N,N*-trimethylammonium)

The diffusion coefficients of  $[\text{Os}(\text{bpy})_2(\text{OH}_2)(\text{py}^L)](\text{PF}_6)_2$  (4-*N*-(pyridin-4-ylmethyl)-*N,N,N*-trimethylammonium) were measured with the same method as described in S3.4.2:

To prepare the sample for the diffusion coefficient test, a bulk recrystallization of the solid was performed:  $[\text{Os}(\text{bpy})_2(\text{OH}_2)(\text{py}^L)](\text{PF}_6)_3$  ( $\text{py}^L=4\text{-}N\text{-(pyridin-4-ylmethyl)-}N,N,N\text{-trimethylammonium}$ ) (20 mg) was suspended in methanol (5 mL). Diethyl ether (100 mL) was added to the mixture with stirring, and the resulting solid was collected by filtration and dried under dynamic vacuum.

**Table S2.** Summary of the diffusion coefficients of  $[\text{Os}(\text{bpy})_2(\text{OH}_2)(\text{py}^L)](\text{PF}_6)_2$  ( $\text{py}^L=4\text{-}N\text{-(pyridin-4-ylmethyl)-}N,N,N\text{-trimethylammonium}$ ) using electrochemical methods at various concentrations.

pH	Concentration (mM)	Diffusion coefficient ( $10^{-6}$ cm <sup>2</sup> /s)
3.50	0.995	2.7
3.50	0.567	2.5
3.50	0.284	2.8

3.50	0.189	2.0
6.80	0.285	3.5
8.15	0.297	2.9

The diffusion coefficient was calculated to be  $(2.8 \pm 0.8) \times 10^{-6} \text{ cm}^2/\text{s}$ . According to the Stokes-Einstein law, the diffusion coefficient of a molecule is inversely proportional to its radius. Therefore, if the dinuclear structure were present in the solution state, there should be a relationship between the concentration of the solute and the diffusion coefficient. Specifically, at low concentrations, the mononuclear structure should dominate, resulting in higher diffusion coefficients, and vice versa. Since we did not observe this trend, we conclude that the dinuclear structure is not present in the solution state. The complex remained mononuclear, as confirmed by testing the diffusion coefficient at various pH values (pH = 6.80 and 8.15, Table S2), which yielded similar results. Further support for this conclusion comes from  $^1\text{H}$  DOSY experiments (Figure S72), which also showed a similar diffusion coefficient at a 1 mM solution concentration.

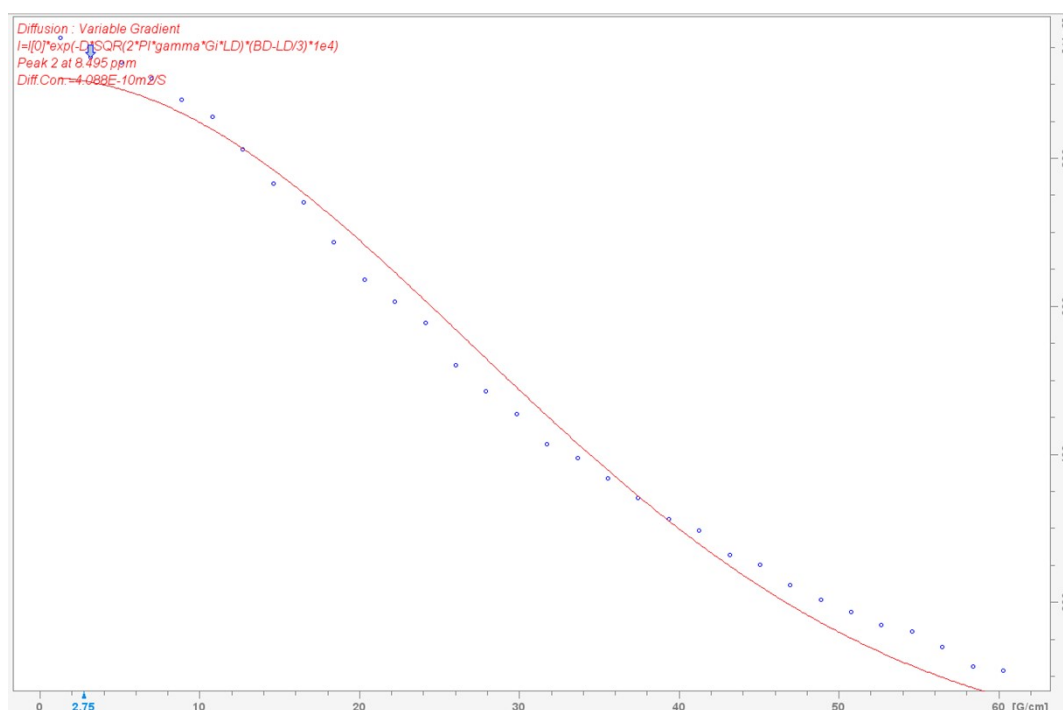
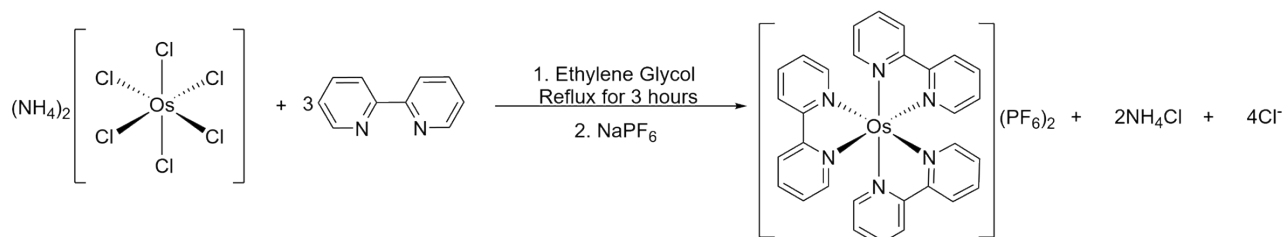


**Figure S72.** Signal attenuation curves for  $^1\text{H}$  DOSY data of  $[\text{Os}(\text{bpy})_2(\text{OH}_2)(\text{py}^L)](\text{PF}_6)_2$  ( $\text{py}^L = 4\text{-}N$ -(pyridin-4-ylmethyl)- $N,N,N$ -trimethylammonium) in deuterated B-R buffer (40 mM) with ascorbic acid (10 equiv, pH = 6.80); the diffusion coefficient was measured to be  $4.0 \times 10^{-6} \text{ cm}^2/\text{s}$ .

### S3.7 Synthesis and diffusion coefficient measurement of $[\text{Os}(\text{bpy})_3](\text{PF}_6)_2$ (bpy=2,2'-bipyridine)



$[\text{Os}(\text{bpy})_3](\text{PF}_6)_2$  was synthesized according to a modified literature procedure.<sup>10</sup> In a 25 mL round-bottom flask,  $(\text{NH}_4)_2\text{OsCl}_6$  (44.3 mg, 0.100 mmol, 1.00 equiv) and bpy (50.0 mg, 0.320 mmol, 3.20 equiv) were heated in ethylene glycol (10 mL) to reflux (200 °C) for 3 hours under  $\text{N}_2$ . After the reaction mixture cooled to room temperature, ascorbic acid (50.0 mg, 0.284 mmol, 2.84 equiv) was added to reduce any Os(III) to Os(II). To isolate the product from the ethylene glycol solvent, diethyl ether (25 mL) was added to the mixture which extracted some of the ethylene glycol into the diethyl ether phase (the desired product is not soluble in ether) and the ether/ethylene glycol phase was decanted and discarded. The procedure was repeated (~10 times) until the addition of diethyl ether could not extract any ethylene glycol. DI water (10 mL) was added to the concentrated oily residue. Solid  $\text{NaPF}_6$  (100 mg, 0.60 mmol, 6.00 equiv) was added to the aqueous solution and the resulting green solid precipitate was isolated by filtration, washed with cold water (20 mL) and diethyl ether (50 mL). The product was dried under dynamic vacuum overnight at room temperature (58.3 mg, 61% yield).  $^1\text{H}$  NMR (400 MHz,  $\text{DMSO}-d_6$ , 298 K)  $\delta$  8.82 – 8.75 (m, 6H), 7.98 – 7.89 (m, 6H), 7.60 (ddd,  $J = 5.9, 1.5, 0.7$  Hz, 6H), 7.39 (ddd,  $J = 7.3, 5.7, 1.3$  Hz, 6H);  $^{13}\text{C}$  NMR (151 MHz,  $\text{DMSO}-d_6$ , 298 K)  $\delta$  158.91, 150.80, 137.71, 128.83, 125.12.

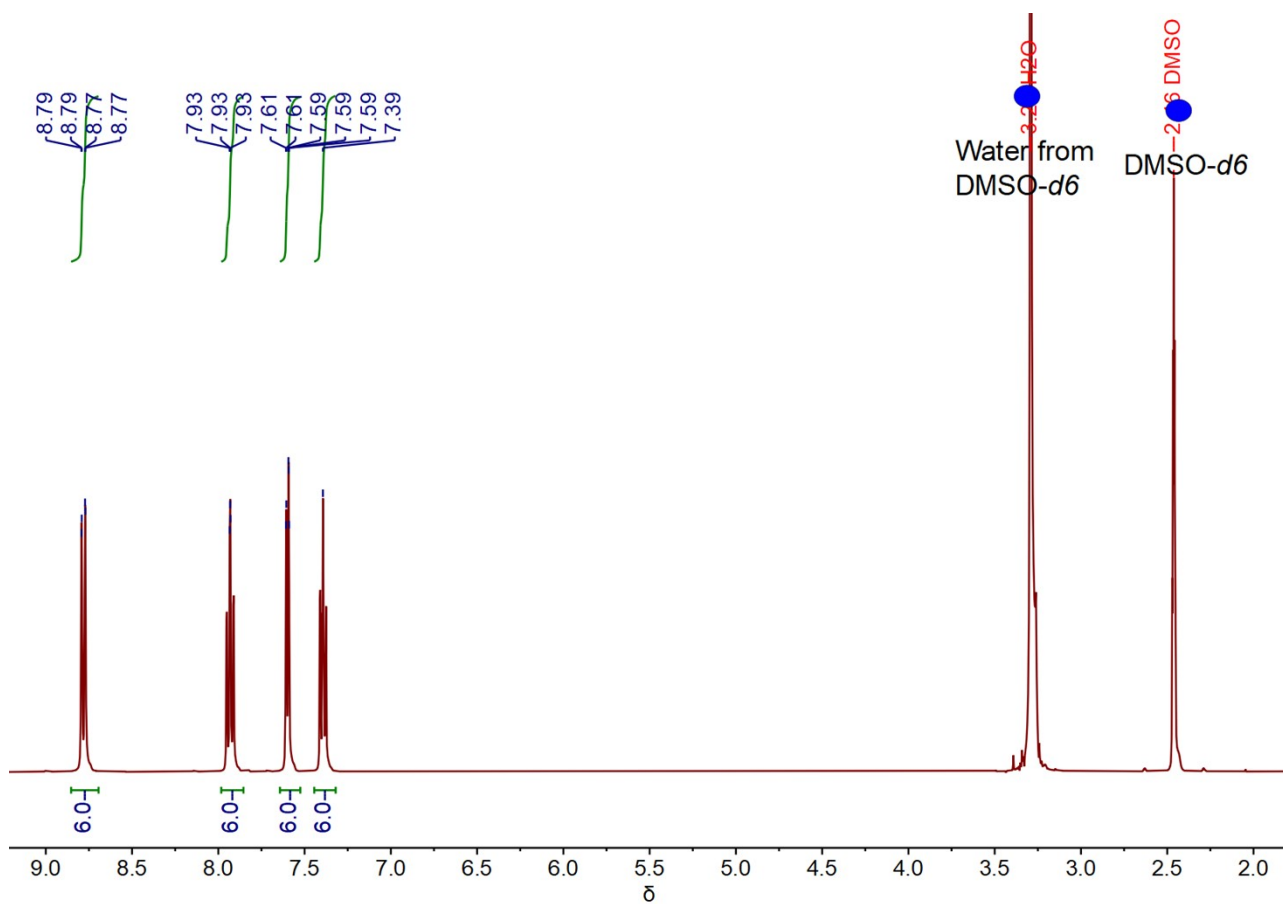


**Figure S73.**  $^1\text{H}$  NMR spectrum of  $[\text{Os}(\text{bpy})_3](\text{PF}_6)_2$  (400 MHz,  $\text{DMSO-}d_6$ , 298 K)

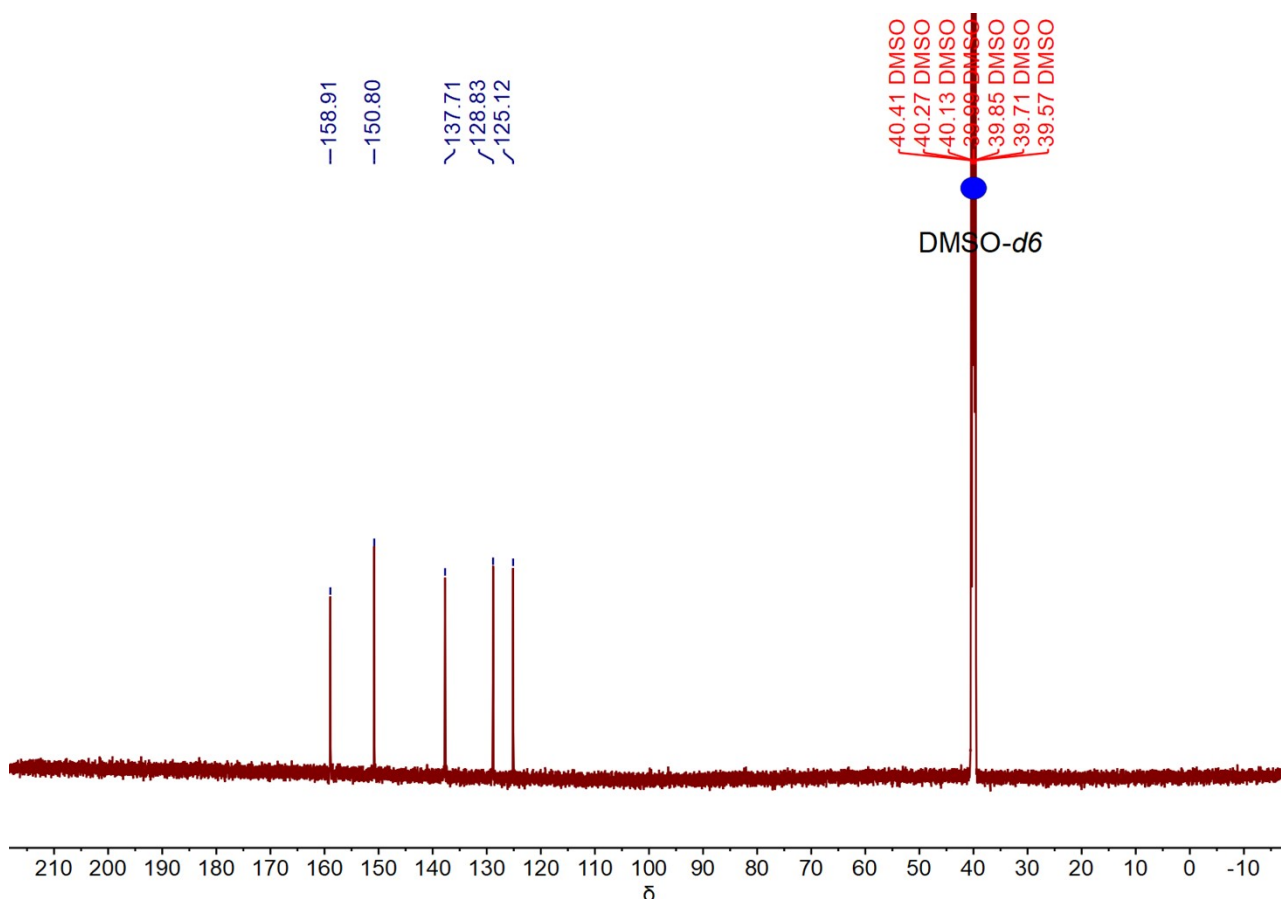


**Figure S74.**  $^{13}\text{C}$  NMR spectrum of  $[\text{Os}(\text{bpy})_3](\text{PF}_6)_2$  (151 MHz,  $\text{DMSO-}d_6$ , 298 K)

The diffusion coefficient of  $[\text{Os}(\text{bpy})_3](\text{PF}_6)_2$  was measured using the same method as described in S3.4.2 and S.3.6.1.

**Table S3.** Summary of the diffusion coefficients of  $[\text{Os}(\text{bpy})_3](\text{PF}_6)_2$  at various concentrations.

Concentration (mM)	Diffusion coefficient ( $10^{-6} \text{ cm}^2/\text{s}$ )
0.457	3.1
0.431	3.7
0.382	3.6
0.379	3.2
0.269	3.8

The diffusion coefficient was calculated to be  $(3.5 \pm 0.3) \times 10^{-6} \text{ cm}^2/\text{s}$ .

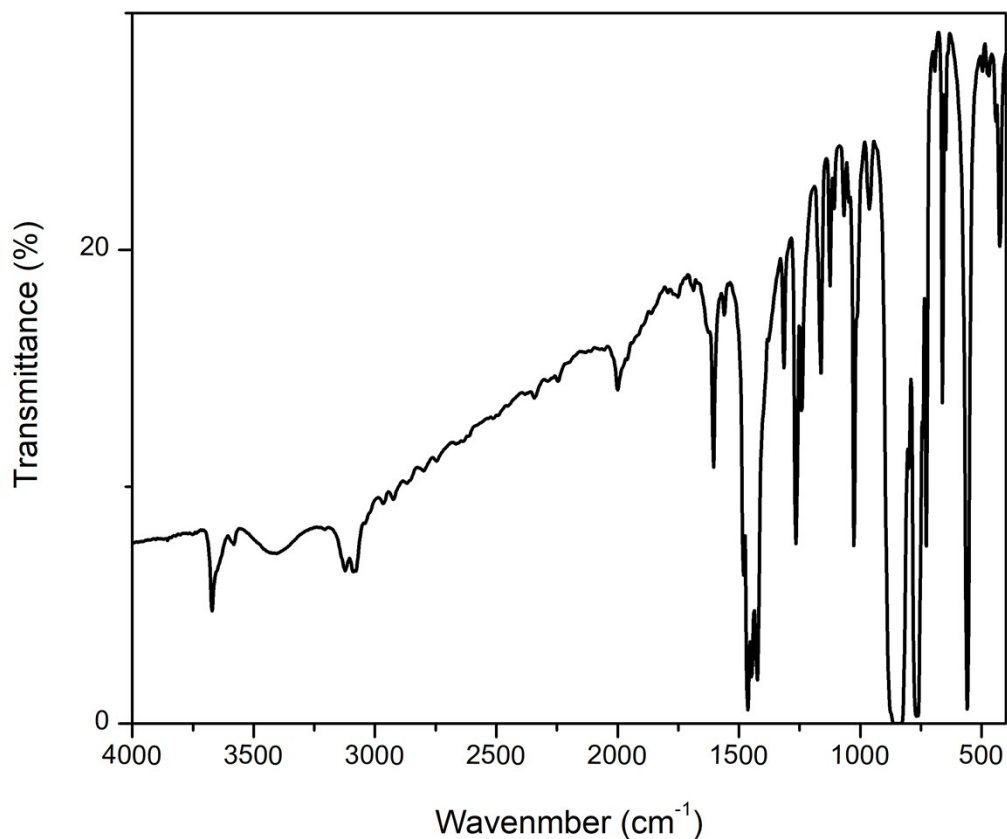
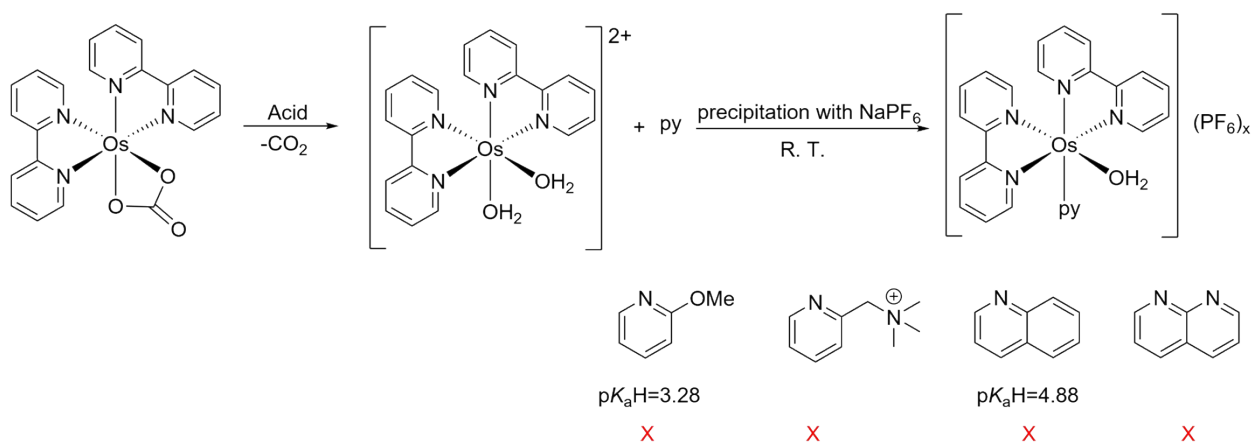


**Figure S75.** Transmission FTIR spectrum of  $[\text{Os}(\text{bpy})_3](\text{PF}_6)_2$ .

**Section S4. Pyridine derivatives that could not be synthesized with the general procedure**



General procedure for the synthesis of pyridine derivatives: In a 10 mL round-bottom flask, pH=3.5 B-R buffer (5 mL) was added to  $\text{Os}(\text{bpy})_2\text{CO}_3$  (47.9 mg, 0.085 mmol, 1 equiv). Pyridine (23 equiv) was added to the mixture with stirring and the pH of the solution was adjusted to 6.8. The solution

was stirred rigorously. CV of the solution was monitored in situ to detect the growth of the peak between -0.1 V and 0.1 V.

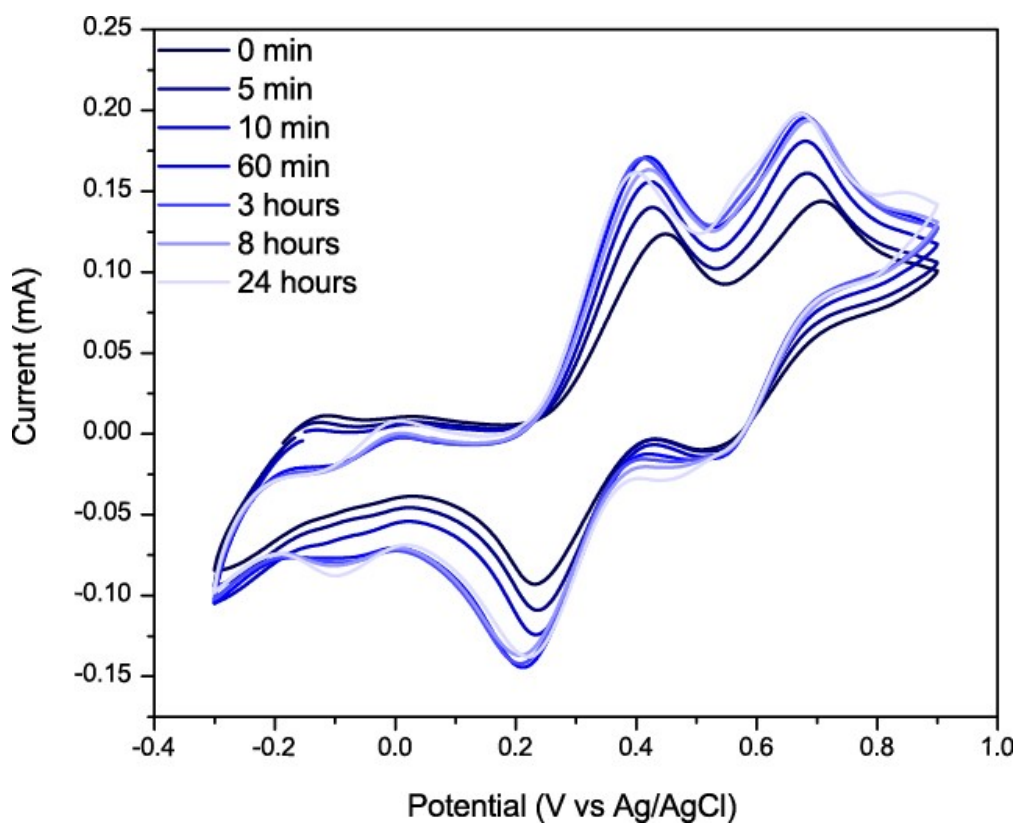


**Figure S76.** In situ CV traces of  $[\text{Os}(\text{bpy})_2(\text{OH}_2)_2]^{2+}$  treated with 2-methoxypyridine in an attempt to prepare  $[\text{Os}(\text{bpy})_2(\text{OH}_2)(\text{py}^L)](\text{PF}_6)_2$  ( $\text{py}^L=2\text{-methoxypyridine}$ ) in pH=6.8 B-R buffer; concentration of  $[\text{Os}(\text{bpy})_2(\text{OH}_2)_2]^{2+} = 17 \text{ mM}$ ; scan rate = 100 mV/s.

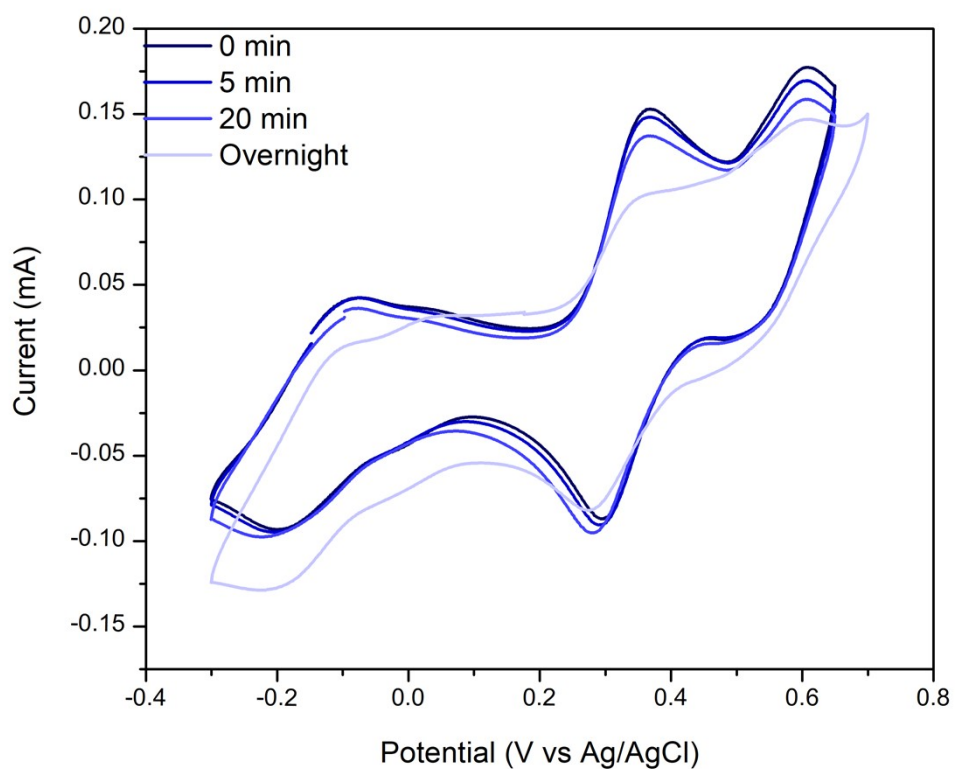


**Figure S77.** In situ CV traces of  $[\text{Os}(\text{bpy})_2(\text{OH}_2)_2]^{2+}$  treated with 2-N-(pyridin-2-ylmethyl)-N,N,N-trimethylammonium bromide in an attempt to prepare  $[\text{Os}(\text{bpy})_2(\text{OH}_2)(\text{py}^L)](\text{PF}_6)_2$  ( $\text{py}^L=2\text{-N-(pyridin-2-ylmethyl)-N,N,N-trimethylammonium}$ ) in pH=6.8 B-R buffer; concentration of  $[\text{Os}(\text{bpy})_2(\text{OH}_2)_2]^{2+} = 17 \text{ mM}$ ; scan rate = 100 mV/s.

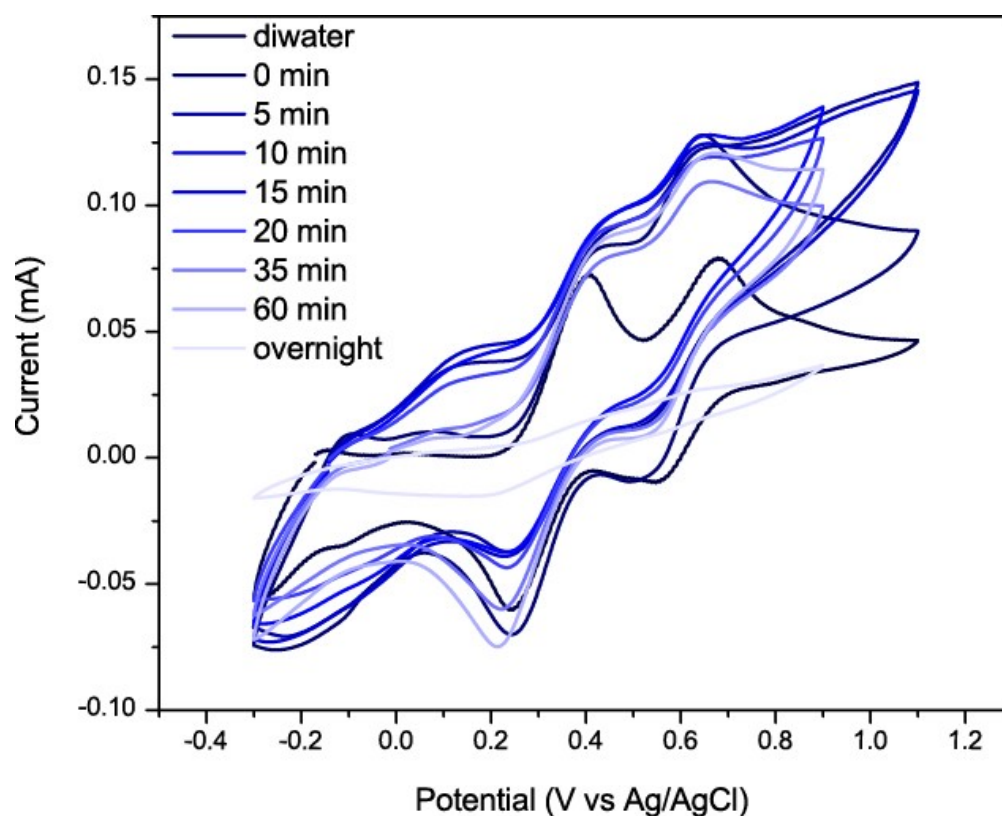


**Figure S78.** In situ CV traces of  $[\text{Os}(\text{bpy})_2(\text{OH}_2)_2]^{2+}$  treated with quinoline in an attempt to prepare  $[\text{Os}(\text{bpy})_2(\text{OH}_2)(\text{py}^L)](\text{PF}_6)_2$  ( $\text{py}^L = \text{quinoline}$ ) in pH=6.8 B-R buffer; concentration of  $[\text{Os}(\text{bpy})_2(\text{OH}_2)_2]^{2+} = 17 \text{ mM}$ ; scan rate = 100 mV/s.

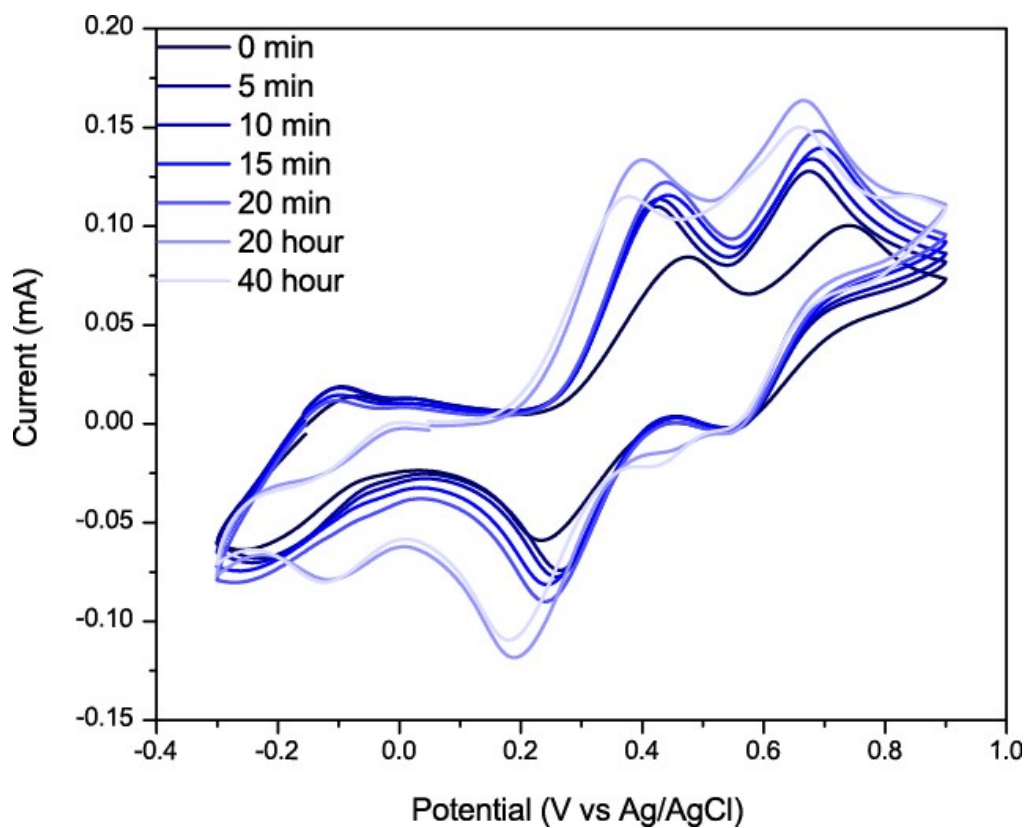


**Figure S79.** In situ CV traces of  $[\text{Os}(\text{bpy})_2(\text{OH}_2)_2]^{2+}$  treated with 1,8-naphthyridine in an attempt to prepare  $[\text{Os}(\text{bpy})_2(\text{OH}_2)(\text{py}^L)](\text{PF}_6)_2$  ( $\text{py}^L=1,8\text{-naphthyridine}$ ) in pH=6.8 B-R buffer; concentration of  $[\text{Os}(\text{bpy})_2(\text{OH}_2)_2]^{2+} = 17 \text{ mM}$ ; scan rate = 100 mV/s.

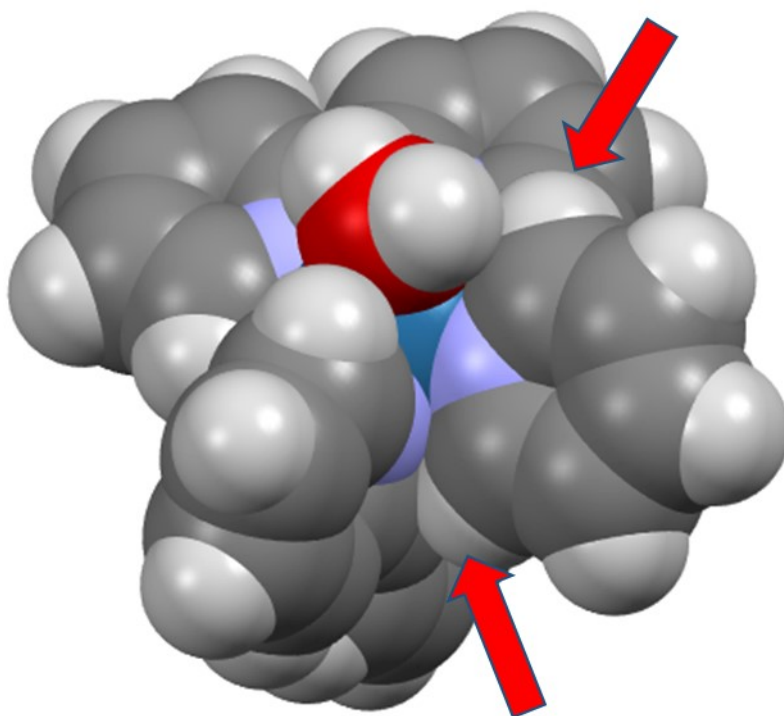


**Figure S80.** Space-filling model generated from the optimized structure of  $[\text{Os}(\text{bpy})_2(\text{OH}_2)(\text{py})](\text{PF}_6)_2$  (py=pyridine). We hypothesize the ortho substituted derivatives could not be synthesized due to steric clashing.

## Section S5. Single Crystal X-ray Crystallography

### S5.1 Single crystal structure of complex $[\text{Os}(\text{bpy})_2(\text{py}^L)(\text{OH}_2)][\text{Cl}]_{0.66}[\text{PF}_6]_{1.33}$ (py<sup>L</sup> = 4-methylpyridine)

Data were collected from a single crystal at 100(2) K on a Bruker D8 Venture Fixed Chi Three-Circle Diffractometer with a Micro Focus Rotating Anode using a Double Bounce Multilayer Mirrors as monochromator and a CPAD Area Detector. The diffractometer was equipped with a low temperature device and used  $\text{MoK}_\alpha$  radiation ( $\lambda = 0.71073 \text{ \AA}$ ). All data were integrated with SAINT and a multi-scan absorption correction using SADABS was applied.<sup>11,12</sup> The structure was solved by direct methods using SHELXT and refined by full-matrix least-squares methods against  $F^2$  by SHELXL-2018/3 following established refinement strategies.<sup>13,14</sup> All non-hydrogen atoms were refined with anisotropic displacement parameters. Unless otherwise noted, all hydrogen atoms were included into the model at geometrically calculated positions and refined using a riding model. The isotropic displacement parameters of all hydrogen atoms were fixed to 1.2 times the U-value of the atoms they are linked to (1.5 times for methyl groups). Details of the data quality and a summary of the residual values of the refinement are listed in Tables S4-S7. Further details can be found in the form of .cif files available from the Cambridge Crystallographic Data Centre.<sup>15</sup> Parts of this report and the .cif file were generated using FinalCif.<sup>16</sup>

A red plate shaped crystal of  $[\text{Os}(\text{bpy})_2(\text{py}^L)(\text{OH}_2)][\text{Cl}]_{0.66}[\text{PF}_6]_{1.33}$  was grown *via* layering an ethanol solution of  $[\text{Os}(\text{bpy})_2(\text{py}^L)(\text{OH}_2)][\text{Cl}]_{0.66}[\text{PF}_6]_{1.33}$  with diethyl ether. Compound  $[\text{Os}(\text{bpy})_2(\text{py}^L)(\text{OH}_2)][\text{Cl}]_{0.66}[\text{PF}_6]_{1.33}$  crystallized in the monoclinic space group  $P2_1/c$ . The asymmetric unit contains one molecule of  $[\text{Os}(\text{bpy})_2(\text{py}^L)(\text{OH}_2)][\text{Cl}]_{0.66}[\text{PF}_6]_{1.33}$  and free ethanol, in addition to chloride-associated ethanol, which was substitutionally disordered with a second  $\text{PF}_6^-$  molecule in a 2:1 ratio. The free ethanol exhibits whole molecule disorder and was refined over two positions with the aid of similarity restraints on bond lengths and angles and on displacement parameters. A DFIX command was used to fix the free ethanol O-H bond distances due to disorder.

**Table S4.** Crystal data and structure refinement for [Os(bpy)<sub>2</sub>(py<sup>L</sup>)(OH<sub>2</sub>)]Cl<sub>0.66</sub>[PF<sub>6</sub>]<sub>1.33</sub> (py<sup>L</sup> = 4-methylpyridine)

CCDC number	2345821
Empirical formula	C <sub>4.51</sub> H <sub>5.43</sub> Cl <sub>0.10</sub> F <sub>1.23</sub> N <sub>0.77</sub> O <sub>0.41</sub> Os <sub>0.15</sub> P <sub>0.21</sub>
Formula weight	139.66
Temperature [K]	100(2)
Crystal system	monoclinic
Space group (number)	<i>P</i> 2 <sub>1</sub> / <i>c</i> (14)
<i>a</i> [Å]	17.1152(10)
<i>b</i> [Å]	8.7658(5)
<i>c</i> [Å]	22.3304(14)
α [°]	90
β [°]	102.552(2)
γ [°]	90
Volume [Å <sup>3</sup> ]	3270.1(3)
<i>Z</i>	26
ρ <sub>calc</sub> [gcm <sup>-3</sup> ]	1.844
μ [mm <sup>-1</sup> ]	4.104
<i>F</i> (000)	1788
Crystal size [mm <sup>3</sup> ]	0.05×0.05×0.01
Crystal colour	red
Crystal shape	plate
Radiation	MoK <sub>α</sub> (λ=0.71073 Å)
2θ range [°]	5.46 to 61.18 (0.70 Å)
Index ranges	-21 ≤ <i>h</i> ≤ 21 -12 ≤ <i>k</i> ≤ 12

			-30 ≤ l ≤ 31		
Reflections collected			63243		
Independent reflections			9264		
			$R_{\text{int}}$	=	0.0652
			$R_{\text{sigma}} = 0.0470$		
Completeness		to	99.6 %		
$\theta = 25.242^\circ$					
Data / Restraints / Parameters			9264/32/531		
Absorption		correction	0.6294/0.7461		
$T_{\text{min}}/T_{\text{max}}$ (method)			(multi-scan)		
Goodness-of-fit on $F^2$			1.080		
Final	$R$	indexes	$R_1$	=	0.0334
[ $I \geq 2\sigma(I)$ ]			$wR_2 = 0.0562$		
Final	$R$	indexes	$R_1$	=	0.0549
[all data]			$wR_2 = 0.0628$		
Largest peak/hole [ $\text{e}\text{\AA}^{-3}$ ]			1.31/-1.45		

**Table S5.** Atomic coordinates and  $U_{\text{eq}}$  [ $\text{\AA}^2$ ] for  $[\text{Os}(\text{bpy})_2(\text{py}^L)(\text{OH}_2)][\text{Cl}]_{0.66}[\text{PF}_6]_{1.33}$  ( $\text{py}^L$  = 4-methylpyridine)

Atom	x	y	z	$U_{\text{eq}}$
P1	0.57175(6)	0.19277(11)	0.63130(4)	0.02067(19)
F1	0.61537(14)	0.0310(2)	0.64565(10)	0.0269(5)
F2	0.65008(14)	0.2595(3)	0.61187(12)	0.0371(6)
F3	0.53708(13)	0.1414(3)	0.56178(9)	0.0298(5)
F4	0.52887(14)	0.3561(2)	0.61752(11)	0.0342(6)
F5	0.49350(13)	0.1271(3)	0.65031(10)	0.0281(5)
F6	0.60672(14)	0.2442(3)	0.70110(10)	0.0307(5)
Cl1	-0.07132(12)	-0.2344(2)	0.55095(7)	0.0308(4)
C29	-0.1889(5)	-0.2993(9)	0.6689(4)	0.048(2)
H29A	-0.169136	-0.219774	0.646626	0.073
H29B	-0.152549	-0.313782	0.707808	0.073
H29C	-0.240595	-0.271333	0.675477	0.073
C30	-0.1956(4)	-0.4433(8)	0.6332(3)	0.0413(17)
H30A	-0.222597	-0.519108	0.653006	0.050
H30B	-0.228116	-0.425153	0.592504	0.050
O3	-0.1201(3)	-0.5017(6)	0.6277(3)	0.0440(13)
H3A	-0.097(4)	-0.437(10)	0.606(5)	0.066
P2	-0.1182(2)	-0.3050(4)	0.61639(15)	0.0313(10)
F7	-0.1091(7)	-0.1893(14)	0.5636(5)	0.078(4)
F8	-0.1800(6)	-0.1925(11)	0.6355(5)	0.066(3)
F9	-0.1909(4)	-0.3833(9)	0.5686(3)	0.0382(19)
F10	-0.1265(5)	-0.4233(11)	0.6677(4)	0.053(3)

F11	-0.0443(5)	-0.2271(9)	0.6616(4)	0.055(3)
F12	-0.0554(5)	-0.4148(11)	0.5949(4)	0.055(3)
Os1	0.25679(2)	0.37790(2)	0.61945(2)	0.01606(4)
O1	0.15924(16)	0.4449(3)	0.54772(12)	0.0264(6)
H1A	0.152442	0.380858	0.512745	0.09(2)
H1B	0.144488	0.548608	0.537961	0.08(2)
N1	0.34025(17)	0.2989(3)	0.69044(13)	0.0163(6)
N2	0.20514(18)	0.1773(3)	0.63735(14)	0.0197(6)
N3	0.31186(18)	0.3044(3)	0.55169(13)	0.0175(6)
N4	0.31677(18)	0.5716(3)	0.60203(13)	0.0178(6)
N5	0.19507(17)	0.4712(3)	0.68300(14)	0.0178(6)
C1	0.4106(2)	0.3662(4)	0.71495(16)	0.0220(7)
H1	0.424704	0.452838	0.695761	0.026
C2	0.4627(2)	0.3144(4)	0.76666(17)	0.0231(8)
H2	0.510289	0.365949	0.782188	0.028
C3	0.4431(2)	0.1846(4)	0.79513(17)	0.0251(8)
H3	0.477362	0.147181	0.830181	0.030
C4	0.3721(2)	0.1112(5)	0.77090(17)	0.0276(8)
H4	0.358057	0.023306	0.789401	0.033
C5	0.3214(2)	0.1695(4)	0.71856(17)	0.0210(7)
C6	0.2446(2)	0.1007(4)	0.68851(17)	0.0219(8)
C7	0.2133(3)	-0.0307(5)	0.70866(19)	0.0329(10)
H7	0.241056	-0.081548	0.743368	0.040
C8	0.1408(3)	-0.0853(5)	0.6769(2)	0.0329(10)
H8	0.118493	-0.171907	0.690443	0.039

C9	0.1016(2)	-0.0107(4)	0.62489(18)	0.0265(8)
H9	0.052929	-0.047105	0.602476	0.032
C10	0.1354(2)	0.1186(4)	0.60648(17)	0.0240(7)
H10	0.108797	0.167718	0.570979	0.029
C11	0.3035(2)	0.1642(4)	0.52618(17)	0.0223(8)
H11	0.274818	0.091098	0.542627	0.027
C12	0.3357(2)	0.1242(5)	0.47678(16)	0.0233(7)
H12	0.329085	0.026041	0.460655	0.028
C13	0.3778(2)	0.2327(4)	0.45164(17)	0.0242(8)
H13	0.399905	0.208528	0.418281	0.029
C14	0.3867(2)	0.3776(5)	0.47677(16)	0.0216(7)
H14	0.414464	0.452245	0.460263	0.026
C15	0.3536(2)	0.4107(4)	0.52723(16)	0.0176(7)
C16	0.3588(2)	0.5593(4)	0.55676(15)	0.0173(7)
C17	0.4036(2)	0.6801(4)	0.54176(17)	0.0210(7)
H17	0.431923	0.668703	0.510935	0.025
C18	0.4059(2)	0.8173(4)	0.57269(17)	0.0215(8)
H18	0.435917	0.898767	0.563326	0.026
C19	0.3623(2)	0.8302(4)	0.61806(17)	0.0212(8)
H19	0.362468	0.921176	0.639503	0.025
C20	0.3187(2)	0.7076(4)	0.63112(17)	0.0208(7)
H20	0.289253	0.718492	0.661286	0.025
C21	0.1146(2)	0.4657(4)	0.67171(18)	0.0223(8)
H21	0.087257	0.425712	0.634452	0.027
C22	0.0707(2)	0.5167(4)	0.71298(18)	0.0243(8)

H22	0.015127	0.509252	0.703372	0.029
C23	0.1093(2)	0.5789(4)	0.76860(18)	0.0244(8)
C24	0.0633(3)	0.6368(6)	0.8144(2)	0.0370(10)
H24A	0.085268	0.732570	0.830830	0.055
H24B	0.067082	0.564155	0.847107	0.055
H24C	0.008081	0.650391	0.794451	0.055
C25	0.1920(2)	0.5848(4)	0.78021(16)	0.0213(8)
H25	0.220353	0.625515	0.817015	0.026
C26	0.2328(2)	0.5308(4)	0.73765(16)	0.0194(7)
H26	0.288423	0.535492	0.746822	0.023
C27	-0.1866(5)	-0.8006(9)	0.5295(4)	0.0433(19)
H27A	-0.222872	-0.824632	0.491499	0.065
H27B	-0.199651	-0.702111	0.543467	0.065
H27C	-0.191157	-0.876181	0.559680	0.065
C28	-0.1026(6)	-0.7986(10)	0.5201(4)	0.040(2)
H28A	-0.066988	-0.755935	0.555931	0.048
H28B	-0.085257	-0.901964	0.514412	0.048
O2	-0.0991(3)	-0.7082(5)	0.46681(19)	0.0362(13)
H2A	-0.0427(16)	-0.685(9)	0.476(4)	0.12(3)
C27A	-0.0611(14)	-0.799(3)	0.5164(13)	0.059(8)
H27D	-0.035254	-0.896332	0.517998	0.089
H27E	-0.039386	-0.743023	0.553327	0.089
H27F	-0.052097	-0.742536	0.481653	0.089
C28A	-0.1500(13)	-0.821(2)	0.5107(12)	0.045(6)
H28C	-0.173129	-0.864717	0.470848	0.054

H28D	-0.158689	-0.892512	0.541844	0.054
O2A	-0.1895(7)	-0.6780(12)	0.5177(5)	0.036(3)
H2B	-0.200(10)	-0.672(9)	0.559(3)	0.054

$U_{eq}$  is defined as 1/3 of the trace of the orthogonalized  $U_{ij}$  tensor.

**Table S6.** Anisotropic displacement parameters [ $\text{\AA}^2$ ] for  $[\text{Os}(\text{bpy})_2(\text{py}^L)(\text{OH}_2)][\text{Cl}]_{0.66}[\text{PF}_6]_{1.33}$  ( $\text{py}^L = 4$ -methylpyridine).

The anisotropic displacement factor exponent takes the form:

$$-2\pi^2 [ h^2(a^*)^2 U_{11} + k^2(b^*)^2 U_{22} + \dots + 2hka^*b^*U_{12} ]$$

Atom	$U_{11}$	$U_{22}$	$U_{33}$	$U_{23}$	$U_{13}$	$U_{12}$
P1	0.0237(5)	0.0168(4)	0.0221(5)	0.0015(4)	0.0062(4)	-0.0004(4)
F1	0.0354(14)	0.0183(11)	0.0272(12)	-0.0005(9)	0.0072(10)	0.0085(9)
F2	0.0284(14)	0.0399(15)	0.0441(15)	0.0104(12)	0.0106(11)	-0.0080(11)
F3	0.0349(13)	0.0349(13)	0.0199(10)	0.0015(10)	0.0067(9)	-0.0017(10)
F4	0.0335(14)	0.0178(12)	0.0484(15)	0.0036(11)	0.0027(11)	0.0036(9)
F5	0.0308(12)	0.0258(11)	0.0316(12)	-0.0032(11)	0.0151(9)	-0.0049(10)
F6	0.0405(14)	0.0240(12)	0.0249(12)	-0.0059(10)	0.0015(10)	-0.0002(10)
Cl1	0.0302(10)	0.0376(10)	0.0229(7)	0.0006(7)	0.0020(6)	-0.0109(7)
C29	0.060(5)	0.049(5)	0.043(4)	-0.012(4)	0.026(4)	-0.015(4)
C30	0.038(4)	0.049(4)	0.040(4)	-0.002(3)	0.014(3)	-0.005(3)
O3	0.049(3)	0.036(3)	0.049(3)	0.014(3)	0.013(3)	0.007(2)
P2	0.032(2)	0.0272(18)	0.0308(18)	-0.0049(14)	-0.0004(13)	0.0042(13)
F7	0.065(9)	0.075(8)	0.088(9)	0.035(7)	0.003(7)	-0.002(6)
F8	0.053(6)	0.065(7)	0.073(7)	-0.041(6)	-0.005(5)	0.022(5)
F9	0.033(4)	0.045(4)	0.031(4)	-0.014(4)	-0.004(3)	0.010(4)
F10	0.044(6)	0.073(7)	0.040(5)	0.006(5)	0.006(4)	-0.013(4)

F11	0.051(6)	0.033(4)	0.069(6)	-0.013(4)	-0.010(4)	-0.004(4)
F12	0.036(5)	0.081(7)	0.043(5)	-0.010(5)	0.001(4)	0.014(5)
Os1	0.01896(7)	0.01445(6)	0.01475(6)	0.00029(6)	0.00359(4)	0.00058(6)
O1	0.0293(16)	0.0250(14)	0.0222(14)	0.0015(12)	0.0000(11)	0.0029(11)
N1	0.0186(16)	0.0175(15)	0.0129(13)	-0.0005(11)	0.0038(11)	0.0022(11)
N2	0.0238(17)	0.0145(14)	0.0216(15)	0.0005(12)	0.0064(12)	0.0042(11)
N3	0.0194(16)	0.0182(15)	0.0153(14)	0.0018(12)	0.0045(11)	0.0024(11)
N4	0.0200(16)	0.0172(14)	0.0161(14)	0.0009(12)	0.0040(11)	0.0006(11)
N5	0.0185(16)	0.0147(14)	0.0221(15)	0.0014(12)	0.0081(12)	0.0016(11)
C1	0.0247(19)	0.0218(18)	0.0206(17)	-0.0023(16)	0.0071(14)	0.0017(15)
C2	0.021(2)	0.0266(19)	0.0216(18)	-0.0074(16)	0.0034(14)	0.0026(15)
C3	0.029(2)	0.0237(19)	0.0202(18)	-0.0012(16)	-0.0010(15)	0.0115(16)
C4	0.038(2)	0.0186(18)	0.0256(19)	0.0021(17)	0.0066(16)	0.0050(17)
C5	0.024(2)	0.0165(17)	0.0225(18)	-0.0001(14)	0.0055(14)	0.0033(13)
C6	0.027(2)	0.0143(18)	0.0241(18)	-0.0015(15)	0.0051(14)	0.0020(14)
C7	0.047(3)	0.021(2)	0.027(2)	0.0077(17)	0.0009(18)	-0.0061(18)
C8	0.043(3)	0.020(2)	0.034(2)	0.0024(17)	0.0069(19)	-0.0104(17)
C9	0.026(2)	0.024(2)	0.029(2)	-0.0075(17)	0.0057(16)	-0.0037(15)
C10	0.027(2)	0.0208(17)	0.0242(18)	-0.0028(17)	0.0059(14)	0.0011(16)
C11	0.027(2)	0.0187(18)	0.0218(18)	0.0005(15)	0.0069(15)	0.0016(14)
C12	0.029(2)	0.0205(17)	0.0210(17)	-0.0007(17)	0.0068(14)	0.0066(16)
C13	0.025(2)	0.026(2)	0.0233(19)	0.0000(16)	0.0098(15)	0.0043(15)
C14	0.0210(18)	0.0235(17)	0.0222(17)	0.0019(17)	0.0089(13)	-0.0001(15)
C15	0.0165(18)	0.0163(17)	0.0190(17)	0.0027(13)	0.0014(13)	0.0025(12)
C16	0.0158(18)	0.0200(17)	0.0157(16)	0.0032(14)	0.0021(13)	0.0037(13)

C17	0.022(2)	0.0200(17)	0.0207(18)	0.0022(15)	0.0039(14)	0.0009(14)
C18	0.022(2)	0.0175(17)	0.0235(19)	0.0051(15)	0.0015(14)	-0.0015(14)
C19	0.025(2)	0.0164(17)	0.0215(18)	-0.0008(14)	0.0028(14)	0.0004(13)
C20	0.024(2)	0.0186(18)	0.0203(18)	0.0004(15)	0.0058(14)	0.0009(14)
C21	0.023(2)	0.0184(18)	0.0255(19)	0.0001(15)	0.0049(15)	-0.0031(14)
C22	0.020(2)	0.0224(19)	0.032(2)	0.0011(16)	0.0090(16)	-0.0016(14)
C23	0.027(2)	0.0214(19)	0.028(2)	0.0030(16)	0.0145(16)	0.0012(14)
C24	0.029(2)	0.047(3)	0.039(2)	-0.005(2)	0.0177(18)	0.001(2)
C25	0.027(2)	0.0207(19)	0.0172(17)	-0.0007(14)	0.0075(14)	0.0011(14)
C26	0.0193(19)	0.0182(17)	0.0207(18)	0.0015(14)	0.0043(14)	-0.0004(13)
C27	0.041(5)	0.047(5)	0.038(4)	-0.001(3)	0.000(3)	-0.006(3)
C28	0.055(8)	0.037(4)	0.029(4)	0.005(3)	0.011(5)	0.010(5)
O2	0.049(3)	0.032(2)	0.028(2)	0.0029(18)	0.010(2)	0.010(2)
C27A	0.07(2)	0.058(14)	0.049(13)	-0.001(11)	0.013(15)	0.020(15)
C28A	0.049(18)	0.039(11)	0.049(14)	-0.001(9)	0.015(12)	0.002(11)
O2A	0.041(7)	0.020(6)	0.044(7)	0.001(5)	0.004(5)	0.002(4)

**Table S7.** Bond lengths and angles for  $[\text{Os}(\text{bpy})_2(\text{py}^L)(\text{OH}_2)][\text{Cl}]_{0.66}[\text{PF}_6]_{1.33}$  ( $\text{py}^L = 4\text{-methylpyridine}$ )

Atom–Atom	Length [Å]
P1–F5	1.598(2)
P1–F3	1.601(2)
P1–F1	1.602(2)
P1–F2	1.606(2)
P1–F6	1.608(2)
P1–F4	1.608(2)

C29–C30	1.484(9)
C30–O3	1.420(8)
P2–F8	1.572(8)
P2–F10	1.575(8)
P2–F7	1.587(10)
P2–F11	1.590(8)
P2–F12	1.592(8)
P2–F9	1.607(7)
Os1–N1	2.012(3)
Os1–N2	2.046(3)
Os1–N3	2.053(3)
Os1–N4	2.064(3)
Os1–N5	2.110(3)
Os1–O1	2.130(3)
N1–C1	1.345(5)
N1–C5	1.368(5)
N2–C10	1.344(5)
N2–C6	1.370(5)
N3–C11	1.350(5)
N3–C15	1.358(4)
N4–C20	1.354(4)
N4–C16	1.367(4)
N5–C21	1.346(5)
N5–C26	1.355(5)
C1–C2	1.374(5)

C2–C3	1.380(6)
C3–C4	1.378(6)
C4–C5	1.392(5)
C5–C6	1.469(5)
C6–C7	1.386(5)
C7–C8	1.374(6)
C8–C9	1.373(6)
C9–C10	1.376(5)
C11–C12	1.380(5)
C12–C13	1.385(5)
C13–C14	1.384(5)
C14–C15	1.398(5)
C15–C16	1.454(5)
C16–C17	1.390(5)
C17–C18	1.383(5)
C18–C19	1.388(5)
C19–C20	1.375(5)
C21–C22	1.384(5)
C22–C23	1.386(5)
C23–C25	1.383(5)
C23–C24	1.509(5)
C25–C26	1.379(5)
C27–C28	1.498(10)
C28–O2	1.441(8)
C27A–C28A	1.512(16)

C28A–O2A	1.451(15)
<b>Atom–Atom– Atom</b>	<b>Angle [°]</b>
F5–P1–F3	90.05(12)
F5–P1–F1	90.52(13)
F3–P1–F1	90.21(13)
F5–P1–F2	179.63(16)
F3–P1–F2	89.75(13)
F1–P1–F2	89.78(13)
F5–P1–F6	90.03(12)
F3–P1–F6	179.90(16)
F1–P1–F6	89.72(12)
F2–P1–F6	90.18(14)
F5–P1–F4	89.86(13)
F3–P1–F4	90.40(13)
F1–P1–F4	179.28(15)
F2–P1–F4	89.83(13)
F6–P1–F4	89.67(13)
O3–C30–C29	112.8(6)
F8–P2–F10	92.4(6)
F8–P2–F7	88.9(7)
F10–P2–F7	178.5(7)
F8–P2–F11	92.7(5)
F10–P2–F11	90.3(5)

F7-P2-F11	90.3(6)
F8-P2-F12	177.8(6)
F10-P2-F12	89.7(5)
F7-P2-F12	88.9(6)
F11-P2-F12	87.5(5)
F8-P2-F9	88.7(5)
F10-P2-F9	91.3(5)
F7-P2-F9	88.1(5)
F11-P2-F9	177.8(5)
F12-P2-F9	91.0(4)
N1-Os1-N2	79.23(12)
N1-Os1-N3	96.41(11)
N2-Os1-N3	99.30(12)
N1-Os1-N4	97.73(12)
N2-Os1-N4	175.75(12)
N3-Os1-N4	78.01(12)
N1-Os1-N5	88.68(11)
N2-Os1-N5	84.32(11)
N3-Os1-N5	174.21(11)
N4-Os1-N5	98.63(11)
N1-Os1-O1	173.57(11)
N2-Os1-O1	94.75(11)
N3-Os1-O1	86.71(11)
N4-Os1-O1	88.40(11)
N5-Os1-O1	88.50(11)

C1–N1–C5	117.1(3)
C1–N1–Os1	126.1(2)
C5–N1–Os1	116.7(2)
C10–N2–C6	117.5(3)
C10–N2–Os1	127.0(3)
C6–N2–Os1	115.4(2)
C11–N3–C15	118.1(3)
C11–N3–Os1	125.0(2)
C15–N3–Os1	116.6(2)
C20–N4–C16	117.5(3)
C20–N4–Os1	126.5(2)
C16–N4–Os1	116.0(2)
C21–N5–C26	116.8(3)
C21–N5–Os1	120.1(2)
C26–N5–Os1	123.0(2)
N1–C1–C2	123.9(4)
C1–C2–C3	118.7(4)
C4–C3–C2	119.1(3)
C3–C4–C5	119.6(4)
N1–C5–C4	121.6(3)
N1–C5–C6	114.0(3)
C4–C5–C6	124.4(3)
N2–C6–C7	121.5(4)
N2–C6–C5	114.2(3)
C7–C6–C5	124.3(3)

C8-C7-C6	119.4(4)
C9-C8-C7	119.4(4)
C8-C9-C10	119.0(4)
N2-C10-C9	123.2(4)
N3-C11-C12	123.0(4)
C11-C12-C13	118.9(4)
C14-C13-C12	119.2(3)
C13-C14-C15	119.3(3)
N3-C15-C14	121.5(3)
N3-C15-C16	114.7(3)
C14-C15-C16	123.8(3)
N4-C16-C17	121.6(3)
N4-C16-C15	114.6(3)
C17-C16-C15	123.8(3)
C18-C17-C16	120.0(3)
C17-C18-C19	118.3(3)
C20-C19-C18	119.6(3)
N4-C20-C19	123.0(3)
N5-C21-C22	123.1(4)
C21-C22-C23	120.1(4)
C25-C23-C22	116.9(3)
C25-C23-C24	121.6(4)
C22-C23-C24	121.4(4)
C26-C25-C23	120.6(3)
N5-C26-C25	122.6(3)

O2-C28-C27	109.7(7)
O2A-C28A-C27A	111.2(16)

### S5.2 Single crystal structure of complex $[\{\text{Os}^{\text{II}}(\text{bpy})_2(\text{py}^{\text{L}})\}_2(\mu\text{-O}_2\text{H}_3)](\text{PF}_6)_5$ ( $\text{py}^{\text{L}} = 4\text{-N-(pyridin-4-ylmethyl)-N,N,N-trimethylammonium}$ )

Diffraction studies of  $[\{\text{Os}^{\text{II}}(\text{bpy})_2(\text{py}^{\text{L}})\}_2(\mu\text{-O}_2\text{H}_3)](\text{PF}_6)_5$  were performed at the UCSD Crystallography Facility. A red, block-shaped crystal of  $[\{\text{Os}^{\text{II}}(\text{bpy})_2(\text{py}^{\text{L}})\}_2(\mu\text{-O}_2\text{H}_3)](\text{PF}_6)_5$  was mounted on the goniometer. Data were collected from a shock-cooled single crystal at 100(2) K on a Bruker D8 Venture fixed chi three-circle diffractometer with a micro focus rotating anode using double bounce multilayer mirrors as monochromator and a CPAD area detector. The diffractometer was equipped with a low temperature device and used  $\text{MoK}_\alpha$  radiation ( $\lambda = 0.71073 \text{ \AA}$ ). All data were integrated with SAINT and a multi-scan absorption correction using SADABS was applied.<sup>11,12</sup> The structure was solved by direct methods using SHELXT and refined by full-matrix least-squares methods against  $F^2$  by SHELXL-2018/3.<sup>13,14</sup> All non-hydrogen atoms were refined with anisotropic displacement parameters. All hydrogen atoms were refined with isotropic displacement parameters. Some were refined freely and some on calculated positions using a riding model with their  $U_{\text{iso}}$  values constrained to 1.5 times the  $U_{\text{eq}}$  of their pivot atoms for terminal  $\text{sp}^3$  carbon atoms and 1.2 times for all other carbon atoms. Disordered moieties were refined using bond lengths restraints and displacement parameter restraints. This report and the CIF file were generated using FinalCif.<sup>16</sup>

#### Refinement Details:

All main molecule non-hydrogen atoms were refined as anisotropic ellipsoids without restraints or constraints. The asymmetric unit contained 2.5 hexafluorophosphate units. One was refined in one position, one was refined with disorder over two positions, and the final was the half occupancy hexafluorophosphate disordered over three positions across a crystallographic inversion center. This highly disordered hexafluorophosphate was refined partly with an ether molecule and partly with a heavily disordered methanol molecule consistent with the occupancies of the disordered parts of the half hexafluorophosphate. All of the hexafluorophosphate ions were refined with DFIX and SAME commands, and the disordered solvents were heavily constrained and restrained in their anisotropic displacement parameters and bond lengths. The refinement of the occupancy of the disordered hexafluorophosphate unit is not in question, but the disordered solvent refinement is presented as a reasonable solution to the significant disorder present.

#### Table S8. Crystal data and structure refinement for $[\{\text{Os}^{\text{II}}(\text{bpy})_2(\text{py}^{\text{L}})\}_2(\mu\text{-O}_2\text{H}_3)](\text{PF}_6)_5$ ( $\text{py}^{\text{L}} = 4\text{-N-(pyridin-4-ylmethyl)-N,N,N-trimethylammonium}$ )

CCDC number	2366172
Empirical formula	$\text{C}_{62.40}\text{H}_{77.80}\text{F}_{30}\text{N}_{12}\text{O}_4\text{Os}_2\text{P}_5$
Formula weight	2165.21

Temperature [K]	100(2)			
Crystal system	triclinic			
Space group (number)	$P\bar{1}$ (2)			
$a$ [Å]	12.0421(5)			
$b$ [Å]	13.5806(6)			
$c$ [Å]	14.2226(6)			
$\alpha$ [°]	62.1400(10)			
$\beta$ [°]	83.454(2)			
$\gamma$ [°]	69.7840(10)			
Volume [Å <sup>3</sup> ]	1926.51(14)			
$Z$	1			
$\rho_{\text{calc}}$ [gcm <sup>-3</sup> ]	1.866			
$\mu$ [mm <sup>-1</sup> ]	3.526			
$F(000)$	1065			
Crystal size [mm <sup>3</sup> ]	0.05×0.04×0.03			
Crystal colour	red			
Crystal shape	block			
Radiation	MoK $\alpha$ ( $\lambda=0.71073$ Å)			
2 $\theta$ range [°]	4.99 to 50.97 (0.83 Å)			
Index ranges	-14 ≤ h ≤ 14			
	-16 ≤ k ≤ 16			
	-17 ≤ l ≤ 17			
Reflections collected	53437			
Independent reflections	7142			
	$R_{\text{int}} = 0.0777$			
	$R_{\text{sigma}} = 0.0446$			
Completeness	to 99.9 %			
$\theta = 25.242^\circ$				
Data / Restraints / Parameters	7142/841/788			
Absorption	correction 0.6768/0.7452			
$T_{\text{min}}/T_{\text{max}}$ (method)	(multi-scan)			
Goodness-of-fit on $F^2$	1.052			
Final $R$ indexes	$R_1 = 0.0358$			
[ $I \geq 2\sigma(I)$ ]	$wR_2 = 0.0762$			
Final $R$ indexes	$R_1 = 0.0502$			
[all data]	$wR_2 = 0.0828$			

Largest peak/hole [ $\text{e}\text{\AA}^{-3}$ ]

0.86/-0.64

**Table S9. Atomic coordinates and  $U_{eq}$  [Å<sup>2</sup>] for  $[\{Os^{II}(bpy)_2(py^L)\}_2(\mu-O_2H_3)](PF_6)_5$  ( $py^L = 4-N$ -  
(pyridin-4-ylmethyl)-N,N,N-trimethylammonium)**

Atom	x	y	z	$U_{eq}$
Os1	0.35269(2)	0.65574(2)	0.58132(2)	0.02794(8)
P1	0.83526(15)	0.63964(14)	0.57242(14)	0.0471(4)
F1	0.7185(3)	0.7407(4)	0.5047(4)	0.0794(13)
F2	0.7859(5)	0.6572(5)	0.6736(4)	0.0862(15)
F3	0.7671(5)	0.5453(4)	0.6016(4)	0.0889(15)
F4	0.8844(4)	0.6232(3)	0.4705(3)	0.0630(10)
F5	0.8967(3)	0.7371(3)	0.5419(3)	0.0580(10)
F6	0.9515(5)	0.5409(4)	0.6397(4)	0.1002(18)
P2	0.2913(4)	0.9088(3)	0.8520(3)	0.0466(9)
F7	0.1574(6)	0.9732(6)	0.8061(6)	0.078(2)
F8	0.3311(6)	0.9122(5)	0.7413(5)	0.0655(18)
F9	0.2770(5)	0.7831(5)	0.8903(6)	0.084(2)
F10	0.2506(7)	0.9036(9)	0.9644(5)	0.100(2)
F11	0.3093(6)	1.0321(5)	0.8139(5)	0.0676(17)
F12	0.4247(5)	0.8445(5)	0.8992(5)	0.087(2)
P2B	0.2880(13)	0.9362(12)	0.8612(11)	0.057(3)
F7B	0.1612(18)	0.936(2)	0.837(2)	0.072(6)
F8B	0.350(2)	0.8792(18)	0.7870(17)	0.078(6)
F9B	0.3031(19)	0.8120(16)	0.9630(16)	0.106(7)
F10B	0.2230(15)	0.9962(18)	0.9356(13)	0.061(4)
F11B	0.260(2)	1.0651(14)	0.7617(15)	0.086(6)
F12B	0.4093(14)	0.9402(19)	0.8863(16)	0.085(5)
P3	0.1522(11)	0.4238(12)	0.9837(11)	0.0758(14)
F13	0.191(2)	0.380(2)	1.1055(12)	0.079(2)
F14	0.2663(15)	0.4592(19)	0.9442(16)	0.078(2)
F15	0.2193(19)	0.2922(14)	0.9983(18)	0.079(2)
F16	0.0331(16)	0.390(2)	1.0239(17)	0.076(2)
F17	0.0854(18)	0.5550(14)	0.9730(18)	0.078(2)
F18	0.096(2)	0.4769(18)	0.8669(12)	0.079(2)
P3B	0.1666(12)	0.4260(12)	0.9803(10)	0.0758(14)
F13B	0.153(2)	0.449(2)	1.0831(14)	0.077(2)
F14B	0.2299(19)	0.5224(17)	0.9238(15)	0.077(2)

F15B	0.2920(15)	0.3244(16)	1.0310(16)	0.079(2)
F16B	0.0931(19)	0.3366(17)	1.0402(15)	0.078(2)
F17B	0.0427(15)	0.5308(16)	0.9253(16)	0.081(2)
F18B	0.177(2)	0.405(2)	0.8790(14)	0.077(2)
P3C	0.0451(15)	0.4801(18)	0.9957(16)	0.0758(14)
F13C	0.133(3)	0.417(3)	0.928(3)	0.078(2)
F14C	-0.017(3)	0.383(3)	1.035(3)	0.077(2)
F15C	-0.043(3)	0.557(3)	0.891(2)	0.078(3)
F16C	0.121(3)	0.569(3)	0.953(3)	0.076(2)
F17C	0.140(3)	0.390(3)	1.097(2)	0.077(2)
F18C	-0.025(3)	0.536(3)	1.068(3)	0.076(2)
O2	-0.251(3)	0.945(3)	0.826(2)	0.071(7)
H2A	-0.177207	0.917104	0.839983	0.106
C30	-0.302(4)	0.853(4)	0.886(3)	0.073(11)
H30A	-0.381234	0.877577	0.854638	0.109
H30B	-0.308029	0.840267	0.959969	0.109
H30C	-0.251713	0.780302	0.884078	0.109
O3	-0.317(3)	0.997(3)	0.935(2)	0.089(8)
H3A	-0.380772	1.005386	0.966429	0.133
C31	-0.327(7)	0.958(5)	0.859(5)	0.064(9)
H31A	-0.250494	0.939834	0.827513	0.095
H31B	-0.387429	1.019930	0.802763	0.095
H31C	-0.349643	0.886283	0.894923	0.095
O4	-0.357(2)	0.950(2)	0.934(3)	0.067(7)
H5A	-0.315630	0.886631	0.983360	0.100
C32	-0.478(2)	0.959(3)	0.947(3)	0.051(8)
H32A	-0.520439	1.004030	0.876585	0.077
H32B	-0.511730	0.999134	0.990224	0.077
H32C	-0.484049	0.879578	0.981770	0.077
O5	-0.229(2)	0.7566(17)	0.9511(17)	0.143(7)
C33	-0.211(4)	0.641(2)	0.963(3)	0.143(7)
H33A	-0.237045	0.652708	0.894405	0.172
H33B	-0.267923	0.610917	1.015526	0.172
C34	-0.089(5)	0.538(5)	0.998(7)	0.143(7)
H34A	-0.038732	0.551694	1.037032	0.215

H34B	-0.050121	0.534924	0.934806	0.215
H34C	-0.102636	0.462959	1.044324	0.215
C35	-0.276(4)	0.854(3)	0.852(2)	0.143(7)
H35A	-0.343305	0.843457	0.828146	0.172
H35B	-0.214667	0.854734	0.799253	0.172
C36	-0.319(7)	0.973(4)	0.852(5)	0.143(7)
H36A	-0.378418	0.972669	0.905366	0.215
H36B	-0.353709	1.035154	0.781736	0.215
H36C	-0.251555	0.987056	0.870478	0.215
O5B	-0.229(2)	0.7566(17)	0.9511(17)	0.143(7)
C33B	-0.211(4)	0.641(2)	0.963(3)	0.143(7)
H33C	-0.142730	0.617686	0.923692	0.172
H33D	-0.282473	0.639743	0.936559	0.172
C34B	-0.184(8)	0.545(6)	1.101(6)	0.143(7)
H34D	-0.118864	0.554425	1.128055	0.215
H34E	-0.161657	0.463167	1.113036	0.215
H34F	-0.255389	0.563534	1.138220	0.215
C35B	-0.276(4)	0.854(3)	0.852(2)	0.143(7)
H35C	-0.343305	0.843457	0.828146	0.172
H35D	-0.214667	0.854734	0.799253	0.172
C36B	-0.319(7)	0.973(4)	0.852(5)	0.143(7)
H36D	-0.404943	0.997977	0.857228	0.215
H36E	-0.297792	1.031172	0.786566	0.215
H36F	-0.280947	0.965729	0.913786	0.215
O1	0.5046(3)	0.5770(3)	0.5195(3)	0.0303(8)
H1A	0.500000	0.500000	0.500000	0.045
H1B	0.577(3)	0.555(5)	0.554(4)	0.045
N1	0.3696(4)	0.8201(4)	0.5023(4)	0.0305(10)
N2	0.2072(4)	0.7520(4)	0.6263(4)	0.0347(11)
N3	0.4491(4)	0.6007(4)	0.7156(4)	0.0321(10)
N4	0.3471(4)	0.4868(4)	0.6720(4)	0.0318(10)
N5	0.2580(4)	0.7025(4)	0.4433(4)	0.0304(10)
N6	0.0326(4)	0.7572(4)	0.1235(4)	0.0413(12)
C1	0.4584(5)	0.8462(5)	0.4409(5)	0.0381(13)
H1	0.518513	0.785066	0.431096	0.046

C2	0.4662(6)	0.9585(5)	0.3911(5)	0.0461(15)
H2	0.531158	0.973856	0.349110	0.055
C3	0.3784(6)	1.0472(5)	0.4035(6)	0.0519(17)
H3	0.381641	1.125166	0.369816	0.062
C4	0.2856(6)	1.0225(5)	0.4651(5)	0.0465(15)
H4	0.224062	1.083441	0.474064	0.056
C5	0.2822(5)	0.9082(5)	0.5140(4)	0.0344(12)
C6	0.1899(5)	0.8703(5)	0.5841(4)	0.0356(13)
C7	0.0938(6)	0.9445(6)	0.6085(5)	0.0473(16)
H7	0.084260	1.025979	0.579252	0.057
C8	0.0120(6)	0.9006(6)	0.6750(5)	0.0551(18)
H8	-0.055257	0.951352	0.691038	0.066
C9	0.0293(6)	0.7821(7)	0.7178(5)	0.0541(18)
H9	-0.025662	0.749678	0.764645	0.065
C10	0.1271(5)	0.7105(6)	0.6922(5)	0.0463(15)
H10	0.138168	0.628641	0.722477	0.056
C11	0.4936(5)	0.6682(5)	0.7364(5)	0.0419(14)
H11	0.476249	0.748993	0.686083	0.050
C12	0.5624(6)	0.6250(6)	0.8268(5)	0.0467(15)
H12	0.592353	0.675136	0.838015	0.056
C13	0.5874(6)	0.5085(6)	0.9008(5)	0.0464(15)
H13	0.635088	0.476704	0.963800	0.056
C14	0.5425(5)	0.4391(5)	0.8822(5)	0.0416(14)
H14	0.558534	0.358545	0.932995	0.050
C15	0.4732(5)	0.4853(5)	0.7895(4)	0.0323(12)
C16	0.4191(5)	0.4207(5)	0.7628(5)	0.0364(13)
C17	0.4362(5)	0.3011(5)	0.8237(5)	0.0414(14)
H17	0.484762	0.256837	0.887860	0.050
C18	0.3826(6)	0.2465(5)	0.7911(5)	0.0467(16)
H18	0.395211	0.164245	0.831136	0.056
C19	0.3110(5)	0.3134(5)	0.7000(5)	0.0423(14)
H19	0.273193	0.277546	0.676171	0.051
C20	0.2933(5)	0.4318(5)	0.6427(5)	0.0366(13)
H20	0.241585	0.476891	0.580382	0.044
C21	0.3130(5)	0.7219(5)	0.3504(4)	0.0337(12)

H21	0.396237	0.706396	0.350955	0.040
C22	0.2529(5)	0.7631(5)	0.2558(5)	0.0357(13)
H22	0.295231	0.774238	0.192983	0.043
C23	0.1321(5)	0.7884(5)	0.2508(4)	0.0336(12)
C24	0.0755(5)	0.7697(5)	0.3455(5)	0.0358(13)
H24	-0.008049	0.787896	0.345700	0.043
C25	0.1403(5)	0.7249(5)	0.4388(5)	0.0343(12)
H25	0.100025	0.709142	0.503011	0.041
C26	0.0649(5)	0.8422(5)	0.1461(5)	0.0396(14)
H26A	0.113167	0.879888	0.088270	0.048
H26B	-0.008933	0.905165	0.144073	0.048
C27	0.1390(6)	0.6557(5)	0.1330(5)	0.0480(16)
H27A	0.117017	0.605837	0.111387	0.072
H27B	0.171186	0.609320	0.207009	0.072
H27C	0.199097	0.685070	0.086721	0.072
C28	-0.0580(6)	0.7133(6)	0.1980(6)	0.0547(17)
H28A	-0.126471	0.780792	0.193729	0.082
H28B	-0.022881	0.666102	0.271086	0.082
H28C	-0.083683	0.664436	0.177722	0.082
C29	-0.0211(7)	0.8229(7)	0.0125(5)	0.066(2)
H29A	0.037531	0.849967	-0.037553	0.100
H29B	-0.090044	0.891222	0.005541	0.100
H29C	-0.046148	0.770675	-0.003576	0.100

$U_{eq}$  is defined as 1/3 of the trace of the orthogonalized  $U_{ij}$  tensor.

**Table S10. Anisotropic displacement parameters [ $\text{\AA}^2$ ] for  $[\{\text{Os}^{\text{II}}(\text{bpy})_2(\text{py}^{\text{L}})\}_2(\mu\text{-O}_2\text{H}_3)](\text{PF}_6)_5$  ( $\text{py}^{\text{L}} = 4\text{-N-(pyridin-4-ylmethyl)-N,N,N-trimethylammonium}$ ). The anisotropic displacement factor exponent takes the form:  $-2\pi^2[h^2(a^*)^2U_{11} + k^2(b^*)^2U_{22} + \dots + 2hka^*b^*U_{12}]$**

Atom	$U_{11}$	$U_{22}$	$U_{33}$	$U_{23}$	$U_{13}$	$U_{12}$
Os1	0.02651(12)	0.02556(11)	0.03264(12)	-0.01511(9)	0.00762(8)	-0.00903(8)
P1	0.0500(10)	0.0390(9)	0.0534(10)	-0.0210(8)	0.0060(8)	-0.0172(8)
F1	0.043(2)	0.080(3)	0.117(4)	-0.057(3)	-0.010(2)	-0.002(2)
F2	0.109(4)	0.115(4)	0.076(3)	-0.061(3)	0.042(3)	-0.070(3)
F3	0.147(5)	0.076(3)	0.074(3)	-0.039(3)	0.027(3)	-0.072(3)
F4	0.065(3)	0.061(2)	0.069(3)	-0.038(2)	0.013(2)	-0.019(2)
F5	0.044(2)	0.044(2)	0.089(3)	-0.035(2)	0.016(2)	-0.0161(17)

F6	0.117(4)	0.055(3)	0.093(4)	-0.026(3)	-0.044(3)	0.016(3)
P2	0.0416(14)	0.0425(17)	0.0442(14)	-0.0100(12)	0.0120(11)	-0.0181(12)
F7	0.058(4)	0.064(5)	0.101(5)	-0.043(4)	-0.006(3)	0.003(3)
F8	0.086(4)	0.059(4)	0.064(4)	-0.033(3)	0.026(3)	-0.037(3)
F9	0.078(4)	0.054(3)	0.096(4)	-0.006(3)	0.012(3)	-0.038(3)
F10	0.109(5)	0.133(6)	0.067(4)	-0.045(4)	0.039(4)	-0.063(5)
F11	0.092(4)	0.041(3)	0.077(4)	-0.030(3)	0.011(3)	-0.027(3)
F12	0.061(3)	0.065(4)	0.107(4)	-0.013(3)	-0.018(3)	-0.019(3)
P2B	0.052(4)	0.055(5)	0.056(4)	-0.016(4)	0.012(4)	-0.026(4)
F7B	0.065(8)	0.062(8)	0.079(9)	-0.019(7)	0.015(7)	-0.033(7)
F8B	0.083(8)	0.049(8)	0.076(9)	-0.017(7)	0.021(8)	-0.014(7)
F9B	0.086(8)	0.073(8)	0.082(8)	0.012(8)	0.019(8)	-0.011(8)
F10B	0.059(8)	0.073(8)	0.045(7)	-0.035(7)	0.017(6)	-0.010(7)
F11B	0.081(9)	0.062(8)	0.080(9)	-0.012(8)	0.011(8)	-0.015(8)
F12B	0.062(8)	0.077(9)	0.093(9)	-0.024(8)	0.009(7)	-0.019(8)
P3	0.101(4)	0.089(3)	0.073(3)	-0.052(3)	0.013(3)	-0.055(3)
F13	0.103(5)	0.096(5)	0.076(3)	-0.054(3)	0.014(3)	-0.056(4)
F14	0.105(4)	0.095(5)	0.076(4)	-0.056(4)	0.016(3)	-0.059(4)
F15	0.103(5)	0.092(4)	0.079(5)	-0.054(3)	0.015(4)	-0.056(4)
F16	0.101(5)	0.087(5)	0.076(4)	-0.050(4)	0.013(3)	-0.054(4)
F17	0.105(5)	0.091(4)	0.077(4)	-0.053(3)	0.014(4)	-0.057(4)
F18	0.111(5)	0.088(5)	0.075(3)	-0.051(3)	0.012(3)	-0.059(4)
P3B	0.101(4)	0.089(3)	0.073(3)	-0.052(3)	0.013(3)	-0.055(3)
F13B	0.104(5)	0.088(5)	0.075(4)	-0.051(4)	0.013(3)	-0.055(4)
F14B	0.100(5)	0.090(5)	0.075(4)	-0.050(4)	0.012(4)	-0.054(4)
F15B	0.103(4)	0.092(4)	0.077(4)	-0.053(4)	0.012(3)	-0.054(3)
F16B	0.102(5)	0.091(5)	0.076(4)	-0.053(4)	0.016(4)	-0.056(4)
F17B	0.101(4)	0.095(4)	0.078(4)	-0.051(3)	0.014(3)	-0.054(3)
F18B	0.097(5)	0.097(5)	0.076(4)	-0.054(4)	0.015(3)	-0.057(4)
P3C	0.101(4)	0.089(3)	0.073(3)	-0.052(3)	0.013(3)	-0.055(3)
F13C	0.104(5)	0.092(5)	0.074(4)	-0.052(4)	0.013(4)	-0.055(4)
F14C	0.103(5)	0.090(5)	0.074(4)	-0.052(4)	0.013(4)	-0.056(4)
F15C	0.104(5)	0.092(5)	0.074(4)	-0.051(3)	0.012(4)	-0.056(4)
F16C	0.102(5)	0.091(5)	0.074(5)	-0.052(4)	0.013(4)	-0.056(4)
F17C	0.102(5)	0.092(5)	0.073(4)	-0.052(3)	0.013(3)	-0.055(4)

F18C	0.100(5)	0.091(5)	0.075(4)	-0.053(4)	0.013(4)	-0.056(4)
O2	0.106(19)	0.053(14)	0.040(13)	0.000(11)	-0.015(14)	-0.037(14)
C30	0.055(18)	0.09(2)	0.039(17)	0.002(17)	-0.021(15)	-0.029(17)
O3	0.11(2)	0.079(17)	0.059(15)	-0.010(14)	-0.002(15)	-0.041(16)
C31	0.09(2)	0.058(16)	0.056(18)	-0.015(16)	-0.033(17)	-0.045(17)
O4	0.072(14)	0.056(13)	0.064(14)	0.000(12)	-0.016(12)	-0.045(11)
C32	0.049(17)	0.030(15)	0.058(18)	-0.007(13)	-0.042(15)	0.001(13)
O5	0.183(16)	0.092(10)	0.130(14)	-0.031(10)	-0.052(13)	-0.027(12)
C33	0.183(16)	0.092(10)	0.130(14)	-0.031(10)	-0.052(13)	-0.027(12)
C34	0.183(16)	0.092(10)	0.130(14)	-0.031(10)	-0.052(13)	-0.027(12)
C35	0.183(16)	0.092(10)	0.130(14)	-0.031(10)	-0.052(13)	-0.027(12)
C36	0.183(16)	0.092(10)	0.130(14)	-0.031(10)	-0.052(13)	-0.027(12)
O5B	0.183(16)	0.092(10)	0.130(14)	-0.031(10)	-0.052(13)	-0.027(12)
C33B	0.183(16)	0.092(10)	0.130(14)	-0.031(10)	-0.052(13)	-0.027(12)
C34B	0.183(16)	0.092(10)	0.130(14)	-0.031(10)	-0.052(13)	-0.027(12)
C35B	0.183(16)	0.092(10)	0.130(14)	-0.031(10)	-0.052(13)	-0.027(12)
C36B	0.183(16)	0.092(10)	0.130(14)	-0.031(10)	-0.052(13)	-0.027(12)
O1	0.028(2)	0.031(2)	0.039(2)	-0.0217(17)	0.0056(16)	-0.0106(17)
N1	0.029(2)	0.026(2)	0.039(3)	-0.016(2)	0.001(2)	-0.009(2)
N2	0.035(3)	0.037(3)	0.032(3)	-0.018(2)	0.003(2)	-0.008(2)
N3	0.030(2)	0.033(3)	0.039(3)	-0.022(2)	0.012(2)	-0.011(2)
N4	0.028(2)	0.032(2)	0.034(3)	-0.016(2)	0.012(2)	-0.012(2)
N5	0.029(2)	0.025(2)	0.037(3)	-0.016(2)	0.009(2)	-0.0091(19)
N6	0.039(3)	0.043(3)	0.038(3)	-0.011(2)	-0.003(2)	-0.019(2)
C1	0.036(3)	0.036(3)	0.044(3)	-0.019(3)	0.008(3)	-0.015(3)
C2	0.048(4)	0.043(4)	0.051(4)	-0.019(3)	0.001(3)	-0.023(3)
C3	0.062(4)	0.029(3)	0.061(4)	-0.015(3)	-0.004(3)	-0.018(3)
C4	0.048(4)	0.028(3)	0.062(4)	-0.025(3)	-0.003(3)	-0.004(3)
C5	0.032(3)	0.029(3)	0.039(3)	-0.018(3)	-0.002(2)	-0.002(2)
C6	0.033(3)	0.035(3)	0.037(3)	-0.021(3)	-0.001(2)	-0.002(3)
C7	0.043(4)	0.044(4)	0.050(4)	-0.029(3)	-0.001(3)	0.002(3)
C8	0.037(4)	0.062(5)	0.053(4)	-0.033(4)	0.002(3)	0.009(3)
C9	0.038(4)	0.075(5)	0.048(4)	-0.034(4)	0.019(3)	-0.014(3)
C10	0.038(3)	0.047(4)	0.051(4)	-0.025(3)	0.017(3)	-0.012(3)
C11	0.044(4)	0.038(3)	0.049(4)	-0.026(3)	0.008(3)	-0.014(3)

C12	0.047(4)	0.058(4)	0.054(4)	-0.040(4)	0.003(3)	-0.019(3)
C13	0.041(4)	0.061(4)	0.041(4)	-0.029(3)	0.004(3)	-0.013(3)
C14	0.039(3)	0.041(3)	0.036(3)	-0.014(3)	0.007(3)	-0.009(3)
C15	0.025(3)	0.037(3)	0.035(3)	-0.018(3)	0.010(2)	-0.009(2)
C16	0.030(3)	0.034(3)	0.041(3)	-0.016(3)	0.011(2)	-0.010(2)
C17	0.035(3)	0.037(3)	0.045(4)	-0.013(3)	0.009(3)	-0.014(3)
C18	0.049(4)	0.036(3)	0.049(4)	-0.010(3)	0.010(3)	-0.022(3)
C19	0.042(4)	0.038(3)	0.052(4)	-0.022(3)	0.018(3)	-0.023(3)
C20	0.034(3)	0.044(3)	0.039(3)	-0.021(3)	0.013(2)	-0.022(3)
C21	0.024(3)	0.035(3)	0.043(3)	-0.019(3)	0.010(2)	-0.011(2)
C22	0.032(3)	0.036(3)	0.040(3)	-0.018(3)	0.008(2)	-0.015(3)
C23	0.034(3)	0.028(3)	0.040(3)	-0.015(2)	0.004(2)	-0.013(2)
C24	0.023(3)	0.035(3)	0.047(3)	-0.021(3)	0.004(2)	-0.005(2)
C25	0.028(3)	0.036(3)	0.041(3)	-0.021(3)	0.012(2)	-0.012(2)
C26	0.035(3)	0.032(3)	0.043(3)	-0.011(3)	0.002(3)	-0.010(3)
C27	0.056(4)	0.045(4)	0.051(4)	-0.028(3)	0.006(3)	-0.018(3)
C28	0.045(4)	0.057(4)	0.064(4)	-0.020(4)	0.007(3)	-0.032(3)
C29	0.066(5)	0.083(5)	0.047(4)	-0.012(4)	-0.014(4)	-0.042(4)

**Table S11. Bond lengths and angles for  $[\{\text{Os}^{\text{II}}(\text{bpy})_2(\text{py}^{\text{L}})\}_2(\mu\text{-O}_2\text{H}_3)](\text{PF}_6)_5$  ( $\text{py}^{\text{L}}$  = 4-N-(pyridin-4-ylmethyl)-N,N,N-trimethylammonium)**

Atom–Atom	Length [Å]
Os1–N3	2.032(5)
Os1–N2	2.033(4)
Os1–N1	2.051(4)
Os1–N4	2.062(4)
Os1–N5	2.098(5)
Os1–O1	2.103(3)
P1–F6	1.575(4)
P1–F2	1.585(4)
P1–F4	1.586(4)
P1–F1	1.590(4)
P1–F5	1.599(4)
P1–F3	1.625(4)
P2–F8	1.576(6)

P2-F12	1.588(6)
P2-F7	1.588(6)
P2-F11	1.588(5)
P2-F10	1.594(6)
P2-F9	1.597(6)
P2B-F12B	1.567(13)
P2B-F8B	1.567(13)
P2B-F9B	1.594(13)
P2B-F7B	1.601(13)
P2B-F11B	1.603(13)
P2B-F10B	1.603(13)
P3-F14	1.569(11)
P3-F18	1.590(11)
P3-F15	1.608(11)
P3-F13	1.613(11)
P3-F16	1.619(11)
P3-F17	1.621(11)
P3B-F18B	1.577(11)
P3B-F14B	1.584(11)
P3B-F15B	1.607(11)
P3B-F16B	1.609(11)
P3B-F13B	1.612(11)
P3B-F17B	1.619(12)
P3C-F18C	1.558(14)
P3C-F14C	1.585(12)
P3C-F15C	1.607(12)
P3C-F16C	1.613(12)
P3C-F17C	1.624(12)
P3C-F13C	1.636(12)
O2-C30	1.44(2)
O3-C31	1.44(2)
O4-C36	1.13(7)
O4-C32	1.405(19)
O5-C35	1.408(19)
O5-C33	1.433(19)

C33–C34	1.57(2)
C35–C36	1.52(2)
O5B–C35B	1.408(19)
O5B–C33B	1.433(19)
C33B–C34B	1.76(8)
C35B–C36B	1.52(2)
O1–H1B	0.93(2)
O1–H1A	1.220(3)
O1–O1 <sup>#1</sup>	2.441(7)
N1–C1	1.338(7)
N1–C5	1.358(7)
N2–C10	1.342(7)
N2–C6	1.372(7)
N3–C11	1.356(7)
N3–C15	1.364(7)
N4–C20	1.357(7)
N4–C16	1.363(7)
N5–C25	1.345(7)
N5–C21	1.361(7)
N6–C27	1.485(8)
N6–C29	1.492(8)
N6–C28	1.505(8)
N6–C26	1.506(7)
C1–C2	1.382(8)
C2–C3	1.369(9)
C3–C4	1.375(9)
C4–C5	1.387(8)
C5–C6	1.469(8)
C6–C7	1.380(8)
C7–C8	1.374(10)
C8–C9	1.373(10)
C9–C10	1.381(8)
C11–C12	1.374(9)
C12–C13	1.375(9)
C13–C14	1.367(9)

C14–C15	1.394(8)
C15–C16	1.450(8)
C16–C17	1.387(8)
C17–C18	1.379(9)
C18–C19	1.364(9)
C19–C20	1.368(8)
C21–C22	1.373(8)
C22–C23	1.377(8)
C23–C24	1.389(8)
C23–C26	1.503(8)
C24–C25	1.376(8)
<b>Atom–Atom– Atom</b>	<b>Angle [°]</b>
N3–Os1–N2	92.30(17)
N3–Os1–N1	96.26(17)
N2–Os1–N1	78.93(18)
N3–Os1–N4	78.23(18)
N2–Os1–N4	101.80(17)
N1–Os1–N4	174.45(18)
N3–Os1–N5	176.59(17)
N2–Os1–N5	90.37(17)
N1–Os1–N5	86.34(16)
N4–Os1–N5	99.14(17)
N3–Os1–O1	90.31(15)
N2–Os1–O1	172.65(16)
N1–Os1–O1	93.97(15)
N4–Os1–O1	85.45(15)
N5–Os1–O1	87.29(15)
F6–P1–F2	90.3(3)
F6–P1–F4	90.0(3)
F2–P1–F4	179.5(3)
F6–P1–F1	179.1(3)
F2–P1–F1	89.3(3)
F4–P1–F1	90.3(2)

F6-P1-F5	89.6(3)
F2-P1-F5	89.2(2)
F4-P1-F5	90.4(2)
F1-P1-F5	89.6(2)
F6-P1-F3	92.9(3)
F2-P1-F3	90.1(2)
F4-P1-F3	90.3(2)
F1-P1-F3	87.9(3)
F5-P1-F3	177.4(3)
F8-P2-F12	90.9(4)
F8-P2-F7	89.8(4)
F12-P2-F7	179.3(5)
F8-P2-F11	89.9(4)
F12-P2-F11	88.9(4)
F7-P2-F11	91.0(4)
F8-P2-F10	179.2(5)
F12-P2-F10	89.2(4)
F7-P2-F10	90.1(4)
F11-P2-F10	90.9(4)
F8-P2-F9	89.5(4)
F12-P2-F9	89.7(4)
F7-P2-F9	90.4(4)
F11-P2-F9	178.5(4)
F10-P2-F9	89.7(4)
F12B-P2B-F8B	90.2(12)
F12B-P2B-F9B	93.5(12)
F8B-P2B-F9B	93.7(12)
F12B-P2B-F7B	177.5(14)
F8B-P2B-F7B	92.1(13)
F9B-P2B-F7B	87.1(12)
F12B-P2B-F11B	90.3(12)
F8B-P2B-F11B	90.0(12)
F9B-P2B-F11B	174.7(13)
F7B-P2B-F11B	89.0(12)
F12B-P2B-F10B	90.4(11)

F8B-P2B-F10B	179.0(14)
F9B-P2B-F10B	87.0(12)
F7B-P2B-F10B	87.2(12)
F11B-P2B-F10B	89.3(11)
F14-P3-F18	94.4(11)
F14-P3-F15	91.9(11)
F18-P3-F15	96.1(11)
F14-P3-F13	90.8(11)
F18-P3-F13	172.1(14)
F15-P3-F13	89.6(11)
F14-P3-F16	179.0(13)
F18-P3-F16	85.3(10)
F15-P3-F16	89.2(11)
F13-P3-F16	89.3(11)
F14-P3-F17	88.3(11)
F18-P3-F17	85.7(11)
F15-P3-F17	178.2(13)
F13-P3-F17	88.5(11)
F16-P3-F17	90.7(11)
F18B-P3B-F14B	91.0(10)
F18B-P3B-F15B	91.5(11)
F14B-P3B-F15B	90.7(11)
F18B-P3B-F16B	92.3(10)
F14B-P3B-F16B	174.8(13)
F15B-P3B-F16B	93.1(11)
F18B-P3B-F13B	178.9(14)
F14B-P3B-F13B	89.2(10)
F15B-P3B-F13B	89.6(11)
F16B-P3B-F13B	87.4(10)
F18B-P3B-F17B	87.3(11)
F14B-P3B-F17B	87.5(11)
F15B-P3B-F17B	177.8(13)
F16B-P3B-F17B	88.7(11)
F13B-P3B-F17B	91.6(11)
F18C-P3C-F14C	94.2(14)

F18C-P3C-F15C	99.9(14)
F14C-P3C-F15C	89.3(14)
F18C-P3C-F16C	91.6(14)
F14C-P3C-F16C	173.4(16)
F15C-P3C-F16C	92.8(14)
F18C-P3C-F17C	86.6(14)
F14C-P3C-F17C	87.4(14)
F15C-P3C-F17C	172.9(16)
F16C-P3C-F17C	89.8(14)
F18C-P3C-F13C	173.1(16)
F14C-P3C-F13C	89.0(14)
F15C-P3C-F13C	86.3(13)
F16C-P3C-F13C	84.9(13)
F17C-P3C-F13C	87.4(14)
C36-O4-C32	121(5)
C35-O5-C33	118(3)
O5-C33-C34	124(4)
O5-C35-C36	115(4)
O4-C36-C35	101(5)
C35B-O5B-C33B	118(3)
O5B-C33B-C34B	106(3)
O5B-C35B-C36B	115(4)
H1B-O1-H1A	111(4)
H1B-O1-Os1	116(4)
H1A-O1-Os1	116.2(2)
H1B-O1-O1 <sup>#1</sup>	111(4)
H1A-O1-O1 <sup>#1</sup>	0.00(13)
Os1-O1-O1 <sup>#1</sup>	116.2(2)
C1-N1-C5	118.6(5)
C1-N1-Os1	125.3(4)
C5-N1-Os1	116.1(4)
C10-N2-C6	117.7(5)
C10-N2-Os1	126.1(4)
C6-N2-Os1	116.2(4)
C11-N3-C15	117.7(5)

C11-N3-Os1	125.5(4)
C15-N3-Os1	116.7(4)
C20-N4-C16	117.9(5)
C20-N4-Os1	126.3(4)
C16-N4-Os1	115.1(4)
C25-N5-C21	116.7(5)
C25-N5-Os1	122.9(4)
C21-N5-Os1	120.2(4)
C27-N6-C29	109.4(5)
C27-N6-C28	109.9(5)
C29-N6-C28	108.2(5)
C27-N6-C26	111.1(4)
C29-N6-C26	107.6(5)
C28-N6-C26	110.6(5)
N1-C1-C2	122.7(6)
C3-C2-C1	118.7(6)
C2-C3-C4	119.5(6)
C3-C4-C5	119.6(6)
N1-C5-C4	120.9(5)
N1-C5-C6	114.4(5)
C4-C5-C6	124.6(5)
N2-C6-C7	121.4(6)
N2-C6-C5	114.3(5)
C7-C6-C5	124.3(5)
C8-C7-C6	120.0(6)
C9-C8-C7	118.8(6)
C8-C9-C10	119.5(6)
N2-C10-C9	122.6(6)
N3-C11-C12	123.1(6)
C11-C12-C13	119.2(6)
C14-C13-C12	118.8(6)
C13-C14-C15	120.7(6)
N3-C15-C14	120.5(5)
N3-C15-C16	114.2(5)
C14-C15-C16	125.3(5)

N4–C16–C17	121.1(5)
N4–C16–C15	114.8(5)
C17–C16–C15	124.0(5)
C18–C17–C16	120.0(6)
C19–C18–C17	118.4(6)
C18–C19–C20	120.5(6)
N4–C20–C19	122.1(6)
N5–C21–C22	122.5(5)
C21–C22–C23	120.7(5)
C22–C23–C24	116.8(5)
C22–C23–C26	120.8(5)
C24–C23–C26	122.2(5)
C25–C24–C23	120.2(5)
N5–C25–C24	123.0(5)
C23–C26–N6	115.2(4)

Symmetry transformations used to generate equivalent atoms:

#1: 1-X, 1-Y, 1-Z;

**Table S12. Torsion angles for  $[\{\text{Os}^{\text{II}}(\text{bpy})_2(\text{py}^{\text{L}})\}_2(\mu\text{-O}_2\text{H}_3)](\text{PF}_6)_5$  ( $\text{py}^{\text{L}}$  = 4-N-(pyridin-4-ylmethyl)-N,N,N-trimethylammonium)**

<b>Atom–Atom–Atom– Atom</b>	<b>Torsion Angle [°]</b>
C35–O5–C33–C34	124(6)
C33–O5–C35–C36	166(5)
C32–O4–C36–C35	–91(5)
O5–C35–C36–O4	–37(7)
C35B–O5B–C33B– C34B	–167(4)
C33B–O5B–C35B– C36B	166(5)
C5–N1–C1–C2	1.6(8)
Os1–N1–C1–C2	–178.8(4)
N1–C1–C2–C3	–1.2(9)
C1–C2–C3–C4	0.3(10)
C2–C3–C4–C5	0.2(10)
C1–N1–C5–C4	–1.1(8)
Os1–N1–C5–C4	179.2(4)
C1–N1–C5–C6	–179.1(5)
Os1–N1–C5–C6	1.2(6)
C3–C4–C5–N1	0.2(9)
C3–C4–C5–C6	178.0(6)
C10–N2–C6–C7	0.1(8)
Os1–N2–C6–C7	179.6(4)
C10–N2–C6–C5	179.2(5)
Os1–N2–C6–C5	–1.2(6)
N1–C5–C6–N2	0.0(7)
C4–C5–C6–N2	–177.9(5)
N1–C5–C6–C7	179.1(5)
C4–C5–C6–C7	1.2(9)
N2–C6–C7–C8	–1.0(9)
C5–C6–C7–C8	180.0(6)
C6–C7–C8–C9	1.3(10)
C7–C8–C9–C10	–0.7(10)
C6–N2–C10–C9	0.5(9)
Os1–N2–C10–C9	–179.0(5)

C8–C9–C10–N2	-0.1(10)
C15–N3–C11–C12	1.0(8)
Os1–N3–C11–C12	-177.2(4)
N3–C11–C12–C13	-0.5(9)
C11–C12–C13–C14	-0.2(9)
C12–C13–C14–C15	0.5(9)
C11–N3–C15–C14	-0.7(7)
Os1–N3–C15–C14	177.7(4)
C11–N3–C15–C16	178.0(5)
Os1–N3–C15–C16	-3.6(6)
C13–C14–C15–N3	0.0(8)
C13–C14–C15–C16	-178.6(5)
C20–N4–C16–C17	-0.5(7)
Os1–N4–C16–C17	-171.3(4)
C20–N4–C16–C15	-179.7(4)
Os1–N4–C16–C15	9.4(6)
N3–C15–C16–N4	-3.9(7)
C14–C15–C16–N4	174.7(5)
N3–C15–C16–C17	176.9(5)
C14–C15–C16–C17	-4.5(9)
N4–C16–C17–C18	1.9(8)
C15–C16–C17–C18	-178.9(5)
C16–C17–C18–C19	-1.7(9)
C17–C18–C19–C20	0.0(9)
C16–N4–C20–C19	-1.2(8)
Os1–N4–C20–C19	168.5(4)
C18–C19–C20–N4	1.4(9)
C25–N5–C21–C22	0.4(8)
Os1–N5–C21–C22	-173.9(4)
N5–C21–C22–C23	1.0(8)
C21–C22–C23–C24	-0.3(8)
C21–C22–C23–C26	175.3(5)
C22–C23–C24–C25	-1.7(8)
C26–C23–C24–C25	-177.2(5)
C21–N5–C25–C24	-2.5(8)

Os1–N5–C25–C24	171.6(4)
C23–C24–C25–N5	3.2(8)
C22–C23–C26–N6	101.3(6)
C24–C23–C26–N6	-83.4(7)
C27–N6–C26–C23	-54.2(6)
C29–N6–C26–C23	-173.9(5)
C28–N6–C26–C23	68.1(6)

### S5.3 Single crystal structure of dinuclear complex **6**

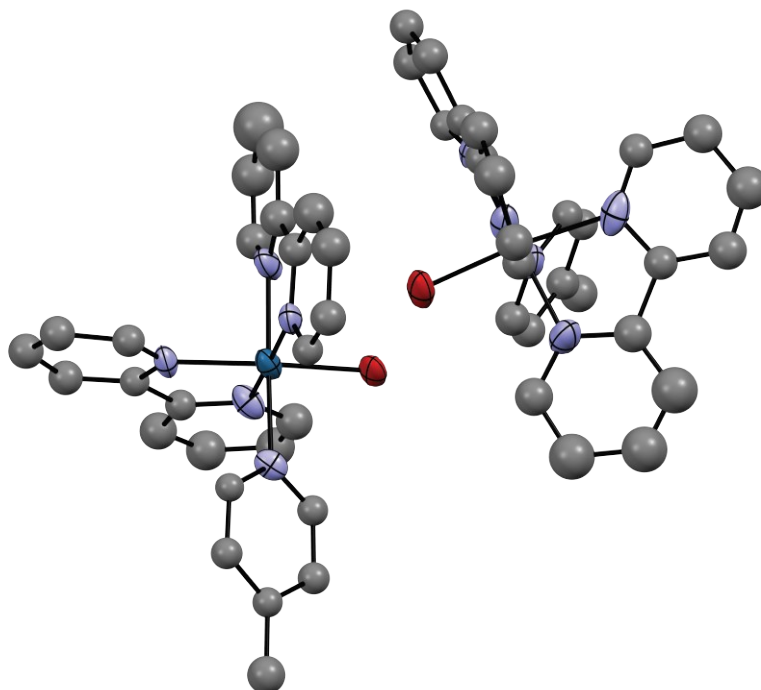


**Figure S81.** Illustration of unrefined solid-state structure of dinuclear complex **6**. Hydrogen atoms, counter anions, and solvent are omitted.

Red crystals of dinuclear complex **6** were grown by layering a concentrated ethanol solution of **6** with diethyl ether in an NMR tube at room temperature for 2 days and crystallized in the monoclinic space group *Cc*. Although we were able to resolve the non-hydrogen atoms of dinuclear complex **6**, we were unable to fully refine the structure due to significant disorder of solvent molecules and the PF<sub>6</sub> counter anions. A depiction of the partially refined structure is shown in Figure S81.

## References

1. E. M. Kober, J. V. Caspar, B. P. Sullivan and T. J. Meyer, Synthetic routes to new polypyridyl complexes of osmium(II), *Inorg. Chem.*, 1988, **27**, 4587–4598.
2. C. Costentin, M. Robert, J. Savéant and A. Teillout, Concerted and stepwise proton-coupled electron transfers in aquo/hydroxo complex couples in water: oxidative electrochemistry of  $[\text{Os}^{\text{II}}(\text{bpy})_2(\text{py})(\text{OH}_2)]^{2+}$ , *ChemPhysChem*, 2009, **10**, 191–198.
3. J. A. Gilbert, Daniel. Geselowitz and T. J. Meyer, Redox properties of the oxo-bridged osmium dimer  $[(\text{bpy})_2(\text{OH}_2)\text{Os}^{\text{III}}\text{O}(\text{OH})(\text{bpy})_2]^{4+}$ . Implications for the oxidation of water to oxygen, *J. Am. Chem. Soc.*, 1986, **108**, 1493–1501.
4. A. D. Allen and J. R. Stevens, Ammine complexes of osmium(II), *Can. J. Chem.*, 1972, **50**, 3093–3099.
5. G. M. Coia, K. D. Demadis and T. J. Meyer, Oxidation of ammonia in osmium polypyridyl complexes, *Inorg. Chem.*, 2000, **39**, 2212–2223.
6. M. Williamson, N. Moustaid-Moussa and L. Gollahon, The molecular effects of dietary acid load on metabolic disease (the cellular pasadoble: the fast-paced dance of pH regulation), *Front. Mol. Med.*, 2021, **1**, 777088.
7. A. Vogler, Photochemistry of  $\text{Os}(\text{bipy})_2(\text{CO}_3)$ . Photoreduction of carbonate to formaldehyde, *Inorg. Chem. Commun.*, 2016, **70**, 175–176.
8. B. Carlson, G. D. Phelan, W. Kaminsky, L. Dalton, X. Jiang, S. Liu and A. K.-Y. Jen, Divalent osmium complexes: synthesis, characterization, strong red phosphorescence, and electrophosphorescence, *J. Am. Chem. Soc.*, 2002, **124**, 14162–14172.
9. E. D. Nacsa and D. W. C. MacMillan, Spin-center shift-enabled direct enantioselective  $\alpha$ -benzylation of aldehydes with alcohols, *J. Am. Chem. Soc.*, 2018, **140**, 3322–3330.
10. C. Zhang, T. Haruyama, E. Kobatake and M. Aizawa, Evaluation of substituted-1,10-phenanthroline complexes of osmium as mediator for glucose oxidase of *aspergillus niger*, *Anal. Chim. Acta*, 2000, **408**, 225–232.
11. D6 PHASER, <https://www.bruker.com/en/products-and-solutions/diffractometers-and-x-ray-microscopes/x-ray-diffractometers/d6-phaser.html>, (accessed 12 June 2024).
12. L. Krause, R. Herbst-Irmer, G. M. Sheldrick and D. Stalke, Comparison of silver and molybdenum microfocus x-ray sources for single-crystal structure determination, *J. Appl. Crystallogr.*, 2015, **48**, 3–10.
13. G. M. Sheldrick, Crystal structure refinement with shelxl, *Acta Crystallogr. Sect. C Struct. Chem.*, 2015, **71**, 3–8.
14. G. M. Sheldrick, SHELXT – integrated space-group and crystal-structure determination, *Acta Crystallogr. Sect. Found. Adv.*, 2015, **71**, 3–8.

15. C. R. Groom, I. J. Bruno, M. P. Lightfoot and S. C. Ward, The cambridge structural database, *Acta Crystallogr. Sect. B Struct. Sci. Cryst. Eng. Mater.*, 2016, **72**, 171–179.
16. Daniel Kratzerts SC-XRD tools, <https://dkratzert.de/finalcif.html>, (accessed 12 June 2024).